WROCŁAW UNIVERSITY
OF ENVIRONMENTAL
AND LIFE SCIENCES

The role of *sanA* in *Salmonella* pathogenicity

Adrianna Aleksandrowicz

PhD thesis

Department of Biochemistry and Molecular Biology
Faculty of Veterinary Science
Wroclaw University of Environmental and Life Sciences

Supervisor

Dr hab. Krzysztof Grzymajło, associate professor

Assistant supervisor

Dr Rafał Kolenda

Wroclaw 2024

This research has been supported by the Polish National Science Centre Research Grant PRELUDIUM BIS number 2019/35/O/NZ6/01590.

Acknowledgments

First and foremost, I am grateful to my supervisor, Prof. Krzysztof Grzymajło, for entrusting me with the opportunity to begin my scientific journey as a PhD student. Your guidance, instruction, and motivation have been invaluable throughout this time. I am thankful for your consistent support and belief in me. This thesis could not have been completed without your exceptional supervision.

I extend my heartfelt thanks to my assistant supervisor, Dr Rafał Kolenda. You introduced me to the laboratory when I began my work as a Master's student in 2018. Your guidance since then has been extremely beneficial, aiding in my growth as a scientist.

I am deeply thankful to Dr Teresa Thurston and her lab members at Imperial College London. The unique opportunity to work with your research group was significant in deepening my skills. Beyond developing my laboratory expertise, you fostered my ability to engage in collaborations with international scientists, making me feel like an integral part of your team.

I extend my gratitude to my colleagues from the Department of Biochemistry and Molecular Biology for the great time we spent together. I am thankful for your valuable feedback during our lab meetings and the enjoyable conversations over coffee in our kitchen.

I owe a special thanks to my future husband, Michał, for your invaluable support throughout my research journey. Your patience, understanding and our long conversations have been an important part of my success. This accomplishment would not have been possible without you by my side.

Z całego serca dziękuję całej mojej rodzinie oraz przyjaciołom. Za nieocenione wsparcie i wyrozumiałość. Za nieustanną wiarę w to, że mogę osiągnąć zamierzone cele i dopingowanie mnie w chwilach zwątpienia. Przede wszystkim dziękuję mojej mamie Monice, za trud wychowania i za to, że dzięki niej mogę być tym, kim jestem obecnie.

Contents

Structure of the thesis

This doctoral thesis is composed of two scientifically coherent articles, which are either published in peer-reviewed journal or preprinted in 2024. These articles are detailed below along with their respective Impact Factor (IF) and scores given by the Ministry of Science and Higher Education (MSHE, Poland). In each manuscript, the PhD student is the first author, having made a major contribution, as confirmed by the statements attached to this work. The research topic addressed in this thesis has been explored over 55 pages across these publications, incorporating references from 105 different academic sources.

List of manuscripts included in the doctoral dissertation:

- **1st manuscript (M1)**

Aleksandrowicz A., Kolenda R., Baraniewicz K., Thurston T., Suchański J., Grzymajło K. Membrane properties modulation by SanA: implications for xenobiotic resistance in *Salmonella* Typhimurium. 2024. Frontiers in Microbiology. 4:1340143 doi: 10.3389/fmicb.2023.1340143
IF: 5.2
MSHE: 140

- **2nd manuscript (M2)**

Aleksandrowicz A., Kolenda R., Thurston T., Grzymajło K. SanA is an inner membrane protein mediating early stages of *Salmonella* infection. 2024. bioRxiv preprint doi: https://doi.org/10.1101/2024.01.05.574334
Preprint of the manuscript; The final version will be published in 2024

The publications that comprise this doctoral dissertation are supplemented with brief descriptions in the subsequent chapters. **Chapters 4** and **5** detail the content of each manuscript, including the primary materials and methods used, which contribute to achieving the objectives outlined in **Chapter 2**. The main scientific contributions of each article are also highlighted. The most significant impacts of the conducted research on the field of veterinary science, along with a summary that includes the verification of research hypotheses, conclusions, and future research directions, are discussed in **Chapters 6** and **7.**

Abbreviation list

- Amp – Ampicillin
- AMP - antimicrobial peptide
- BCA- Bicinchoninic Acid
- CCCP - carbonyl cyanidem-chlorophenylhydrazone
- CDC - Centers for Disease Control and Prevention
- CFU - Colony Forming Unit
- Cm - chloramphenicol
- CSF - Classical Swine Fever
- DMSO – Dimethylsulfoxide
- EB – Ethidium Bromide
- EFSA - European Food Safety Authority
- EU – European Union
- FBS - Fetal Bovine Serum
- GALT - Gut-Associated Lymphoid Tissue
- GFP – Green Fluorescent Protein
- Gm – Gentamycin
- HisHF - Imidazole Glycerol Phosphate Synthase
- iBMDMs - immortalized Bone Marrow-Derived Macrophages
- IM – Inner Membrane
- IMP - Inner Membrane Protein
- IPTG - Isopropylthio-β-galactoside
- KLH - Keyhole Limpet Hemocyanin
- Km – Kanamycin
- LB - Lysogeny Broth
- LPS – Lipopolysaccharide
- MATE - Multidrug and toxic compound extrusion
- MF - Major Facilitator
- MHB - Mueller Hinton Broth
- MOI - Multiplicity Of Infection
- MOPS - 3-(N-Morpholino) propanesulfonic acid

- NR – Nile Red
- OD – Optical Density
- OM – Outer Membrane
- OMP – Outer Membrane Protein
- PACE - Proteobacterial Antimicrobial Compound Efflux
- pBMDMs - primary Bone Marrow-Derived Macrophages
- PBP - Penicillin-Binding Proteins
- PBS - Phosphate Buffered Saline
- PCR – Polymerase Chain Reaction
- RND – Resistance Nodulation-Division
- rpm - revolutions per minute
- SCV - *Salmonella*-Containing Vacuole
- SDS - Sodium Dodecyl Sulfate
- SEM - Standard Error of Mean
- SMR - Small Multidrug Resistance
- SPI-1 – *Salmonella* Pathogenicity Island 1
- SPI-2 – *Salmonella* Pathogenicity Island 2
- T3SS – Type III Secretion System
- Ttr - Tetrathionate reductase
- WHO - World Health Organization Collaborating Centre
- WT – Wild Type
- YE - Yeast Extract

Abstract

The increasing prevalence of multidrug-resistant Gram-negative bacteria, such as *Salmonella*, underscores the urgent need for deeper insights into their survival and resistance strategies, aiding in the development of effective prevention and treatment of salmonellosis. These bacteria deploy various mechanisms, including the modification of their membranes composition, to counteract antibiotic treatments and enhance interaction with the host. In this context, the bacterial envelope, embedded with various proteins, plays a pivotal role. One of such molecules with considerable research potential is SanA, which is associated with vancomycin resistance and potentially involved in the initial phases of infection.

In this study, a comprehensive analysis of SanA's properties and biological functions was conducted. The aim was to understand how SanA influences the *Salmonella* membrane, affecting the bacterium's resistance to environmental stressors, including the harsh conditions within host. A *ΔsanA* deletion mutant was employed to assess the effects of SanA on membrane properties, including charge, hydrophobicity, and permeability, through a range of assays. An extensive phenotypic analysis involving 240 xenobiotics was performed to gain deeper insight into SanA's biological role. The study also delved into SanA's expression pattern and its subcellular localization, utilizing techniques such as luciferase activity measurement in a transcriptional fusion and fractionation followed by immunoblotting. In addition, following invasion assays, a newly-created reporter system was utilized to investigate the relationship between SanA and a key virulence factor, *Salmonella* Pathogenicity Island I (SPI-1).

The findings demonstrate that SanA is an inner membrane protein which absence increases membrane permeability, hydrophilicity, and positive charge, leading to heightened resistance against envelope-targeting antibiotics. This genetic alteration also correlates with increased replication rates in primary macrophages, suggesting a potential evasion of immune system defenses. Invasion assays revealed that the deletion of *sanA* in early stationary phase bacteria significantly boosts their invasiveness, partially due to upregulated SPI-1 expression, which is modulated in a nutrient availability-dependent manner.

In conclusion, our research highlights the importance of SanA in regulating *Salmonella*'s response to environmental stress. This includes playing a crucial role in the pathogen's entry, survival within the host, and xenobiotic resistance, thus underlining the significance of inner membrane proteins in understanding the complexities of *Salmonella* pathogenicity.

Streszczenie

Rosnąca częstość występowania wielolekoopornych bakterii Gram-ujemnych, takich jak *Salmonella*, podkreśla konieczność zrozumienia mechanizmów oporności, będących podstawą do opracowania skutecznych metod zapobiegania i leczenia salmonellozy. Bakterie te wykorzystują szereg mechanizmów, w tym modyfikacje w obrębie osłon komórkowych, aby przeciwdziałać terapiom antybiotykowym i zwiększyć efektywność infekcji. W tym kontekście, błony bakteryjne, będące miejscem zakotwiczenia różnorodnych białek, odgrywają kluczową rolę. Jednym z takich białek o wysokim potencjale badawczym jest SanA, związane z opornością na wankomycynę i potencjalnie uczestniczące w początkowych fazach infekcji.

W ramach pracy doktorskiej przeprowadzono kompleksową analizę właściwości i funkcji biologicznej SanA. Celem było zrozumienie, jak SanA wpływa na charakterystykę błon *Salmonella*, skutkując w fenotypie oporności bakterii na stresory środowiskowe. W tym celu wykorzystano szereg testów funkcjonalnych z użyciem mutanta z delecją *ΔsanA*, aby ocenić cechy błon takie jak ładunek, hydrofobowość i przepuszczalność. Przeprowadzono również rozległą analizę fenotypową z udziałem 240 ksenobiotyków. W ramach projektu analizie poddano także poziom ekspresji SanA i jego lokalizację subkomórkową, wykorzystując techniki takie jak pomiar aktywności lucyferazy w konstrukcie fuzyjnym oraz frakcjonowanie i immunoblotting. Ponadto, na podstawie rezultatów testów inwazyjnych, wykorzystano system reporterowy, celem zbadania korelacji SanA z Wyspą Patogenności Typu I (SPI-1).

Wykazano, iż SanA jest białkiem błony wewnętrznej, którego brak skutkuje zwiększoną przepuszczalnością błony, jej hydrofilowością i dodatnim ładunkiem, co powoduje zmienioną oporność na antybiotyki, których celem działania są osłony bakteryjne. Delecja *sanA* związana jest również z podwyższonym poziomem replikacji *Salmonella* w makrofagach, sugerując zmniejszoną wrażliwość na składowe układu immunologicznego gospodarza. Ponadto wykazano, że mutacja ta w bakteriach we wczesnej fazie stacjonarnej wzrostu, znacznie zwiększa ich inwazyjność, częściowo korelując z nadekspresją SPI-1, która z kolei zależna jest od dostępności składników odżywczych.

Podsumowując, niniejsze badania podkreślają znaczenie SanA w regulowaniu odpowiedzi *Salmonella* na stres środowiskowy. Obejmuje to kluczową rolę w inwazji, namnażaniu w organizmie gospodarza oraz oporności na ksenobiotyki, co podkreśla znaczenie białek błony wewnętrznej w zrozumieniu złożoności procesu patogenezy pałeczek *Salmonella*.

1. Introduction

In 1885, American veterinarians Theobald Smith and Daniel Elmer Salmon, discovered a new bacterium during their investigation of Classical Swine Fever (CSF), commonly known as swine cholera. Initially, this bacterium was named "Bacillus cholerae suis" (1). By the turn of the century, in 1900, French bacteriologist Lignières reclassified these bacteria, acknowledging their distinct nature and establishing them as a separate genus. To honor one of its discoverers, he named the genus *Salmonella* (1).

Current data from numerous countries indicate that *Salmonella* ranks as one of the most common bacterial pathogen transmitted through food. The increase in global travel and the heightened interconnectivity of nations significantly contribute to the spread of these bacteria, resulting in a higher number of foodborne diseases. The transmission of *Salmonella* via food and agricultural products, especially those exposed to contaminated manure, leads to a greater number of individuals harbouring the pathogen asymptomatically. Such trends pose major health threats, have potential economic consequences, and emphasize the importance of monitoring these microorganisms.

1.1. Taxonomy and serological classification

Salmonella is a genus within the *Enterobacteriaceae* family, comprising a rod-shaped, facultatively anaerobic bacteria. These Gram-negative bacteria, which are catalase-positive and oxidase-negative, typically exhibit motility. They do not form spores and are generally sized between 0.7-1.5 µm in width and 2.0-5.0 µm in length. *Salmonella* colonies usually measure about 2-4 mm in diameter (2).

Currently, the nomenclature system used by the Centers for Disease Control and Prevention (CDC) for the genus *Salmonella* is based on recommendations from the World Health Organization Collaborating Centre (WHO), which is responsible for the updating of the scheme every year. At this time, two primary species are recognized within this genus: *S. enterica* and *S. bongori*. The former is further divided into six subspecies: I. *S. enterica* subsp. *enterica*; II. *S. enterica* subsp. *salamae*; IIIa. *S. enterica* subsp. *arizonae*, IIIb. *S. enterica* subsp. *diarizonae*, IV. *S. enterica* subsp. *houtenae,* and VI. *S. enterica* subsp. *indica* (**Fig. 1**) (3). Most serovars pathogenic to humans and warm-blooded animals belong to the *S. enterica* subsp. *enterica* (I), while the other five subspecies are most commonly found in the environment or in cold-blooded

animals. Each subspecies can be further categorized into various serotypes or serovars under the White-Kauffmann-Le Minor scheme (4). This classification is based on the differences and combinations of antigens found in capsular polysaccharides (Vi antigen), lipopolysaccharides (O antigen), and flagellar proteins (H antigen). Out of the over 2,600 serovars currently identified in the genus, about 99 % are associated with *S. enterica* and share a DNA sequence similarity ranging from 96-99 % (5).

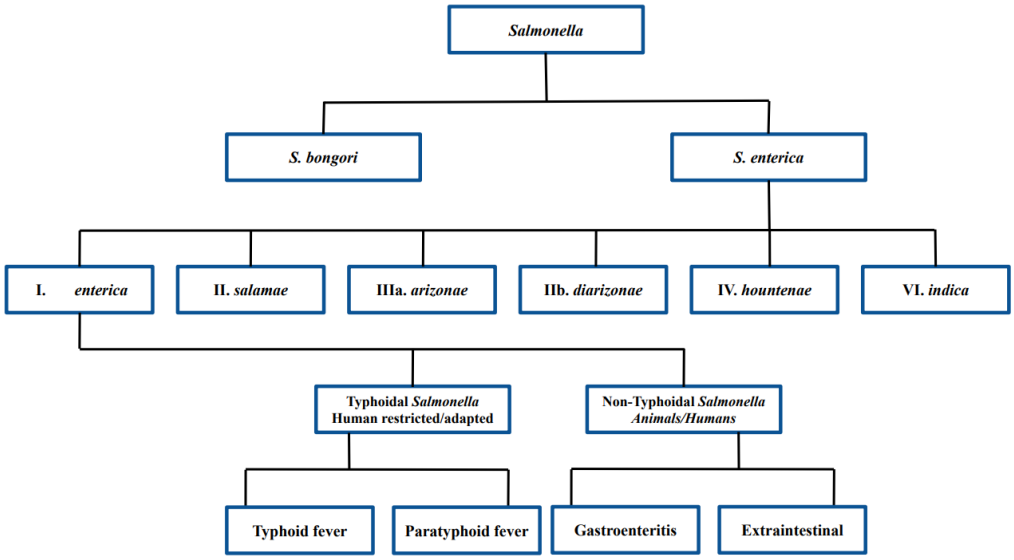

Fig. 1 Taxonomy and classification of *Salmonella* (3)

Each serovar is characterized by varying degrees of host adaptations and can be classified into one of the following groups: host-restricted specialists; host-adapted specialists or host-unrestricted generalists (6). The former group includes serotypes that trigger diseases in a limited range of closely related species. For instance, *S.* Typhi and *S.* Paratyphi are exclusively linked to systemic diseases in humans. Similarly, *S.* Gallinarum and *S.* Pullorum are specific to poultry, while *S.* Abortusovis affects sheep and *S.* Abortusequi targets equine species. Host-adapted specialists are predominantly adapted to a specific host species, yet they are capable of infecting others as well. For example, *S.* Choleraesuis mainly causes systemic disease in pigs, and *S.* Dublin is primarily associated with cattle. However, these serotypes can also infect and cause disease in various other hosts, including humans. Most serovars, including *S.* Enteritidis and *S.* Typhimurium, belong to host-unrestricted generalists and are capable of infecting different hosts, which makes them a major causes of foodborne diseases globally (6, 7).

Based on clinical patterns, there are two types of salmonellosis identified: typhoidal, caused by serotypes *S.* Typhi and *S.* Paratyphi, and non-typhoidal (NTS) caused by other serotypes (8). *S.* Typhimurium is responsible for nontyphoidal food poisoning with gastrointestinal symptoms. However, in some cases, potentially life-threatening bacteremia has been observed (9).

For a deeper analysis of taxonomy and pathogenesis, serotypes are subdivided into biotypes and phagotypes. The term 'biotype' refers to the biochemical variations, whereas 'phagotype' denotes the varying levels of susceptibility to bacteriophage lysis among organisms of a particular serotype (10).

1.2. *Salmonella* as zoonose with antimicrobial resistance threat

S. enterica ranks as the second most reported zoonotic gastrointestinal pathogen, causing significant illness and associated costs in human societies. Annually, there are approximately 93.8 million human salmonellosis cases worldwide, resulting in 155,000 deaths (11). Most of these cases (85.6 %) are linked to foodborne sources (12). The economic impact of human salmonellosis is substantial, with costs averaging over $1,000 per case of diarrheal illness. In the United States, the CDC recognized *Salmonella* as the second most common source of foodborne diseases, after *Campylobacter*. It accounts for 56 % of hospitalizations and is responsible for 33 % of both outbreaks and individual cases of illness (13). Similarly, the EFSA (*European Food Safety Authority*) reported it as the second most common zoonosis in Europe, with 91,662 confirmed cases, 18.3 % of which required hospitalization and a fatality rate of 0.25 % (7). Despite a decrease in incidents since 2008, *Salmonella* remains the leading cause of foodborne outbreaks in the EU. It is important to acknowledge that these statistics likely represent only a fraction of the actual cases, as a considerable number of them are not reported.

Salmonella is commonly found in environments like water and soil, where it can survive for extended periods (14). Importantly, the intestinal tracts of various domestic and wild animals serve as typical reservoirs for *Salmonella*, leading to diverse food sources being implicated in infections. Vectors such as rats, flies, and birds can carry *Salmonella,* shedding it in their feces for weeks or months (14). The broad range of environments that can harbor *Salmonella* and its presence in multiple species of animals create several transmission pathways (15). Monitoring these bacteria in wild and food-producing animals is therefore crucial, as these animals are key in transmitting the bacteria into the human food chain. It is necessary to highlight that controlling salmonellosis is challenging due to numerous exposure areas. A primary route of

human infection is through contaminated food, including undercooked or improperly washed poultry meat, eggs, and egg products or fruits. Nevertheless, infections are also acquired through direct or indirect animal contact at homes, in veterinary offices, zoos, farms, or other public and private places (14, 15). *S*. Typhimurium is frequently linked to contaminated pork, poultry, and bovine meat, while *S*. Enteritidis is most often associated with contaminated eggs and broiler meat. *S*. Typhimurium contributed to the pandemic of food-borne salmonellosis in humans, partly because it can contaminate eggs while the birds are infected asymptomically (16).

Given the high level of cases around the world *Salmonella's* ability to survive under diverse conditions, adaptability to new environments, and capacity for facultative intracellular survival and replication, make the prevention and treatment of salmonellosis more challenging. It often leads to an over-reliance on antibiotic therapies, especially in less developed countries. Consequently, this results in global selective pressure from antimicrobial therapy and a crisis of antibiotic resistance. According to certain models, antimicrobial resistance could lead to as many as 10 million deaths per year globally in the human population by 2050 (17). The development of this phenomenon is largely a consequence of using the drugs in food-producing animals for treatment, prevention, or as production enhancers (18). Despite regulations intended to limit antimicrobial usage in food animal production, there has been a significant increase in the occurrence of resistance in non-typhoidal *Salmonella* over recent years. The most pressing issue now is *S*. Enteritidis and *S*. Typhimurium (7). **Table 1** summarizes the most important classes of antibiotics with the targets of action and examples of the resistance mechanism among these serovars.

Pathogenic bacteria have developed various defense mechanisms to withstand different environmental challenges, including exposure to xenobiotics. These mechanisms include: (I) efflux pumps, which eliminate drugs from bacterial cells, thus reducing their concentration to non-toxic levels and causing loss of potency; (II) antibiotic inactivation by bacterial enzymes that alter or degrade antibiotic structures; (III) target site modification by spontaneous mutation and changing the chemical structure of their molecular targets; and (IV) preventing drug entry by altering bacterial membrane compositions (19) (**Table 1**). Their phenotype is also associated with acquiring mobile genetic elements, including plasmids with various replicons, such as ncP, HI2, A/C, FIIs, FIA, FIB, and I1which are often linked to multidrug resistance (MDR) (20, 21).

Typical antibiotics for treating non-typhoidal *Salmonella* infections in adults include ciprofloxacin, amoxicillin, ceftriaxone, ampicillin, and trimethoprim-sulfamethoxazole (22). With the reduced effectiveness of ampicillin and trimethoprim in the 1980s, quinolones gained

popularity in treating salmonellosis, subsequently leading to heightened ciprofloxacin resistance and the rise of MDR strains (21). In 2020 the group of Nadi et al. showed complete ampicillin resistance in all *S*. Typhimurium strains from sick patient feces. Conversely, these strains remained sensitive to ciprofloxacin and nalidixic acid (22). Although various reports indicate the sensitivity of non-typhoidal *Salmonella* strains to ciprofloxacin, an observed rise in the minimum inhibitory concentration (MIC) for fluoroquinolones poses a considerable challenge in epidemiology (23). Importantly, plasmid-mediated quinolone resistance determinants like *qnrABCDS*, *aac(6')lb-cr*, and *oqxAB* are more frequently observed (24).

A worrying trend identified by numerous researchers is the rise of extended-spectrum β-lactamase producers (ESBLs) in *S*. Enteritidis and *S*. Typhimurium strains. These ESBL-producing isolates can be a source of genes linked to antibiotic resistance and pathogenicity, leading to an increased number of hard-to-treat, resistant, and virulent bacterial infections (25). Qiao et al. reported that all of the 96 ESBL-producing strains isolated from chicken carcasses were resistant to ampicillin, and approximately 84 % showed resistance to nalidixic acid, with one-third being resistant to 11 different antibiotics (25). In a study by Ma et al., more than 60 % of clinical and food isolates of *S*. Enteritidis, which showed MDR to ampicillin, chloramphenicol, streptomycin, sulfamethoxazole, and tetracycline (ACSSuT), were found to possess ESBL genes. The same type of resistance, known as pentaresistance, was also identified in *S*. Typhimurium definitive type 104, which has been associated with global epidemics (16, 26).

Table 1 The summary of the most important classes of antibiotics with the target of action and examples of the resistance mechanism (27–31)

Antibiotic	Target of action	Mechanism of resistance
β-lactams	interrupt bacterial cell-wall formation as a result of covalent binding to penicillin-binding proteins (PBPs)	reduced access to the PBPs; reduced PBP binding affinity; and destruction of the antibiotic through the expression of β-lactamase
Aminoglycosides	inhibit membrane protein (bind to P10 protein in 30S ribosome complex)	enzymatic modification and inactivation of the aminoglycosides; increased efflux; reduced permeability; altered target site
Cephalosporins (2^{nd} and 3^{rd} generation)	inhibit enzymatic reaction required for stable cell wall synthesis (bind to PBPs)	altered membrane permeability; enzyme modifications (β-lactamases); alternation of target site (PBP)
Chloramphenicol	inhibits protein synthesis (binds to 50S ribosome to inhibit transpeptidation)	enzyme modification (chloramphenicol transacetylases)
Glycopeptides	inhibit the synthesis of peptidoglycan by binding to amino acids (d-alanyl-d-alanine) in the cell wall	altered target site
Macrolides	inhibit protein synthesis (bind the bacterial 50S ribosomal subunit)	target modification; efflux; enzymatic inactivation
Quinolones	bind topoisomerase II and block DNA replication; bind topoisomerase IV and interferes with separation of interlocked replicated DNA molecules	altered target site (mutations in topoisomerase II or IV); active efflux system
Trimethoprim-Sulfamethoxazole	interferes sequentially with folic acid synthesis	reduced permeability; insensitive target

The prevalence of MDR patterns in non-typhoidal *Salmonell*a isolates emphasizes that the challenge of antibiotic resistance is becoming increasingly evident and requires immediate action. In response, the FDA implemented the final rule (FVD rule) to gradually eliminate the use of antibiotics in production agriculture (32). This rule restricts the use of antibiotics that are clinically important for production purposes, and require veterinary supervision for their therapeutic use in livestock and poultry. In light of this, various alternatives such as phytobiotics, prebiotics, probiotics, metals, antimicrobial enzymes, and others are being explored to combat drug-resistant pathogens, due to their wide range of antimicrobial effects (33). These alternatives should be non-toxic, leave no residues in meat or eggs, be harmless to animals, remain stable in the gut, enhance beneficial gut flora, and neutralize harmful pathogens. They are also being evaluated for their potential to improve feed efficiency and growth, without negatively impacting the environment. Although research on using these methods against various *Salmonella* serovars is expanding, most studies are still in the early stages. More research is necessary to fill significant knowledge gaps before these methods can be recommended for enhancing food safety. There is a substantial challenge ahead in developing, optimizing, and scaling interventions to achieve the effectiveness and safety that antibiotics have provided over the past decades.

1.3. Pathogenesis and key virulence factors

The pathogenic mechanisms of *Salmonella* in humans are complex and multifaceted, largely dependent on factors such as the type of serovar involved, the strain's virulence, the infectious dose, the nature of the contaminated food, and the host's immune status. The infectious process typically begins with the oral ingestion of the bacteria, with an infective dose ranging from 10^3 to 10^7 cells. Once ingested, the bacteria encounter the acidic environment of the stomach, where approximately 99 % of them are eradicated. However, the resilient 1 % that survives, progresses into the small intestine, where it faces the antimicrobial effects of bile salts (34).

As *Salmonella* passes through the small intestine, peristalsis ensures that the majority of the bacteria remain within the gut lumen. Approximately 15 % of the surviving cells are retained in the small intestine, while the remainder are expelled in the feces (34). The bacteria that manage to persist in the intestine initiate the infection by adhering to the apical surface of the enterocytes, the cells lining the intestinal wall. Pathogens employ various surface structures such as flagella, apical appendages, and long polar fimbriae for this attachment, subsequently penetrating the intestinal wall to access the gut-associated lymphoid tissue (GALT) (34, 35).

Salmonella utilizes multiple pathways to invade the intestinal mucosa. The bacteria can be absorbed by antigen-sampling M cells, captured by phagocytes expressing CD18 in the lumen that penetrate the epithelial layer, or they can actively invade non-phagocytic enterocytes (36). Once inside non-phagocytic cells, *Salmonella* is enclosed in a phagosomal compartment, known as the *Salmonella*-containing vacuole (SCV). As the SCV matures, it moves towards the Golgi apparatus, selectively interacting with the host's endocytic pathway. Positioned near the cell nucleus, the SCV-enclosed bacteria multiply, developing tubulovesicular structures - *Salmonella*-induced filaments (Sifs) (37, 38). If the host's immune response fails to control the infection, clinical symptoms of gastroenteritis emerge, characterized by vomiting, fever, diarrhea, and abdominal cramps, typically appearing 12 to 72 hours after ingestion. These symptoms, which occur due to enterotoxins produced by the bacteria, are often self-limiting and generally resolve within a week (8).

Although most *Salmonella* infections remain localized within the intestines, triggering inflammatory reactions that cause diarrhea, in typhoid fever, *Salmonella* continues to survive in intestinal macrophages and disseminates to the liver and spleen through the bloodstream and lymphatic system (8). The subsequent dissemination of live bacteria and lipopolysaccharides (LPS or endotoxin) into the circulatory system can lead to septicemia. It is a critical condition associated with cardiovascular dysfunction, largely attributed to the impact of endotoxins on the neurovegetative centers of the ventriculus (39). Notably, in humans with compromised immune systems, even non-typhoidal *Salmonella* can lead to systemic diseases. It is estimated that up to 5 % of food poisoning cases may develop into invasive extraintestinal diseases leading to bacteremia (8). Moreover, individuals infected with *Salmonella*, particularly in the case of typhoid fever, can become asymptomatic carriers. These carriers excrete a large number of bacteria in their feces, posing a significant risk for the spread of infection to humans and livestock animals (40).

The complex, multi-stage infection process is controlled by the delivery of a variety of specialized effector proteins by *Salmonella* into eukaryotic host cells. This is achieved through clusters located on both its chromosomes and plasmids, referred to as *Salmonella* Pathogenicity Islands (SPIs). To date, researchers have identified and characterized 23 SPIs (41, 42). Of these, SPIs 1 to 5 are found in all *Salmonella* serotypes, while SPIs 19 to 23 are absent in *S*. Typhi and *S*. Typhimurium, only occurring in a few *S.* Dublin, Gallinarum, and Derby (43). Among SPIs 1 to 18, only SPI-1, 4, 9, 14, and 18 encode effectors crucial for the invasion of *Salmonella* into macrophages and epithelial cells. In turn, the virulence effectors secreted by SPI-2, 3, 5 to 8, 10 to 13, and 16 are essential for *Salmonella* to survive the acidic environment, facilitate

intracellular replication, and evade the host's immune system (43). The most important are SPI-1 and SPI-2 as they contain a substantial number of virulence genes related to intracellular pathogenesis (44, 45).

1.3.1. *Salmonella* Pathogenicity Island 1 (SPI-1)

SPI-1 is critical for the invasion of non-phagocytic host cells and plays a significant role in the inflammation-induced immune responses by *Salmonella*. The process involves injecting a set of effector proteins into the host cell, leading to cytoskeletal rearrangement and facilitating bacterial uptake through macropinocytosis. Once the SCVs are internalized into eukaryotic host cells, these proteins are vital for their growth and maturation (46).

Spanning nearly 40 kb, SPI-1 encodes a Type III Secretion System (T3SS), intricate macromolecular assemblies, which due to their ability to transfer proteins in a contact-dependent manner are often referred to as 'injectisomes' or 'molecular needles' (47). They comprise at least 20 different components and are found not only in *Salmonella*, but also in various Gram-negative bacteria, such as *Yersinia, Shigella, Escherichia coli*, and *Pseudomonas*. It has been shown that *Salmonella* lacking a functional SPI-1 T3SS are unable to invade epithelial cells in tissue culture, highlighting the critical role of this system in the bacterial invasion process (48).

Numerous effector proteins encoded by SPI-1 have been discovered in *Salmonella*. These proteins play diverse functions during the infection process, such as participating in the reorganization of the host's cytoskeletal structure, attracting immune cells, influencing cell metabolism, stimulating fluid secretion, and modulating the host's inflammatory response (49). During the invasion phase, key effectors like SopE, SopE2, and SopB influence the Rho-family small GTPases, altering signal transduction. SopE and SopE2 act as G-nucleotide exchange factors on CDC42 and Rac1 (50). Other effectors, such as SptP, mediate the restoration of the cytoskeleton, previously modified by SipA and SipC, through GTPase activity. SipA and SipC directly promote the polymerization and assembly of actin filaments (51).

The activation of SPI-1 is coordinated by the central transcription factor HilA, a member of the OmpR/ToxR family of transcription regulators (**Fig. 2A**) (52). The process is affected by a unique combination of environmental signals such as osmolarity, antimicrobial peptides, oxygen, pH, and other yet-unidentified signals (53). These signals are detected by two-component regulatory systems, including BarA/SirA, OmpR/EnvZ, PhoBR, and PhoPQ (52, 54, 55). The phosphorylated forms of these response regulators can either enhance or

inhibit SPI-1 expression by modulating the expression of HilD or HilE, respectively. PhoB, PhoP, and FimZY can stimulate *hilE* expression, which in turn can negatively affect *hilA* expression (56). HilD, in conjunction with HilC and RtsA, forms a feed-forward loop where each element can enhance its own expression as well as the expression of *rtsA, hilC,* and *hilA*, thereby boosting the signal significantly (57). Nucleoid-associated proteins HU and Fis are critical for the expression of *hilA*. HilA interacts with cis-elements in specific promoters, activating the *prg/org* and *inv/spa* operons within SPI-1. This activation leads to the production of InvF, a member of the AraC family of transcriptional regulators. InvF, along with the chaperone SicA, triggers the expression of a set of genes within SPI-1 and at various loci on the chromosome (**Fig. 2A**) (58). RtsA/HilD/HilC also activates the expression of *dsbA*, which is essential for the functionality of the T3SS encoded by SPI-1 as it is involved in the formation of periplasmic disulfide bonds which contribute to the proper folding and assembly of specific proteins (56).

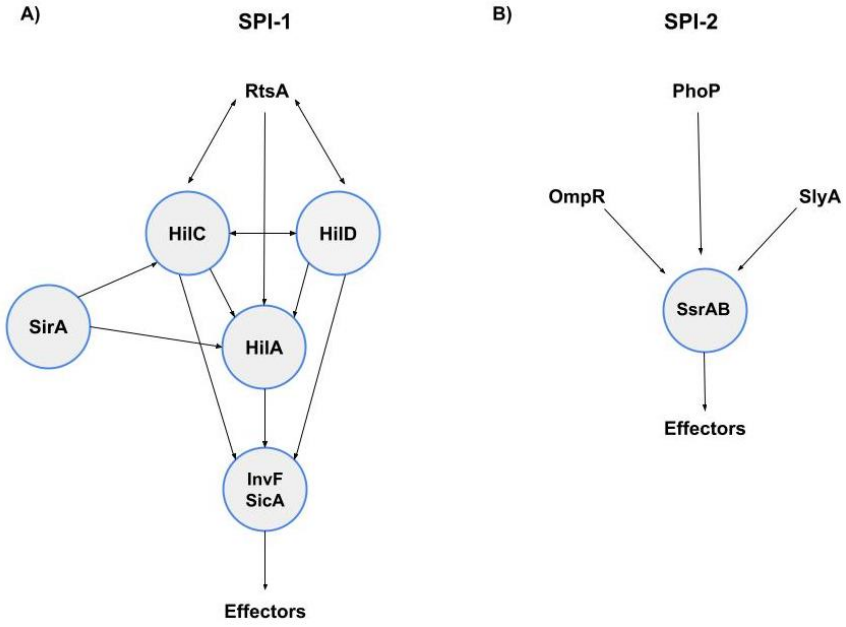

Fig. 2 Regulatory cascades activating the expression of SPI1 (**A**) and SPI2 (**B**) related type III effectors (59)

The expression of SPI-1 genes is coupled with the expression of flagellar genes (60). These genes encode a structure that enables bacteria to navigate through liquids and swarm over surfaces, enabling the connection with the host cells. Their regulation, similar to that of SPI-1

genes, is controlled by multiple transcription factors (61). The primary regulator of flagellar gene expression is $FlhD_4C_2$, which not only activates the expression of flagellar structural genes but also induces the expression of FliZ. FliZ indirectly regulates $FlhD_4C_2$ by repressing YdiV (also known as RflP), which binds to $FlhD_4C_2$, inhibiting the activation of class 2 flagellar promoters and promoting its degradation (62, 63). Significantly, FliZ is involved in the regulation of SPI-1 gene expression as well, by activating HilD via a post-translational mechanism that is not yet fully understood (64). Moreover, HilD can initiate the transcription of *flhDC*. Concurrently, RtsB, which is part of the same operon as RtsA, can inhibit the transcription of *flhDC* (65). These interrelated regulatory mechanisms serve to coordinate the expression of both SPI-1 and flagellar genes.

It is worth highlighting that not only genetic factors affect the T3SS activity. It was discovered that acetate and nutrients, supplied in the form of yeast extract, collectively enhance SPI-1 gene expression (60, 66). Each of these components can independently trigger SPI-1 gene expression, but their combined presence in the growth medium significantly improves it. Acetate is the predominant short-chain fatty acid in the distal small intestine, the primary site of *Salmonella* invasion. It is believed that *Salmonella* utilizes acetate as a signal to detect its presence in the small intestine. Acetate stimulates SPI-1 gene expression through the BarA/SirA two-component system (52). Yeast extract, in contrast, is a complex nutrient mixture known to induce flagellar gene expression via RflP (67). This induction is thought to result not from any specific metabolite in the yeast extract, but from the overall improved growth facilitated by these nutrients. Although the exact role of yeast extract in invasion remains unclear, the combined effect of acetate and yeast extract in synergistically boosting SPI-1 gene expression arises from transcriptional interplay with flagellar genes through the post-translational activation of HilD (64).

1.3.2. *Salmonella* Pathogenicity Island 2 (SPI-2)

SPI-2 is crucial for the survival inside macrophages and the establishment of a systemic infection by the formation and maintenance of the SCV. SPI-2 spans roughly 40 kb and consists of two separate regions. The larger region, about 25 kb, encodes T3SS-2, is exclusive to *S. enterica* and plays a role in systemic pathogenesis. The smaller region, about 15 kb was found in *S. bongori* and encodes the tetrathionate reductase (Ttr) which is involved in anaerobic respiration (46, 47). The T3SS-2 translocates proteins across the SCV membrane into the cytosol of the macrophages, where they perform a wide range of functions. Studies using

mutants lacking SPI-2, or those involving individual effectors, demonstrated that SPI-2 is essential for impeding various endocytic trafficking processes (68). This includes preventing the fusion of lysosomes with SCV, evading the NADPH oxidase-dependent killing mechanisms of macrophages, delaying apoptosis-like cell death, managing the dynamics of the SCV membrane, and orchestrating the formation of an F-actin meshwork around the SCV. Furthermore, SPI-2 is involved in accumulating cholesterol around the SCV and disrupting the localization of inducible nitric oxide synthase to the SCV. These varied functions suggest the involvement of multiple different effector proteins (46, 68).

Seventeen effectors are known to be translocated through the SCV membrane into the host cell cytoplasm, with most encoded outside the SPI-2 locus (69). Only three of these effectors, including SpiC, SseF, and SseG, are encoded within SPI-2. The SPI-2 translocated proteins such as SifA, SifB, SseJ, SopD2, PipB, and PipB2 are located on the SCV surface, contributing to either tubulation or other phagosome modifications (70).

The regulation of SPI-2 gene expression is controlled by a global regulatory system, specifically the SsrAB system (**Fig. 2B**). This is a classic two-component system essential for the expression of the SPI-2 regulon in intracellular bacteria. Key global regulatory systems influencing SPI-2 gene expression levels include the EnvZ/OmpR and PhoPQ two-component systems, along with SlyA and Fis (**Fig. 2B**) (54, 71). They induce SPI-2 expression in response to the acidic pH and poor nutrient level in the lumen of the SCV (71).

Recent findings indicated that the expression of SPI-1 and SPI-2 genes and their functions at various stages of the infection process are not as isolated and specific to certain niches as was previously believed. The study of Bustamante et al. uncovers a transcriptional interaction between SPI-1 and SPI-2, in which the SPI-1–encoded regulator HilD is crucial for activating both regulons at varying times during the stationary growth phase in the Luria-Bertani medium (72).

1.4. Cell envelope – composition and role in pathogenicity

Bacteria must adapt to an environment that is often unpredictable and resource-limited. To survive under these conditions, they have developed a complex and highly specialized cell envelope. This structure not only provides protection but also facilitates the selective passage of nutrients from the outside and the removal of waste products from the inside (73). Given the diverse functionalities of the bacterial envelope, Gram-negative pathogens utilize various modifications to the membranes, aiming to enhance their resilience to environmental stress and

to successfully establish infections. For instance, *Enterobacteriaceae* have been shown to decrease porin expression as a quick response to toxic agents (74). Additionally, they modify LPS to alter the characteristics of the outer membrane, which helps in avoiding recognition by the host's immune system and enhances their resilience to antimicrobial peptides. These modifications include altering lipid A phosphates, the core oligosaccharide phosphates, and lipid A acylation (75). Further adding to the complexity, other membrane attributes, such as charge and hydrophobicity, modulate bacterial resistance to external stresses and were shown to affect pathogenicity indirectly. It has been demonstrated that the efficiency of phagocytosis increases with the hydrophobicity of bacterial cells and that hydrophilic bacteria resist ingestion by phagocytes (76).

The layered structure of the Gram-negative cell envelope was first clearly demonstrated in 1969 by Glauert and Thornley who identified its three principal compartments; the outer membrane (OM), the peptidoglycan cell wall, and the cytoplasmic or inner membrane (IM) (**Fig. 3**) (77).

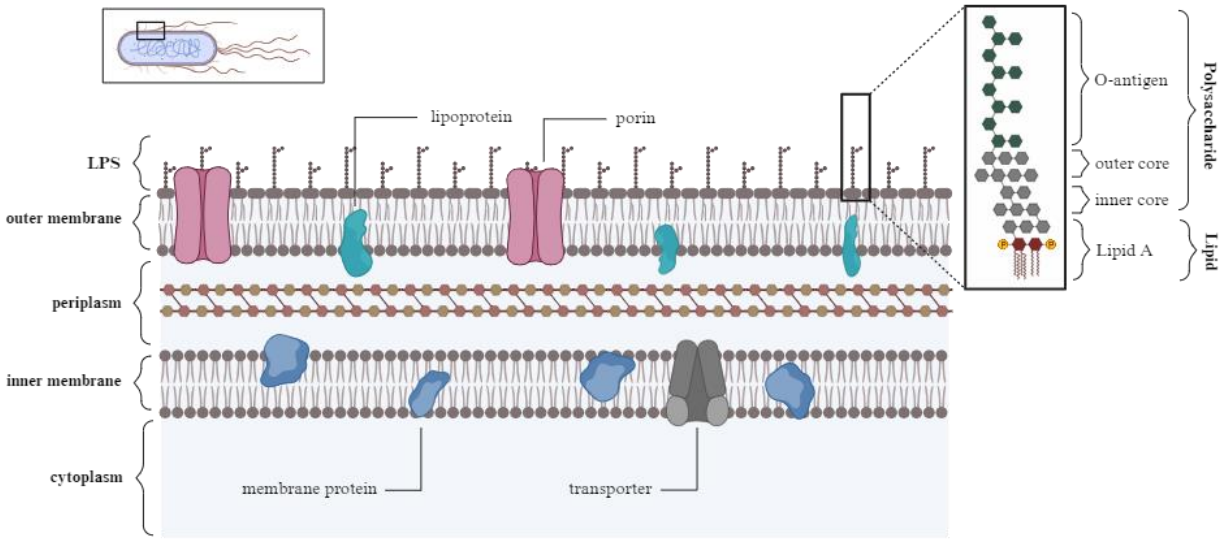

Fig. 3 Gram-negative bacterial cell wall with the structure of lipopolysaccharide (prepared in *BioRender*)

1.4.1. Outer membrane

Beginning at the outer surface and moving inwards, the first layer encountered is the OM. This membrane sets Gram-negative bacteria apart from Gram-positive ones, which lack that

structure (78). The OM, is a lipid bilayer, similar to other biological membranes. However, in the OM, phospholipids are found only in the inner leaflet, while the outer leaflet is mainly composed of glycolipids, especially LPS (79). LPS typically consists of three structural domains: Lipid A, which includes fatty acids linked to N-acetylglucosamine, core polysaccharide (inner and outer), and O-specific polysaccharide (**Fig. 3**). The LPS layer forms a non-fluid barrier, highly effective against hydrophobic molecules and is crucial for causing endotoxic shock in septicemia, triggering the human innate immune system (80).

The OM additionally comprises lipoproteins and a variety of outer membrane proteins (OMPs). The former group has lipid parts attached to a cysteine residue at their N-terminus, whose role is to anchor the lipoproteins in the OM's inner leaflet, rather than spanning across the whole membrane (73). In Gram-negative bacteria, there are more than 90 different OM lipoproteins, with most of their roles still being investigated (81). The OM's integral proteins, in turn, usually display a cylindrical structure known as a β-barrel, extending across both the inner and outer leaflets. These porins facilitate the movement of numerous small hydrophilic molecules (under 600 Da) from the environment to the periplasmic space via passive diffusion serving as a selective permeability barrier (81). Conversely, larger molecules exceeding 0.6 kDa or those present in low concentrations, such as Vitamin B12 or siderophores are transported through an energy-dependent active uptake process, such as the TonB system. The TonB-dependent receptors facilitate the transport of specific substrates across the outer membrane, drawing on energy from the proton motive force. The energy for this process is relayed by the TonB−ExbB−ExbD complex (TonB complex) situated in the inner membrane (82). TonB system, with passive transporters and substrate-specific channels, also plays a role in the transport of nutrients (82).

The proximity to the external environment makes OM a key site for a large number of environmental sensors and an anchor point for attachment structures (83). The OM serves as a crucial interface for interactions with the host immune system and other bacterial cells, either through direct surface contact or via vesicles. Additionally, the OM acts as a significant barrier to many large and hydrophobic antibiotics that are otherwise effective against Gram-positive bacteria, contributing to the resistance of Gram-negative bacteria to these antibiotics (84). This resistance poses a considerable threat to human health and has been a major obstacle in the development of new antibiotics. The OM also functions as a barrier to large molecules like antibodies and phages, preventing them from binding to surface targets (85). Although the barrier function of the outer membrane (OM) is significant, this alone does not fully explain its essential nature, considering that this compartment contains only a few enzymes. These include

a phospholipase (PldA), a protease (OmpT), and an enzyme-modifying LPS (PagP) [72]. In fact, the only essential proteins in the OM are those necessary for building this compartment.

1.4.2. Peptidoglycan

Peptidoglycan (murein) is a polymer that forms part of the cell wall surrounding the cytoplasmic membrane of most bacteria. The OM is anchored to the peptidoglycan layer by a lipoprotein known as Lpp, also referred to as murein lipoprotein or Braun's lipoprotein (86). Murein is composed of N-acetylglucosamine (GlcNAc) and N-acetylmuramic acid (MurNAc) residues linked by β-1,4 bonds, further cross-linked by short peptides (81). Bacterial peptidoglycans undergo various post-synthetic changes to strengthen their defense against antimicrobial substances and to protect pathogens from degradation by host factors (87, 88). Besides differences between species, the composition of peptidoglycan can also change within a single species, influenced by factors like the stage of growth and external environmental conditions. The diversity in peptidoglycan composition among different bacteria has been extensively documented (87, 89). Examples of this diversity include alterations in glycan chains, peptide stems, and the nature of peptide cross-links (89).

The biosynthesis of peptidoglycan is a complex process comprising about 20 enzymatic reactions that occur both in the cytoplasm and on the inner and outer sides of the cytoplasmic membrane (90). Any disturbances in the structure of peptidoglycan can lead to cell lysis, which is why the biosynthesis of this structure is often the target of antibiotics. Indeed, the murein is crucial for the survival of microorganisms (90).

One of the most important feature of murein is rigidity, which provides a species-specific shape, cell integrity, and protection against osmotic lysis. Additionally, the porosity of peptidoglycan allows the diffusion of nutrients, virulence factors, and facilitates signal transduction (81).

1.4.3. Periplasm

Periplasm is an aqueous space created by the OM and IM. This compartment is densely filled with proteins and possesses a higher viscosity compared to the cytoplasm (91). This compartmentalization in Gram-negative bacteria is crucial for isolating potentially harmful enzymes, like RNAse or alkaline phosphatase (73). The periplasm's unique functions are also similar to those of the endoplasmic reticulum in eukaryotic cells, involving protein transport,

folding, and oxidation. Furthermore, the periplasm enhances the cell's resistance to turgor pressure through structural components like peptidoglycan and lipoproteins, working in tandem with the outer membrane. This includes multidrug efflux systems and specific solutes that maintain an ionic potential across the outer membrane. Additionally, the periplasm contains assembly platforms for secreting distinct beta-barrel proteins, lipoproteins, and glycerolphospholipids to the outer membrane (92).

1.4.4. Inner membrane

The IM separates the periplasm from the cytoplasm. It consists of a phospholipid bilayer, primarily made up of phosphatidyloethanolamine (75 %) and phosphatidyloglycerol (15-20 %). It also contains a smaller amount (5-10 %) of phosphatidyloserine or cardiolipin, and minor lipids such as polyisoprenoid carriers (C55), which are essential for the transport of activated sugar intermediates necessary for the formation of the envelope (93). The lipid composition of a bacterial membrane plays a critical role in determining its properties and functionality, contributing to its fluidity, permeability, and overall structural integrity (94, 95). Beyond lipids, the IM contains approximately 25 % of all cellular proteins, which are crucial for various functions like the translocation of small molecules and proteins, chemotaxis and motility, respiration, and energy production (96). Keeping in mind a high diversity of inner membrane proteins, the function of many of them remains unknown or uncertain even in *E. coli*. One such protein is SanA, as described in the further part of this work.

Unlike the OM, the IM is semi-permeable due to its amphipathic nature and the absence of unregulated protein channels like the porins in the OM. The transfer of molecules between the periplasm and cytoplasm is highly selective, necessitating active, energy-driven transport across the IM via specialized transport systems composed of α-helical integral IM proteins (81). There are three types of transport systems in the IM: (1) Simple transporters, which do not modify the substrate during transport; these include uniporters that transport only the substrate across the IM; symporters that co-transport a second molecule with the substrate in the same direction, like LacY, and antiporters that transport a second molecule in the opposite direction to the substrate, such as the Na+/H+ antiporter NhaB in *E. coli;* (2) Group translocators, where the substrate undergoes chemical modification during transport, and (3) ABC-transporters, such as the maltose transport system, which involve multiple proteins and several steps. They include the binding of the substrate by a periplasmic protein, transfer to the IM transporter and translocation and release of the substrate through the IM transporter, coupled with ATP

hydrolysis by an ATPase (81, 97, 98). ABC-transporters are one of the groups within drug efflux pumps. They comprise six families, each distinguished by structural differences and variations in coupling energy. In addition to ABC-transporters, this group also includes the MF (major facilitator), RND (resistance-nodulation-division), MATE (multidrug and toxic compound extrusion), SMR (small multidrug resistance), and the more recently identified PACE (proteobacterial antimicrobial compound efflux) family (99). While the study of efflux pumps in bacteria often focuses on their contribution to MDR, emerging research highlights their broader roles. Evidence of this has been seen in studies with *Salmonella*, where strains deficient in efflux pumps, demonstrate their crucial function in the pathogenicity of bacteria using a mouse model (100).

The primary role of the bacterial cytoplasmic membrane is to act as a selective barrier. This membrane is crucial for retaining vital metabolites and macromolecules within the cell, actively transporting nutrients into the cell against concentration gradients, and blocking the influx of specific environmental compounds. The cytoplasmic membrane's barrier function is particularly vital for the cell's energy transduction processes (73).

1.5. SanA – the current state of knowledge

In 1998, Mouslim et al. identified *sfiX* as a gene responsible for the pleiotropic response of the HisC *S*. Typhimurium strains (101). Further analysis showed it was an ortholog of the *sanA* in *E. coli*, with approximately 97 % identity of nucleotide sequence. This gene was positioned downstream of the encoding cytidine deaminase *cdd*, thereby creating a conserved *cdd-sanA* (*cdd-sfiX*) operon in *E. coli* and *S*. Typhimurium, respectively (101). The *sanA* encodes a protein with a molecular weight of ~20 kDa, composed of 239 amino acids (102). This molecule includes a cytoplasmic domain, which comprises six amino acids, a transmembrane helix, and a segment located in the periplasm. Within the periplasmic part, SanA harbors a DUF218 domain designated as the domain of unknown function (103). DUF218 domains contain multiple charged amino acids, implying potential enzymatic activity, and are prevalent across various bacterial species. In *E. coli*, there are four proteins containing this domain: SanA, ElyC, YgjQ, and YdcF, however, their functions are not fully understood (104). It is believed that all of them (except YdcF) are integral membrane proteins with periplasmic domains.

To analyze the role of the *sanA* in *E. coli*, Rida et al. used a vancomycin-sensitive mutant that also exhibited other properties typical to defects in outer membrane permeability: sensitivity to SDS, MacConkey agar components, ethidium bromide, cold (18°C), and

hypersensitivity to kanamycin and chloramphenicol (102). Their research showed that overexpression of *sanA* restores resistance to vancomycin and also negates sensitivity to SDS. The analyzed mutant was transformed with two different plasmids (pJRD9.5 and pJRD1) carrying the *sanA* insert, but only one of them (pJRD1) eliminated sensitivity to MacConkey components. These results suggest that the SanA does not affect the mechanism of antibiotic action, sequestration, modification, or targeting blockage but has a more general effect on barrier functions or the formation of bacterial cell envelopes. Furthermore, other permeability mutants with similar phenotypes were also transformed with the same plasmids, but no defect was reversed by *sanA* overexpression (102). Similar effects of the gene defect is observed in the *tolA* deletion mutant. The TolA protein, anchored in the inner membrane, maintains the integrity of the cell envelopes by interacting with the inner part of the outer membrane (105, 106). A *tolA* gene defect also leads to bacterial sensitivity to vancomycin and detergents, indicating that *sanA* might perform a similar function.

Additionally, Rida et al. constructed a mutant *sanA*::Tc by replacing *sanA* with a cassette conferring tetracycline (Tc) resistance. The fact that the strain carrying the damaged allele in the wild-type gene's loci could grow, indicates that the *sanA* is not essential for survival. Moreover, growth inhibition of *sanA*::Tc mutants at 43°C, but not at 42°C, in the presence of vancomycin was observed (102). Therefore, it could be concluded that the SanA is a protein expressed only in stress conditions such as high temperature. Alternatively, *sanA* might encode a broad-specificity transporter, normally not expressed but activated only under extreme conditions or artificial expression from a plasmid. It is worth noting however that the Panther database's classification of SanA as a potential permease may not align with biological reality, given that SanA has only one transmembrane helix (107). The same database assigns a similar classification to YdcF, a cytoplasmic protein containing a DUF218 domain (107).

The location of the C-terminus of the SanA in the periplasm, a place of cell wall synthesis, suggests its role in blocking the activity of vancomycin at its site of action (101). The hydrophobic nature of this protein, meanwhile, implies its involvement in the barrier functions of bacterial cell envelopes (102). The inactivation of *sanA* in *S.* Typhimurium also eliminates the cell division defect induced by overproduction of HisHF (imidazole glycerol-phosphate synthase), further suggesting the role of *sanA* in cell envelope biogenesis (108). HisHF catalyzes the formation of imidazole glycerol phosphate, releasing a purine precursor known as AICAR. The synthase subunits are HisH and HisF – two polypeptides encoded by the histidine operon of enteric bacteria. In *S.* Typhimurium, overexpression of HisHF triggers a complex pleiotropic response, characterized by inhibition of cell division, sensitivity to osmotic pressure,

and loss of methionine at 42°C. A similar response is observed in *E. coli* following HisHF overproduction. Besides *hisH* and *hisF*, the HisC pleiotropic response requires the involvement of loci unrelated to histidine biosynthesis. These genes are homologous to *rfe* and *sanA* found in *E. coli*. Both Rfe and SanA functions appear to inhibit cell division (101).

Contrary to the abovementioned studies, our previous research from 2021 showed that a 10-nucleotide deletion in the *sanA* gene in the *S*. Enteritidis 6203 impairments the bacteria's ability to survive in the presence of vancomycin at 37°C (109). Complementation of this mutation with the full sequence of this gene from the *S*. Enteritidis PT4 P125109 caused a reduction of the vancomycin resistance (from 62.5 μg/ml to 31.25 μg/ml). Moreover, both the strain containing the wild variant of the gene and the mutant were tested for adhesion and invasion on the human cell line Caco-2. The results showed that complementing the 6203 strain with the unmutated version of the *sanA* reduced invasiveness 20 % compared to the strain with the deletion, indicating the contribution of SanA to initial stages of *Salmonella* infection (109).

Although SanA is speculated to be involved in the synthesis of bacterial cell walls or to serve as an efflux pump in response to extreme conditions like cold/heat shocks or bile exposure, these functions have not been conclusively established. In this context, identifying the exact location of a protein within a cell would be essential for the understanding of its role. Indeed, it was shown the subcellular localization of bacterial proteins has a significant impact on their function as it determines interactions with other cellular components. Nevertheless, the SanA subcellular localization has not been confirmed experimentally, and various *in silico* predictions provide inconsistent results. Furthermore, the influence of SanA on the membrane characteristics is yet to be investigated, and the link between changes in the physicochemical properties of the cell envelope and the effect on environmental stress, including antibiotic treatment, remains unclear. Likewise, the specific mechanism by which SanA contributes to infection processes is still unknown.

The research on the *sanA* represents a significant breakthrough in understanding bacterial physiology and forms the basis of this PhD dissertation. It explores the interplay between bacterial genetics, membrane physiology, antibiotic resistance, and host-pathogen interactions, underscoring its significance in understanding *Salmonella* pathogenicity. Each feature sheds light on vital processes and alongside cognitive aspects, paves the way for novel interventions in these fields.

2. Research objectives

The aim of the study designed and carried out as part of the doctoral dissertation was to investigate the role of *sanA* in *Salmonella* pathogenicity. Its implementation involved the following stages:

1. Generation and characterization of a *sanA* deletion mutant strain.
2. Investigation into the role of *sanA* in xenobiotic resistance.
3. Examination of the impact of *sanA* on the physicochemical properties of the bacterial membrane.
4. Determination of SanA subcellular localization.
5. Evaluation of environmental factors influencing *sanA* expression.
6. Investigation of the *sanA* role in invasion and intracellular survival using *in vitro* models.
7. Analysis of the correlation between SanA and *Salmonella* Pathogenicity Island 1 (SPI-1).

3. Hypotheses

Considering the preliminary data and existing literature, the following research hypotheses have been proposed:

H1: SanA, as an inner membrane protein, enhances membrane integrity and influences the physicochemical properties of the bacterial cell envelope, such as hydrophobicity and surface charge.

H2: These alterations contribute to *Salmonella'*s response to environmental stress, particularly by modulating sensitivity to certain classes of antibiotics targeting cell envelope and by enhancing intracellular survival within phagocytic cells.

H3: SanA plays a role in the early stages of *Salmonella* infection, as its deletion leads to increased invasiveness in mammalian cell models.

H4: The observed infection phenotype of the deletion mutant is a consequence of heightened membrane permeability, which facilitates greater access to nutrients, upregulating the expression of SPI-1, a critical virulence factor of *Salmonella*.

4. 1st manuscript

4.1. Foreword to the 1st manuscript

A) Rationale of research objectives and hypotheses

While it is speculated that SanA may be linked to bacterial cell wall synthesis or act as an efflux pump in response to harsh conditions, experimental evidence for these roles is still lacking (**Chapter 1.5**). Furthermore, the influence of SanA on membrane properties remains unexplored, and the correlation between physicochemical changes in the envelope and their subsequent effects on xenobiotic resistance has not been investigated (**Chapter 1.5**).

Given the abovementioned, the research objective of **M1** was to address hypotheses **H1** and **H2**, which indicate that the deletion of *sanA* alters the membrane permeability in *Salmonella*, leading to changes of its physicochemical properties. We also suggest that these changes may influence the bacterium's resistance to various antibiotics and potentially enhance its capacity for replication within primary macrophages. This understanding provides insights into the mechanism of antibiotic resistance and potentially guides the development of more effective methods of prevention and treatments.

B) Methodology and techniques

- Generation of *sanA* gene deletion mutant in *S.* Typhimurium 4/74 (4/74WT) strain by recombineering antibiotic resistance cassette into the locus of *sanA* gene,
- Characterisation of the newly-created mutant by comparison of growth rate between 4/74WT and 4/74*ΔsanA* in LB medium and cell line infection medium,
- Cloning *sanA* into low copy expression plasmid pWSK29 and complementation of 4/74*ΔsanA* strain *in trans* with plasmid-encoded *sanA* gene and empty pWSK29 plasmid,
- Screening for chemical sensitivity with the use of Phenotype MicroArrays for Microbial cells with 4/74WT and 4/74*ΔsanA* strains,
- Confirmation of results from screens for selected chemical compounds with the use of minimal inhibitory concentrations tests with 4/74WT, 4/74*ΔsanA*, 4/74*ΔsanA*+pWSK29-*sanA,* and 4/74*ΔsanA*+pWSK29 strains,

- Examination of membrane permeability, surface charge, and hydrophilicity across the 4/74WT, 4/74*ΔsanA*, 4/74*ΔsanA*+pWSK29-*sanA* and 4/74*ΔsanA*+pWSK29 strains. It employed ethidium bromide/Nile red uptake for analysis of permeability; cytochrome c binding to assess surface charge; and hexadecane adhesion tests to evaluate hydrophobicity,
- Quantification of bacterial intracellular survival using gentamycin protection assays of 4/74WT, 4/74*ΔsanA*, 4/74*ΔsanA*+pWSK29-*sanA* and 4/74*ΔsanA*+pWSK29 strains on the mouse primary bone marrow macrophages (pBMDM) model.

C) Results

Our main findings demonstrated that:

- The absence of *sanA* results in a remarkably increased rate of ethidium bromide and nile red uptake, indicating a higher membrane permeability (**Fig. 3** in **M1**).
- Deletion of *sanA* displays significantly lower affinity to cytochrome (**Fig. 4A** in **M1**), and lower adhesion to hexadecane, suggesting a more positive charge and hydrophilicity of the membrane (**Fig. 4B** in **M1**).
- The *ΔsanA* strain exhibits improved growth in the presence of approximately 35 % of tested xenobiotics, grouped mostly as cell wall- and replication-associated antibiotics. The same strain demonstrates lower resistance to membrane-targeting and transcription and protein-associated antibiotics (fluoroquinolones, glycopeptides, nucleic acid analogues) (**Table 5, Fig. 2** in **M1**).
- The deletion mutant shows a significantly increased number of intracellular bacteria 24 h post-infection of primary bone marrow mouse macrophages (**Fig. 5B** in **M1).**

D) Conclusions

This study offers crucial understanding into the dynamics of antibiotic resistance, underscoring how alterations in membrane properties influence bacterial susceptibility to various xenobiotics and harsh hostile conditions. The insights regarding SanA's influence on membrane physicochemical properties shed a new light on the role of membrane proteins in *Salmonella*'s resistance to environmental stressors. Furthermore, the presented outcome emphasizes the need for additional investigation into the role of *sanA* in *Salmonella* infection.

4.2. Copy of the 1st manuscript

Aleksandrowicz A., Kolenda R., Baraniewicz K., Thurston T., Suchański J., Grzymajło K. Membrane properties modulation by SanA: implications for xenobiotic resistance in *Salmonella* Typhimurium. 2024. Frontiers in Microbiology. 4:1340143 doi: 10.3389/fmicb.2023.1340143

frontiers | Frontiers in Microbiology

TYPE Original Research
PUBLISHED 05 January 2024
DOI 10.3389/fmicb.2023.1340143

OPEN ACCESS

EDITED BY
George Grant,
University of Aberdeen, United Kingdom

REVIEWED BY
Yuanyuan Li,
Soochow University, China
Etienne Giraud,
Institut National de Recherche Pour L'agriculture, L'alimentation et L'environnement (INRAE), France
Changyong Cheng,
Zhejiang A&F University, China

*CORRESPONDENCE
Krzysztof Grzymajlo
krzysztof.grzymajlo@upwr.edu.pl

RECEIVED 17 November 2023
ACCEPTED 11 December 2023
PUBLISHED 05 January 2024

CITATION
Aleksandrowicz A, Kolenda R, Baraniewicz K, Thurston TLM, Suchański J and Grzymajlo K (2024) Membrane properties modulation by SanA: implications for xenobiotic resistance in *Salmonella* Typhimurium.
Front. Microbiol. 14:1340143.
doi: 10.3389/fmicb.2023.1340143

Membrane properties modulation by SanA: implications for xenobiotic resistance in *Salmonella* Typhimurium

Adrianna Aleksandrowicz[1], Rafał Kolenda[1], Karolina Baraniewicz[1], Teresa L. M. Thurston[2], Jarosław Suchański[1] and Krzysztof Grzymajlo[1]*

[1]Department of Biochemistry and Molecular Biology, Faculty of Veterinary Medicine, Wrocław University of Environmental and Life Sciences, Wrocław, Poland, [2]Department of Infectious Disease, Centre for Bacterial Resistance Biology, Imperial College London, London, United Kingdom

Introduction: Multidrug resistance in bacteria is a pressing concern, particularly among clinical isolates. Gram-negative bacteria like *Salmonella* employ various strategies, such as altering membrane properties, to resist treatment. Their two-membrane structure affects susceptibility to antibiotics, whereas specific proteins and the peptidoglycan layer maintain envelope integrity. Disruptions can compromise stability and resistance profile toward xenobiotics. In this study, we investigated the unexplored protein SanA's role in modifying bacterial membranes, impacting antibiotic resistance, and intracellular replication within host cells.

Methods: We generated a *sanA* deletion mutant and complemented it *in trans* to assess its biological function. High-throughput phenotypic profiling with Biolog Phenotype microarrays was conducted using 240 xenobiotics. Membrane properties and permeability were analyzed via cytochrome c binding, hexadecane adhesion, nile red, and ethidium bromide uptake assays, respectively. For intracellular replication analysis, primary bone marrow macrophages served as a host cells model.

Results: Our findings demonstrated that the absence of *sanA* increased membrane permeability, hydrophilicity, and positive charge, resulting in enhanced resistance to certain antibiotics that target peptidoglycan synthesis. Furthermore, the *sanA* deletion mutant demonstrated enhanced replication rates within primary macrophages, highlighting its ability to evade the bactericidal effects of the immune system. Taking together, we provide valuable insights into a poorly known SanA protein, highlighting the complex interplay among bacterial genetics, membrane physiology, and antibiotic resistance, underscoring its significance in understanding *Salmonella* pathogenicity.

KEYWORDS

antibiotics, *Salmonella*, inner membrane proteins, membrane permeability, SanA

Introduction

Salmonellosis is a major intestinal foodborne disease, globally affecting approximately 200 million people and causing 60,000 fatalities annually (Havelaar et al., 2015). Thus, it is an epidemiological threat and an impediment to socio-economic development worldwide. Considering the ability of *Salmonella* to survive in various conditions, adapt to new environments, and facultatively survive and replicate inside cells, the prevention and treatment of salmonellosis become quite challenging. This often results in an over-reliance on antibiotic therapy, particularly in developing countries (Ayukekbong et al., 2017). Predictive models suggest that by 2050, antimicrobial resistance (AMR) may result in 10 million annual fatalities worldwide (O'Neil, 2016). Hence, non-typhoidal *Salmonella* and *Salmonella ser.* Typhi have been categorized by the Center for Disease Control as "Serious Threats," alongside other pathogens such as multidrug-resistant *Pseudomonas aeruginosa* and methicillin-resistant *Staphylococcus aureus* (Centers for Disease Control and Prevention, 2019).

Primarily, pathogenic bacteria have developed various defense mechanisms to withstand different environmental challenges, including exposure to xenobiotics. These mechanisms include (I) efflux pumps, which eliminate drugs from bacterial cells, thus reducing their concentration to non-toxic levels and causing loss of potency; (II) antibiotic inactivation by bacterial enzymes that alter or degrade antibiotic structures; (III) target site modification by spontaneous mutation and changing the chemical structure of their molecular targets; and (IV) preventing drug entry by altering bacterial membrane compositions (Alenazy, 2022). In all these processes the cell envelope, consisting of two lipid bilayers—inner membrane (IM) and outer membrane (OM) plays a critical role in protecting microorganisms from environmental stresses, as well as in cell viability and growth (Silhavy et al., 2010). The interdependence between OM and IM proteins is essential for preserving structural integrity of the bacterial cell envelope. Mutations in genes encoding IM proteins, such as *dedA* or *tat* may alter the membrane composition, potentially impacting membrane permeability and consequently resulting in antibiotic resistance (Boughner and Doerrler, 2012).

The outer membrane (OM) is a distinctive feature of gram-negative bacteria (Sun et al., 2022). It consists of an asymmetric lipid bilayer with the outer leaflet made of lipopolysaccharide (LPS) and the inner leaflet made of phospholipids (Nikaido, 2003; Sun et al., 2022). OM proteins can be classified as integral transmembrane β-barrel proteins (OMPs) and lipoproteins anchored in the inner leaflet (Malinverni and Silhavy, 2011). The most common lipoprotein is Lpp, which maintains periplasmic distance (Asmar and Collet, 2018). The OM's essential role is to protect against hydrophobic molecules, and some OMPs act as channels for small or large molecules (Nikaido, 2003). It also provides mechanical strength to compensate for the thin cell wall (Nikaido, 2003). Changes in OM composition can lead to drug resistance, emphasizing its importance in antibiotic sensitivity. They may also influence the efficiency of phagocytosis and the intracellular survival of pathogens within macrophages, as a result of an increased resistance toward antimicrobial activity of these host cells (Matz and Jürgens, 2001; Lei et al., 2019).

In addition to the OM, the bacterial cytoplasm is surrounded by a phospholipid bilayer IM, regulating the movement of nutrients and ions in and out of the cytoplasm. It serves as the site for various metabolic processes such as energy production, lipid and peptidoglycan biosynthesis, protein transport, and translocation (Silhavy et al., 2010). IM proteins vary extensively, from peripheral and integral proteins to lipoproteins attached to the periplasmic side of the IM. Together, they constitute approximately 25% of the bacterial proteome (Papanastasiou et al., 2016). Despite their abundance, the functions of several IM proteins are still unclear. One such IM protein is SanA, which is potentially involved in envelope biogenesis (Rida et al., 1996).

sanA multi-copy expression suppresses the vancomycin sensitivity of *Escherichia coli* K-12 mutant, showing OM permeability defect which was confirmed using compounds such as Sodium Dodecyl Sulfate (SDS), Ethidium Bromide (EB), and the ingredients of MacConkey medium (Rida et al., 1996). The *S.* Typhimurium *sfiX* (*sanA* ortholog) deletion mutant is also vancomycin-sensitive, which suggests that SanA may constitute a barrier that denies antibiotic access to its site of action (Mouslim et al., 1998). Furthermore, our previous study demonstrated the role of SanA in the initial stages of *Salmonella* pathogenicity—invasion and adhesion (Kolenda et al., 2021). Although SanA is hypothesized to be potentially associated with bacterial cell wall synthesis or may function as an efflux pump activated during extreme conditions such as cold/heat shock or bile exposure, these roles lack conclusive establishment. Notably, the subcellular localization of the SanA protein has not been experimentally demonstrated, and prediction tools provide inconsistent results in this context. Furthermore, the influence of SanA on membrane properties remains unexplored, and the correlation between physicochemical changes in the envelope and their subsequent effects on antibiotic resistance has not been investigated.

Considering all these aspects, we hypothesized that *sanA* deletion affects the membrane permeability of *Salmonella* and induces shifts in the membrane's physicochemical properties. These modifications are postulated to alter resistance to multiple antibiotic classes and enhance the bacterium's ability to replicate within primary macrophages.

Materials and methods

Bacteria, plasmids, and growth conditions

All bacterial strains, plasmids, and primers used in this study are listed in Tables 1–3, respectively. All *Salmonella* strains used in this work were derived from the *Salmonella enterica* serovar Typhimurium 4/74. Unless stated otherwise, bacterial cultures were routinely grown at 37°C for 16 h under dynamic or static conditions in Lysogeny Broth (LB) or on agar plates, respectively. According to manufacturer's recommendations, Biolog Universal Growth agar with 5% sheep blood was used to grow bacteria for the Biolog Phenotype Microarray. Mueller Hinton Broth (MHB) was used to measure antimicrobial activity. When necessary, ampicillin (Amp, 100 μg/mL) or kanamycin (Km, 50 μg/mL) was added. For *lac* promoter induction, isopropylthio-β-galactoside was added to a final concentration of 0.5 mM. Cell growth was monitored by measuring the optical density (OD) at 600 nm.

Xenobiotics

The following xenobiotic stock solutions were used: 5,7-dichloro-8-hydroxyquinaldine [55 mg/mL in dimethyl

TABLE 1 Bacterial strains used in this study.

Strain	Relevant feature(s)	References
S. Typhimurium 4/74	Wild type (WT)	Dr Derek Pickard, Cambridge Institute for Therapeutic Immunology and Infectious Disease, University of Cambridge Department of Medicine, Cambridge, United Kingdom
S. Typhimurium 4/74 Δ*sanA*	*S.* Typhimurium 4/74 with *sanA* gene knockout (Δ*sanA*)	This study
S. Typhimurium 4/74 Δ*sanA*-pWSK29	*S.* Typhimurium 4/74 Δ*sanA* with pWSK29 empty plasmid	This study
S. Typhimurium 4/74 Δ*sanA-pWSK29-sanA*	*S.* Typhimurium 4/74 Δ*sanA* complemented with *sanA* carrying pWSK29 plasmid	This study
E. coli XL1-Blue	*recA1 endA1 gyrA96 thi-1 hsdR17 supE44 relA1 lac [F´ proAB lacIq Z¨M15 Tn10 (Tetr)]*	Wroclaw University of Environmental and Life Sciences, Department of Biochemistry and Molecular Biology collection

TABLE 2 Plasmids used in this study.

Plasmid	Relevant feature(s)	References
pKD46	pBAD λ redαβγ ts ori; AmpR	Datsenko and Wanner (2000)
pKD4	template plasmids for FRT-flanked kanamycin cassette	Datsenko and Wanner (2000)
pCP20	Helper plasmid FLP ts *ori*; AmpR, KanR	Cherepanov (1995)
pWSK29	Expression vector under the IPTG-induced lac promoter, AmpR	prof. dr hab. Dariusz Bartosik, Institute of Microbiology, Department of Bacterial Genetics, University of Warsaw
pWSK29-*sanA*	pWSK29 vector with *sanA* sequence insert, AmpR	This study

sulfoxide (DMSO)]; bleomycin (2.56 mg/mL in sterile water); carbenicillin (20.5 mg/mL in sterile water); ceftriaxone (4 mg/mL in sterile water); cetylpyridinium chloride (164 mg/mL in sterile water); chlorhexidine acetate (25.6 mg/mL in ethanol); norfloxacin (0.8 mg/mL in DMSO); phosphomycin (40 mg/mL in sterile water); polymyxin B (1 mg/mL in sterile water); spectinomycin [100 mg/mL in DMSO:water (1:1)]; streptomycin (1 mg/mL in sterile water); sulfamonomethoxine (5 mg/mL in ethanol); thioridazine (16 mg/mL in DMSO); tobramycin (43.2 mg/mL in sterile water); umbelliferone (40 mg/mL in ethanol); and vancomycin (100 mg/mL in sterile water). All xenobiotic solutions were sterilized using 0.22 µm membrane filters and diluted in MHB medium to the appropriate concentration.

Bioinformatic analysis

In the study, a comprehensive array of open-access bioinformatics tools was utilized to investigate the SanA in *S.* Typhimurium 4/74. The nucleotide and protein sequences of SanA (accession number CP002487.1: 2277943-2278662; protein ID: ADX17941.1) were extracted from the NCBI database in a FASTA format for the analyses. Orthologs of the SanA across various taxonomic groups were identified using the EggNOG tool, enabling the generation of a report on the prevalence of SanA in different taxa (Huerta-Cepas et al., 2019).

To compare the sequence similarity of SanA between *Salmonella* and *Escherichia coli*, BLASTN and BLASTP were employed for nucleotide and protein sequence analysis, respectively. Furthermore, the investigation included an in-depth analysis of subcellular protein localization. For this purpose, several tools such as Phobius, SignalP-5.0, PsortB, THMM 2.0, and TMpred were applied (Krogh et al., 2001; Käll et al., 2007; Yu et al., 2010; Petersen et al., 2011; Finn et al., 2014).

Subsequently, Phyre2 was employed to conduct a comparative analysis of SanA against homologous sequences available in the database (Kelley et al., 2015). Additionally, the Panther classification system was utilized to categorize the protein and predict its function, providing insights into its potential biological roles and activities (Thomas et al., 2003).

Bacterial mutant construction

Salmonella Typhimurium 4/74 with *sanA* gene knockout was generated using the protocol described by Datsenko and Wanner (2000), with slight modifications (Datsenko and Wanner, 2000). Initially, electrocompetent cells of the wild-type (WT) strain were transformed with a Red recombinase-carrying plasmid pKD46. The positive clones were further transformed with a kanamycin cassette flanked by FRT sites, which was obtained via polymerase chain reaction (PCR) using primers sanA_del_for and sanA_del_rev on the pKD4 template, and selected on LB agar plates containing kanamycin at 37°C. The FRT flippase present on the pCP20 plasmid was then utilized to eliminate the kanamycin cassette. Colony PCR using locus-specific primer pairs, sanA_upstream_for, sanA_upstream_rev, and sanA_internal_rev was performed to confirm the correct integration and removal of the marker cassette. To determine whether the newly-created strain differed in growth rate or morphology from the parental isolate, growth curves were determined, and acridine orange staining was used to examine them using a fluorescence microscope. Furthermore, the absence of any unintended mutations was confirmed using Next Generation Sequencing.

TABLE 3 Primers used in this study.

Name	Sequence (5′-3′)	References
sanA_del_for	ATGTTAAAGCGCGTGTTTTACAGCCTGTTGGTCCTGGTAGGCTTGCTGCTGTGTAGGCTGGAGCTGCTTC	Datsenko and Wanner (2000) and this study
sanA_del_rev	TCATTTCCCTTTTTTCTTTTCCAGTTCAAGCAATTGTTCCGGCGTAACTGCATATGAATATCCTCCTTAG	Datsenko and Wanner (2000) and this study
sanA_upstream_for	CGATACAAGGGAAATCATGCTG	This study
sanA_downstream_rev	TTCCAGGCCTCACGGAAG	This study
sanA_internal_rev	GCCCTGGATACGATAACGA	This study
O1646 k1	CAGTCATAGCCGAATAGCCT	Datsenko and Wanner (2000)
O1647 k2	CGGTGCCCTGAATGAACTGC	Datsenko and Wanner (2000)
sanA_XbaIpWSK_for	ACATTCTAGAAGGAGGACAGCTATGTTAAAGCGCGTGTTTTAC	This study
sanA_PstIpWSK_rev	ATCTGCAGTCATTTCCCTTTTTTCTTTTCCAG	This study
pWSK_T7_up	CTTCGCTATTACGCCAGCTG	This study

Cloning of *sanA* into pWSK29 plasmid and mutation complementation

The *sanA* from *S.* Typhimurium 4/74 was amplified using sanA_XbaIpWSK_for, sanA_PstIpWSK_rev primers, and Phusion polymerase (Thermo), according to the manufacturer's protocol. The PCR products were purified using the GeneJET PCR purification kit (Thermo) and the plasmid DNA was isolated using the GeneJET Plasmid Miniprep Kit (Thermo). To insert *sanA* into the pWSK29 plasmid, the gene was cloned into the XbaI/PstI digestion sites using the classical ligation method. DNA sequence of the insert was confirmed using colony PCR via the use of a specific primer pair sanA_internal_rev and pWSK_T7_up, and Sanger sequencing. For complementing the deletion mutant, electrocompetent *S.* Typhimurium 4/74 Δ*sanA* was transformed with a plasmid carrying complementing gene as well as pWSK29 vector plasmid alone (without insert) as a control. All clones were analyzed in positive selection on LB agar with ampicillin.

Growth curve determination

To determine the growth curves of *Salmonella* strains, a single bacterial colony of each isolate was inoculated in LB and incubated overnight at 37°C with shaking (180 rpm). The resulting cultures were diluted to $OD_{600} = 0.05$ using LB and incubated until the early logarithmic growth phase ($OD_{600} = 0.5$, 37°C, 220 rpm). Each culture was then centrifuged, washed, and suspended in 0.9% NaCl solution. The OD_{600} values were measured, and the cultures were diluted in LB to obtain 5×10^6 CFU/mL bacterial suspensions. For determining the antimicrobial effect of vancomycin and bile salts, the assay was performed in LB or MHB medium, respectively with 0%–15% bile salts and 0–500 μg/mL vancomycin. The samples were then applied to a polystyrene or polypropylene 96-well plate in triplicate and incubated in a spectrophotometer (Tecan) at 37°C with measurements taken at 15-min intervals for 16 h, with shaking before each reading. The experiment was performed in at least three independent biological replicates, and dilution series on LB agar were prepared to verify initial bacterial concentrations.

Phenotype microarray analysis

The susceptibility of mutant and the parental strain to 240 chemical compounds was determined in three independent experiments using the Phenotype MicroArray (PM) PM11-PM20 (Biolog), as described in a previous study (Shea et al., 2012). Briefly, strains were grown overnight on Biolog Universal Growth agar with 5% sheep blood at 37°C, colonies were then picked using a sterile cotton swab and suspended in 15 mL of 1× inoculation fluid (IF-0a GN/GP Base, Biolog). The cell density was adjusted to 85% transmittance (T) using a Biolog turbidimeter. The inoculation fluid for PM11-20 was prepared by mixing 100 mL of IF-10a GN Base (1.2X; Biolog), 1.2 mL of Biolog Redox Dye A (100X; Biolog), 0.6 mL of cell suspension at 85% T, and sterile water to reach a final volume of 120 mL. The mixture was then inoculated in the PM plates (100 μL per well) and color development was monitored every 15 min for 48 h at 37°C using an Omnilog reader (Biolog). The kinetic curves of both strains were compared using Omnilog-PM software to identify the phenotypes. Raw data were obtained for 10 plates, which included 240 antibiotics arranged as a dilution series across four wells (960 wells in total). Data were recorded in the RA format and filtered using differences of average height with standard thresholds to identify statistically significant differences using Student's t-test (Guard-Bouldin et al., 2007). The reproducibility of our results was ensured by excluding any differences greater than 50 Omnilog units between biological replicates from the analysis (see Supplementary Table S1).

Antimicrobial susceptibility testing

As the manufacturer of PM plates (Biolog) does not disclose the concentrations of compounds in their plates, on the basis of available

literature, we selected 8 different concentrations for all compounds by making two-fold dilutions. Polypropylene and polystyrene plates were utilized for cationic and anionic compounds, respectively. Bacterial strains were incubated in LB for 16 h at 37°C, 180 rpm. Further, the OD_{600} was determined, and bacteria were diluted in MHB to get a total density of 10^6 CFU/mL. The suspensions were aliquoted at 50 µL per well into previously prepared 96-well plates and incubated at 37°C. After 16 h, OD_{600} of each well was measured with using the Tecan microplate reader (Spark®). MHB without xenobiotics serves as a positive control of growth. At least three technical and biological repetitions were performed for each strain. All xenobiotics and tested concentration ranges are listed in Table 4. Antibiotic susceptibility testing results determine the fold change of OD_{600} values between the *ΔsanA* and WT strain at concentrations showing a significant difference. The standard error of mean (SEM) was calculated using the standard deviation of the sample and the square root of the sample size.

TABLE 4 Antimicrobial concentration ranges included in the study.

Compound	Concentration range (µg/mL)	Solvent
5,7-Dichloro-8-hydroxyquinaldine	0.100–27.700	DMSO
Bleomycin	0.025–6.400	Water
Carbenicillin	0.400–102.400	Water
Ceftriaxone	0.002–0.4192	Water
Cetylpyridinium chloride	3.250–832	Water
Chlorhexidine acetate	0.250–64	Ethanol
Norfloxacin	0.010–2	DMSO
Phosphomycin	0.200–39.600	Water
Polymyxin B	0.020–5	Water
Spectinomycin	1.953–500	DMSO:water (1:1)
Streptomycin	0.390–100	Water
Sulfamonomethoxine	1–248	Ethanol
Thioridazine	6.250–1,600	DMSO
Tobramycin	0.084–21.600	Water
Umbelliferone	7.810–2000	Ethanol
Vancomycin	1.953–500	Water

Membrane permeability

The OM permeability was investigated by utilizing the influx of either the cationic Ethidium Bromide (EB) or the neutral Nile Red dye (NR; Murata et al., 2007; Viau et al., 2011). Overnight bacterial cultures were diluted to $OD_{600} = 0.05$ using LB, incubated until early stationary growth phase ($OD_{600} = 2.0$, 37°C, 220 rpm) and rinsed twice with assay buffer (50 mM KH_2PO_4, 137 mM NaCl, pH 7.0). To perform dye uptake assays, the proton motive force inhibitor carbonyl cyanide-m-chlorophenylhydrazone (CCCP) was added at a final concentration of 10 µM. Fluorescence was measured for 30 min at 1-min intervals using a Tecan microplate reader (Spark®) immediately upon mixing cells (final $OD_{600} = 0.2$) with EB at a final concentration of 6 µM (with excitation at 545 nm and emission at 600 nm) or NR at a final concentration of 2 µM (with excitation at 540 nm and emission at 630 nm). Membrane permeability was measured in at least three independent experiments. According to Murata et al., the dye uptake rates of different strains varied between experiments, but the pattern of dye uptake remained consistent across repetitions (Murata et al., 2007).

Hexadecane adhesion assay

Bacterial surface hydrophobicity was determined using the hexadecane adhesion assay (Oguri et al., 2016). Overnight bacterial cultures were diluted to $OD_{600} = 0.05$ using LB and incubated until early stationary growth phase ($OD_{600} = 2.0$, 37°C, 220 rpm). Subsequently, the cultures were harvested, washed twice with phosphate buffered saline (PBS), and resuspended in 1 mL of PBS. Following this, 100 µL of cells were diluted 10× in PBS and the OD_{600} was measured (C_0). Next, 900 µL of the cell suspension was mixed with 200 µL of hexadecane (Merck Millipore), vortexed for 1 min, and left undisturbed at room temperature until the phases separated. Cell samples (100 µL) from the lower, aqueous phase were then diluted in 900 µL PBS and OD_{600} was measured (C_H). The percentage of hexadecane adherence was determined in three independent experiments, using the following formula: % hexadecane adherence = $[(C_0 - C_H)/C_0] \times 100$.

Cytochrome c binding assay

The cytochrome c binding assay was performed as described previously, with minor modifications (Kristian et al., 2005). Briefly, overnight bacterial cultures were diluted to $OD_{600} = 0.05$ using LB and incubated until early stationary growth phase ($OD_{600} = 2.0$, 37°C, 220 rpm). Bacteria were then collected, washed twice in 3-(N-morpholino)propanesulfonic acid (MOPS) buffer (20 mM, pH 7.4), and adjusted to a final $OD_{600} = 7.0$ in the same buffer. Next, bacteria were mixed with cytochrome c (Merck Millipore) to a final concentration of 0.5 mg/mL, incubated for 10 min at room temperature, and centrifuged at 18,000 × g for 6 min. Cytochrome c without bacteria in the same buffer was also incubated as a negative control. The cytochrome c contents in the supernatants were measured at the absorption maximum of the prosthetic group (530 nm). The percentage of bound cytochrome c was calculated from three independent experiments, each performed in triplicate.

Bone marrow-derived macrophages derivation and culture

The isolation of primary bone marrow-derived macrophages (pBMDMs) was performed in accordance with a UK Home Office Project License in a Home Office designated facility, as previously described (Thurston et al., 2016; Bailey et al., 2020). Briefly, bone marrow was obtained from 6 to 8 week-old female C57BL/6 mice (Charles River) by flushing the tibias and femurs. The collected cells were then added to non-tissue culture-treated petri plates at a concentration of 3×10^6 cells per plate in 8 mL Dulbecco's modified Eagle's medium (DMEM) with high glucose supplemented with 20% (v/v) L929-MCSF supernatant, 10% (v/v) fetal bovine serum (FBS),

10 mM HEPES, 1 mM sodium pyruvate, 0.05 mM β-mercaptoethanol, and 100 U/mL penicillin/streptomycin. After 3–4 days, 10 mL fresh medium was supplemented and the differentiated BMDMs were harvested on day 7. The macrophages were then seeded into 24-well tissue culture-treated plates at a concentration of 2×10^5 macrophages per well and infected the following day with DMEM media supplemented with the above concentrations of FBS, HEPES, sodium pyruvate, and β-mercaptoethanol but without antibiotics.

Infection assay

The macrophage monolayer was infected with stationary phase bacteria opsonized in mouse serum for 20 min at room temperature at a multiplicity of infection of 10:1. To synchronize the infection, the culture plates were centrifuged for 5 min at 165 × g, followed by a 30-min incubation at 37°C (5% CO_2). Fresh DMEM supplemented with 100 μg/mL gentamicin (Gm) was added to kill extracellular bacteria, and the macrophage monolayers were incubated with added Gm for 90 min (Monack et al., 1996). After washing with DMEM, the monolayers were lysed in 1% Triton X-100 and diluted with PBS. Dilutions of the suspension were then plated on LB agar to quantify the number of viable bacteria. To evaluate intracellular growth, the medium containing 100 μg/mL Gm was replaced with DMEM supplemented with 10 μg/mL Gm, and parallel cell cultures were examined for viable bacteria 24 h following infection (Monack et al., 1996).

Statistical analyses

Statistical analyses were performed using GraphPad Prism (GraphPad Software, Inc., La Jolla, CA, United States). The Shapiro–Wilk normality test was used to determine data distribution. Depending on the data distribution, either Student's *t*-test, two-way ANOVA analysis of variance with Tukey's correction, or the Kruskal–Wallis test with Dunn's multiple comparison post-hoc test was used. For each condition, data were collected from at least three independent experiments. $p \leq 0.05$ was considered statistically significant. The results were presented as mean ± SEM. The symbols $^{*}p < 0.05$; $^{**}p < 0.01$; $^{***}p < 0.001$; and $^{****}p < 0.0001$ were used to indicate significance levels.

Results

Insights into SanA protein: analysis using bioinformatic tools

According to our analysis of the eggNOG database, we found that the *sanA* is present across a diverse range of bacterial taxa. Specifically, the gene was identified in both, gram-negative and gram-positive bacteria with a prevalence of 44.1% in species classified under *Gammaproteobacteria*, 17.2% of *Bacteroidetes*, 18.9% of *Actinobacteridae*, 5.72% of *Clostridia*, and 3.37% of *Spirochaetia*. Additionally, all SanA homologs have an unknown domain, DUF218. We performed a BLAST comparison and found that SanA in *E. coli* and *Salmonella* share 94% identity, with an estimated 97% amino acids having identical or similar chemical properties, suggesting its high conservative among bacteria.

The predictions for the subcellular localization were inconsistent: Phobius suggested a location outside the cytoplasm, SignalIP-5.0 detected no signal peptide implying a cytoplasmic protein, PsortB indicated a cytoplasmic position, while both THMM 2.0 and TMpred identified a transmembrane domain. Since proteins with similar structures can have similar functions, we elucidated the potential function of SanA by predicting its structure using Phyre2 and comparing it to homologous sequences. Our findings suggested that SanA shares structural similarities with the YdcF protein of *E. coli*, which is involved in binding S-adenosyl-L-methionine; transferases (5-methyltetrahydrofolate homocysteine s-methyltransferase); OmpA like protein; peptide binding protein; membrane protein, and structural protein. Moreover, the Panther classification system revealed that SanA is an IM protein with potential permease activity and is classified into the transporters group.

Impact of *sanA* knockout on resistance profile toward vancomycin and bile salts

As SanA is known as a vancomycin exclusion protein, the first stage of our investigation incorporated analysis of the WT and Δ*sanA* mutant bacteria growth in the presence of vancomycin or bile salts. Surprisingly, the mutant strain showed higher resistance to vancomycin than the WT (Figure 1A). While the WT grew only up to 125 μg/mL vancomycin, *sanA* deletion allowed the strain to grow up to a concentration of 250 μg/mL vancomycin. Moreover, a significant difference in the optical density between the two strains was observed in the presence of 62.5 and 125 μg/mL vancomycin, and the highest contrast was visible in the stationary growth phase—after 10 h (Figure 1A). Additionally, the two strains displayed contrasting growth patterns in the presence of bile salts. The deletion mutant strain demonstrated decreased resistance with growth up to only 3.75% bile salts compared to the WT, which grew up to 7.5% bile salts. Significant growth variations were also noted between the two strains at bile salt concentrations of 0.47%–1.88% (Figure 1B). The phenotypic parallels observed between the strain complemented with *sanA* and the one transformed with the empty pWSK29 plasmid further underscore the function of SanA in these resistance profiles (Supplementary Figure S2).

High-throughput analysis of xenobiotic resistance phenotype

WT and Δ*sanA* were further characterized using Biolog (Biolog®) phenotypic arrays to investigate potential gene knockout-induced changes in resistance profiles. The arrays featured various compounds with some known antimicrobials included on plates PM11a to PM20. Prior to testing, no significant differences in growth kinetics were observed among the strains (Supplementary Figure S1).

Our results revealed distinct resistance patterns for more than 20% (49/240) of the analyzed compounds with different mechanisms of action ($p < 0.05$; Table 5). The Δ*sanA* strain exhibited improved growth in the presence of approximately 35% (17/49) of these 49 agents, grouped mostly as cell wall-and DNA-associated antibiotics.

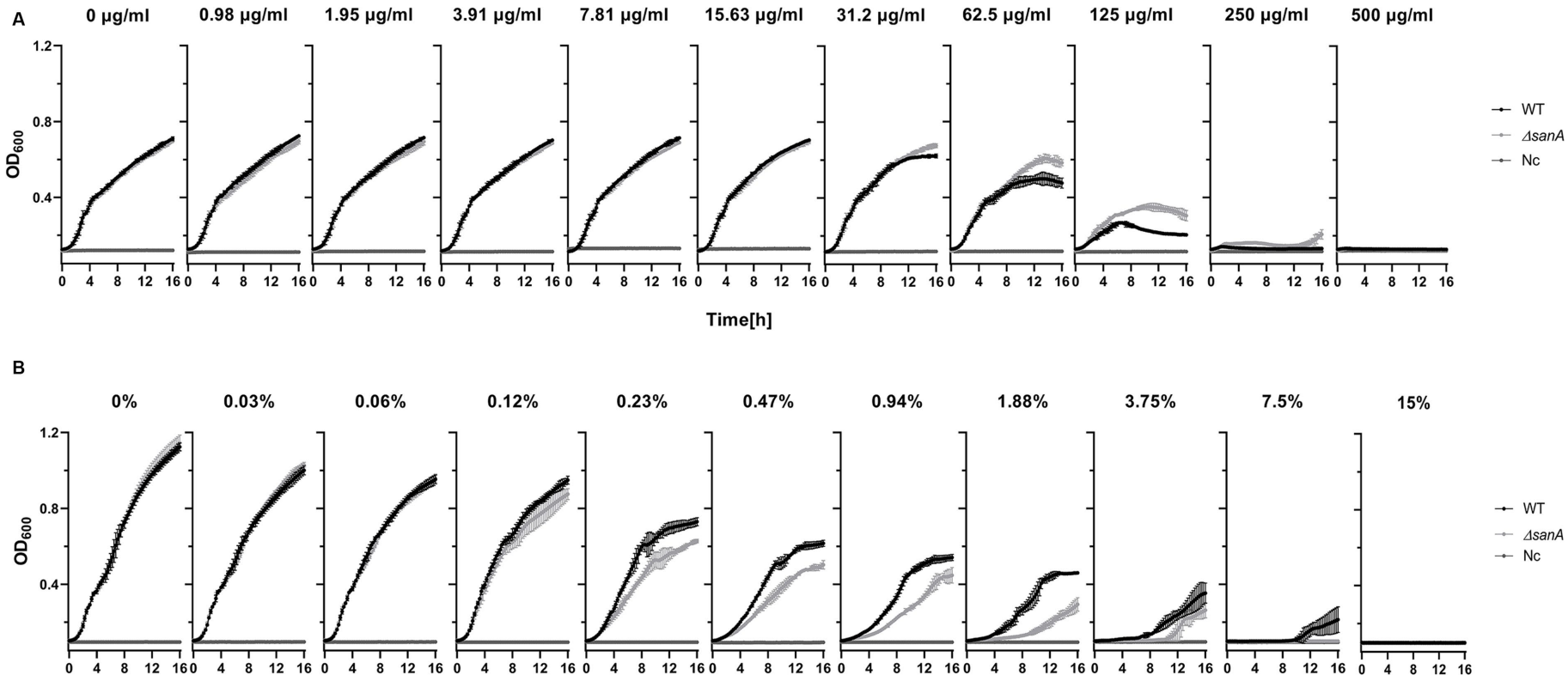

FIGURE 1
Growth curve of *Salmonella* Typhimurium 4/74 and its deletion mutant *ΔsanA* strains in the presence of: **(A)** vancomycin in the concentration range between 0 and 500 µg/mL, **(B)** bile salts in the concentration range between 0% and 15%. The data comprises of median values and median absolute deviation (MAD) of at least three separate experiments in triplicate. Nc represents a negative control: medium containing xenobiotics but lacking bacteria.

10.3389/fmicb.2023.1340143

10.3389/fmicb.2023.1340143

TABLE 5 Schematic representation of statistically significant data obtained from PM (from PM11a to PM20) analyses.

Compound	Difference	Mode of action
PHENOTYPE LOST (lower optical density after sanA knockout) BY Salmonella Typhimurium ΔsanA RELATIVE TO S. Typhimurium WT		
Umbelliferone	**−67.59**	**DNA intercalator**
Thioridazine	**−63.98**	**Membrane, phenothiazine, efflux pump inhibitor, anti-psychotic**
Cetylpyridinium chloride	**−62.62**	**Membrane, detergent, cationic**
Norfloxacin	**−58.49**	**DNA topoisomerase, fluoroquinolone**
DL-Serine hydroxamate	−51.68	tRNA synthetase
Pentachlorophenol	−51.56	Respiration, ionophore, H+
Chlorhexidine diacetate	**−51.28**	**Membrane, electron transport**
5,7-Dichloro-8-hydroxyquinaldine	**−51.18**	**RNA synthesis inhibitor, interference with transcription**
Sulfamonomethoxine	**−50.87**	**Folate antagonist, sulfonamide**
Ethionamide	−50.21	Anti-tuberculosic
Bleomycin	**−43.09**	**Inhibition DNA replication, oxidation, glycopeptide**
Sulfamethazine	−42.3	Folate antagonist, PABA analog, sulfonamide
Fusaric acid	−40.02	chelator, lipophilic
Trifluorothymidine	−35.2	Nucleic acid analog, pyrimidine, DNA synthesis
Sulfadiazine	−34.56	Folate antagonist, PABA analog, sulfonamide
Sulfisoxazole	−33.73	Folate antagonist, PABA analog, sulfonamide
1-Hydroxypyridine-2-thione (pyrithione)	−32.27	Biofilm inhibitor, chelator, anti-fungal
Sorbic acid	−31.04	Respiration, ionophore, H+, preservative
Sulfanilamide	−30.64	Folate antagonist, PABA analog, sulfonamide
Nitrofurantoin	−29.41	Nitro compound, oxidizing agent, DNA damage
Vancomycin	**−29.24**	**Wall, glycopeptide**
Tetraethylthiuram disulfide	−26.81	Nucleic acid inhibitor, purine
trans-Cinnamic acid	−26.7	Respiration, ionophore, H+
Sulfachloropyridazine	−23.02	Folate antagonist, PABA analog, sulfonamide
Phosphomycin	**−22.85**	**Wall, phosphonic**
5-Fluorouracil	−21.73	Nucleic acid analog, pyrimidine
5-Azacytidine	−21.54	DNA methylation, methyltransferase inhibitor
Polymyxin B	**−20.89**	**Membrane, cyclic peptide, polymyxin**
Ruthenium red	−19.28	Respiration, mitochondrial Ca++ porter
Penimepicycline	−15.34	Protein synthesis, 30S ribosomal subunit, tetracycline
Diamide	−11.06	Oxidizes sulfhydryls, depletes glutathione
Captan	−3.28	Fungicide, carbamate
PHENOTYPE GAINED (higher optical density after sanA knockout) BY S. Typhimurium ΔsanA RELATIVE TO S. Typhimurium WT		
Menadione, sodium bisulfite	4.87	Respiration, uncoupler
Spectinomycin	**10.16**	**Protein synthesis, 30S ribosomal subunit, aminoglycoside**
Poly-L-lysine	10.67	Membrane, detergent, cationic
2-Phenylphenol	13.67	DNA intercalator, preservative
Streptomycin	**15.65**	**Protein synthesis, 30S ribosomal subunit, aminoglycoside**
Cytosine-1-beta-D-arabinofuranoside	17.12	Nucleic acid analog, pyrimidine
Chromium (III) chloride	19.38	Toxic cation
Hydroxylamine	20.87	DNA damage, mutagen, antifolate (inhibits thymine and methionine synthesis)
3,5-Diamino-1,2,4-triazole (Guanazole)	22.31	Ribonucleotide DP reductase inhibitor, aromatic amine
Thiosalicylate	22.44	Biofilm inhibitor, anti-capsule agent, chelator, prostaglandin syntetase inhibitor

(Continued)

TABLE 5 (Continued)

Compound	Difference	Mode of action
Phenyl-methylsulfonyl-fluoride (PMSF)	24.9	Protease inhibitor, serine
Chelerythrine chloride	26.82	Protein kinase C inhibitor
Myricetin	28.82	DNA & RNA synthesis, polymerase inhibitor
Cesium chloride	29.38	Toxic cation
Ceftriaxone	**31.69**	**Wall, cephalosporin**
Tobramycin	**35.91**	**Protein synthesis, 30S ribosomal subunit, aminoglycoside**
Carbenicillin	**57.92**	**Wall, lactam**

Data from Omnilog were recorded in the RA format and filtered using differences of average height values between *S.* Typhimurium 4/74 WT and *ΔsanA* to identify statistically significant differences. Phenotype lost indicates lower optical density after *sanA* knockout (negative values in the Table), and gained—higher optical density as a result of mutation (positive values in the Table). The bold text indicates agents which were chosen for further analysis with the use of microbroth dilution assay.

The same strain demonstrated lower resistance to folate antagonists (sulfonamides), membrane-targeting antibiotics, and DNA and protein-associated antibiotics (fluoroquinolones, glycopeptides, nucleic acid analogs; Table 5).

Considering the known adjustments of the PM plates method with MIC measurements, we cross-checked PM results using a microbroth dilution assay. We focused on 16 compounds with the most significant differences between strains, particularly those targeting the membrane and cell wall (Table 5). The results, showing fold changes at OD_{600} between the *ΔsanA* and WT at specific concentrations (Supplementary Figure S3), led to further investigation using complemented strains (Figure 2B).

In the presence of 16 different agents, the *ΔsanA* strain exhibited reduced resistance to ten xenobiotics but displayed increased resistance to six others (Figure 2A). We grouped these agents into the following five categories: (1) membrane, (2) protein synthesis, (3) cell wall and efflux pumps, (4) replication, and (5) transcription (Figure 2A). The *sanA* knockout resulted in compromised growth with certain membrane-associated xenobiotics such as chlorhexidine acetate (2 μg/mL; $p = 0.0003$), cetylpyridinium chloride (6.5 μg/mL; $p = 0.0093$), umbelliferone (500 μg/mL; $p = 0.0465$), and polymyxin B (0.625 μg/mL; $p = 0.0205$). Notably, reintroducing *sanA* restored the resistance pattern on these agents to resemble WT bacteria (Figure 2B).

The *ΔsanA* exhibited lower resistance to agents targeting protein synthesis, such as tobramycin (0.675 μg/mL; $p = 0.0070$), streptomycin (100 μg/mL; $p = 0.0152$), and spectinomycin (31.250 μg/mL; $p = 0.0359$), as well as those targeting transcription, such as norfloxacin (0.010 μg/mL; $p = 0.0052$) and 5,7-dichloro-8-hydroxyquinaldine (3.5 μg/mL; $p = 0.0065$; Figure 2A). Notably, the *ΔsanA* strain showed a different resistance pattern to protein synthesis agents than that suggested by PM. However, when the mutation was complemented, the resistance pattern was mostly attributed to the *sanA* deletion, except for tobramycin (0.675 μg/mL; $p = 0.9998$; Figure 2B).

As anticipated, *sanA* deletion resulted in greater resistance to cell wall and efflux pumps associated compounds, like ceftriaxone (0.002 μg/mL; $p = 0.016$), vancomycin (125 μg/mL; $p = 0.0044$), carbenicillin (3.200 μg/mL; $p = 0.0281$), and thioridazine (1,600 μg/mL; $p = 0.027$). Surprisingly, this strain showed reduced resistance to phosphomycin (9.900 μg/mL; $p = 0.0483$; Figure 2A). Complementation mostly restored WT phenotypes, with the exception of thioridazine (1,600 μg/mL; $p = 0.2196$). In contrast to the PM data, *ΔsanA* demonstrated reduced susceptibility to replication agents, such as bleomycin (0.400 μg/mL; $p = 0.0104$) and sulfamonomethoxine (248 μg/mL; $p = 0.0432$). This phenotype was further validated by complementing *sanA*, highlighting its critical role in this phenotype (Figure 2B).

SanA is responsible for membrane integrity

The impact of *sanA* on resistance to vancomycin along with other antimicrobial agents suggests a general effect on membrane integrity rather than specific vancomycin sensitivity. Thus, OM permeability was determined by measuring influx of the cationic dye, EB or the neutral dye, NR. Dye uptake assays were performed in the presence of CCCP, which enables the inward transport of H^+ across lipid membranes. Therefore, it prevents the efflux of compound by active pumps, so that only passive permeability is measured. In the experiment without CCCP, a minimal increase in dye uptake was noted, suggesting that the increased retention of EtBr in the *ΔsanA* is not due to pump inactivation, but increased membrane permeability (Supplementary Figure S4).

When CCCP was present, the *ΔsanA* bacteria demonstrated a notably higher OM permeability baseline than the WT for both EB and NR, with a remarkably increased rate of dye uptake observed particularly after approximately 10 min of assay initiation (Figure 3; Supplementary Figure S5). Importantly, complementation of the mutation restored the WT phenotype for NR and further reduced the permeability for EB, strongly suggesting that the observed phenotype was primarily due to *sanA* deletion. Moreover, the permeabilities differed between WT and *ΔsanA*, as well as between *ΔsanA*-pWSK29 and its complemented *ΔsanA*-pWSK29-*sanA* counterpart, consistently throughout the assay (Figure 3).

SanA knockout decreases hydrophobicity and negative charge of the bacterial membrane

Considering the distinct resistance phenotype observed for different groups of xenobiotics, we hypothesized that the surface charges and hydrophobicity of bacterial cells could be contributing factors. To investigate potential alterations in the surface properties of the *ΔsanA*, we performed the following two assays: (1) determining

10.3389/fmicb.2023.1340143

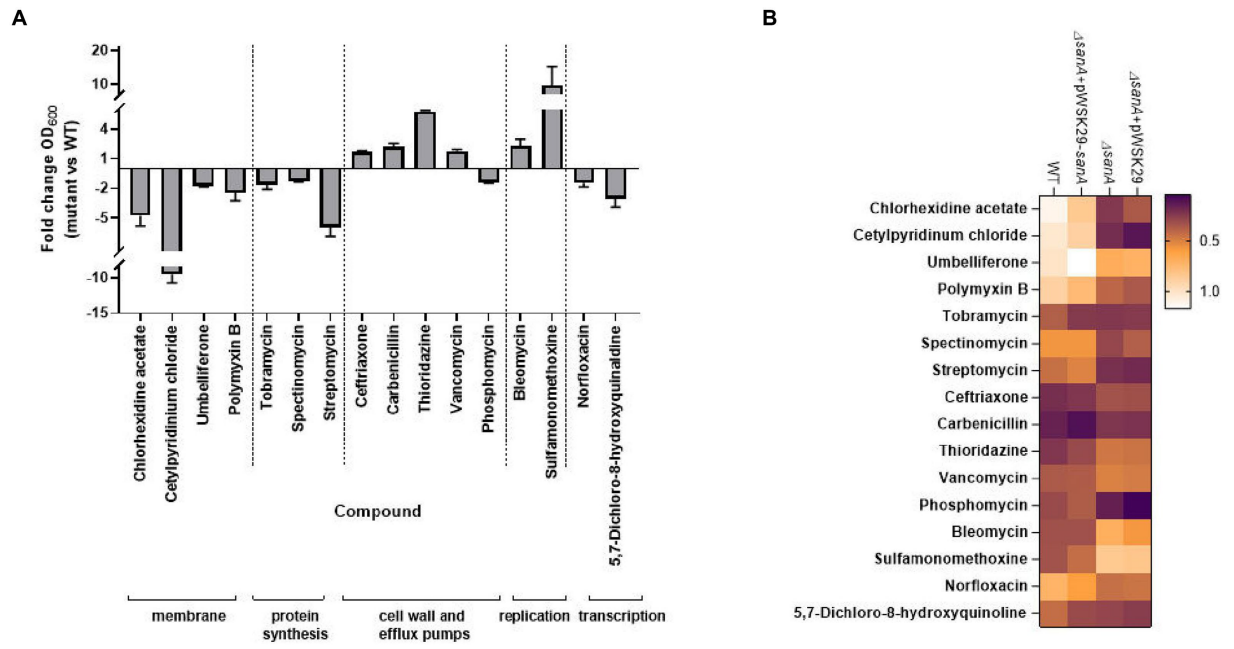

FIGURE 2
Antibiotic susceptibility testing represented by **(A)** bar chart with fold change OD_{600} of *Salmonella* Typhimurium 4/74 deletion mutant *ΔsanA* and WT after 16 h incubation in MHB medium with the presence of indicated agents. Data shown are means and SEM for at least three independent experiments **(B)** heatmap of OD_{600} of *S.* Typhimurium 4/74, its deletion mutant *ΔsanA* and *ΔsanA* transformed with empty pWSK29 plasmid or vector with *sanA* after 16 h incubation in MHB medium with the presence of indicated agents. Brown represents low relative growth in a given condition while white represents high growth.

surface charges by evaluating the binding of the cationic protein cytochrome c to bacterial cells, and (2) determining surface hydrophobicity by measuring the adherence of cells to the hydrophobic solvent hexadecane.

The *ΔsanA* cells displayed significantly lower affinity to cytochrome c (80%) than that of WT cells (90%; $p = 0.0046$; Figure 4A). Additionally, approximately 10% of *ΔsanA* cells adhered to hexadecane, in contrast to approximately 16% of WT cells ($p = 0.0256$; Figure 4B). This suggests a decrease in the negative charge and hydrophobicity on the cell surface of *ΔsanA* mutant, respectively. Moreover, all these changes were attributed entirely to *sanA*, as introduction of *sanA* to the deletion mutant restored the WT phenotype ($p = 0.0199$; $p = 0.005$).

SanA influences the replication of *Salmonella* Typhimurium within primary bone marrow macrophages

Alterations in bacterial membranes significantly influence antimicrobial efficacy and bacterial replication within phagocytes (Ernst et al., 1999). To further investigate this, we monitored *Salmonella* replication in primary BMDMs, which provide a relevant physiological context to examine the interactions between *Salmonella* and host cells. Our results showed that the uptake of *S.* Typhimurium by BMDMs was similar for the WT and *ΔsanA* ($p = 0.0572$; Figure 5A), but the mutant exhibited a significantly increased number of intracellular bacteria 24 h post-infection ($p = 0.0051$; Figure 5B). Furthermore, we observed a marked difference between *ΔsanA* + pWSK29 and *ΔsanA* + pWSK29-*sanA*, whereby expression of *sanA* reduced replication ($p = 0.0351$; Figure 5B).

Discussion

Multidrug resistance among bacteria, including prominent species such as *Salmonella*, *Pseudomonas*, and *Campylobacter*, constitutes a major public health concern (Centers for Disease Control and Prevention, 2019). These bacteria utilize diverse mechanisms, including the creation of enzymatic barriers and altering membrane compositions, to mitigate the impact of surface disinfection or antibiotic therapies (Reygaert, 2018). Gram-negative bacteria exhibit a complex cellular envelope with the OM forming an extra line of defense. Its permeability properties have significant implications for the bacterium's sensitivity to antibiotics (Silhavy et al., 2010). Moreover, although less studied, the IM proteins play a crucial role in coordinating processes pivotal for bacterial survival and resistance to extreme environmental conditions. Mutations in the genes encoding these proteins could increase membrane permeability, thereby promoting antibiotic resistance (Ize et al., 2003; Boughner and Doerrler, 2012).

Our study emphasizes on a lesser-known protein, SanA, and examines its role in altering the physicochemical properties of bacterial membranes, which consequently affect the bacterium's resistance phenotype.

SanA is composed of 239 amino acids and is predicted to primarily localize in the inner membrane, featuring a small N-terminal cytoplasmic domain spanning just six amino acids. It possesses a

10.3389/fmicb.2023.1340143

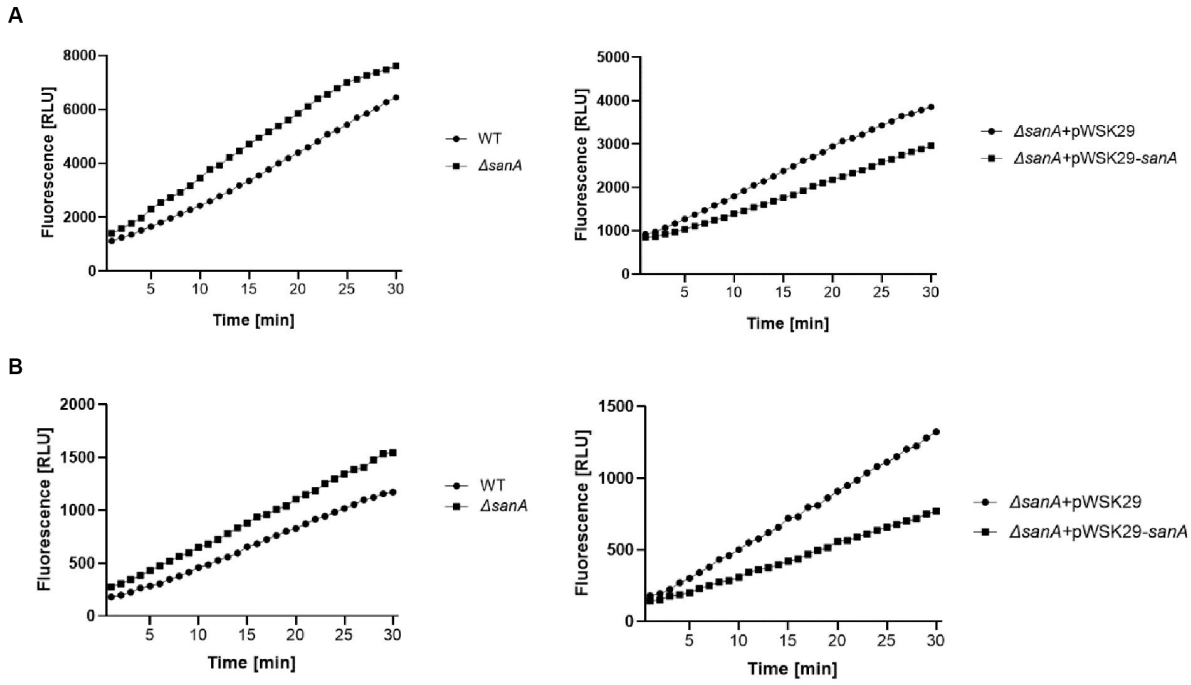

FIGURE 3
Outer membrane permeability of *Salmonella* Typhimurium 4/74, its deletion mutant *ΔsanA* and *ΔsanA* transformed with empty pWSK29 plasmid or vector with *sanA* **(A)** cationic dye Ethidium Bromide or **(B)** neutral dye Nile Red. The assay was conducted in the presence of CCCP to prevent the efflux of compound by active pump to measure only passive permeability. Data shown are representative of at least three independent experiments with similar results.

single transmembrane helix, with the remainder of the protein predominantly situated in the periplasmic space (Krogh et al., 2001; Petersen et al., 2011). Within the periplasmic part, SanA harbors a DUF218 domain designated as a domain of the unknown function (Finn et al., 2014). DUF218 domains contain multiple charged amino acids, implying potential enzymatic activity, and are prevalent across various bacterial species. These domains are primarily associated with proteins whose functions remain elusive (Mitchell et al., 2017). SanA was initially discovered as a multicopy suppressor in response to unknown mutations that affected the OM permeability. This included not only the deletion of the *sanA* gene but also other mutations that were associated with impairments in the OM (Rida et al., 1996). Moreover, in a study on *sanA* ortholog (97% identity of nucleotide sequence), the *S.* Typhimurium *sfiX-strain* failed to grow in the presence of vancomycin in high temperature (Mouslim et al., 1998).

Thus, we initially aimed to determine how *sanA* deletion affects the growth of *S.* Typhimurium 4/74 in the presence of vancomycin and bile salts, a key substrate of McConkey medium at 37°C, what corresponds to the host's physiological temperature. Apparently, our findings aligned with previous outcome, indicating that a *Salmonella* strain carrying a 10-nucleotide deletion in *sanA* displays enhanced vancomycin resistance than that with wild-type *sanA* at the same temperature (Kolenda et al., 2021). It is crucial to highlight that the variance in these findings compared to Rida et al.'s study may arise from various factors, including the higher temperature utilized in their assay and the use of a less well-characterized mutant with additional to *sanA* mutations (Rida et al., 1996). Additionally, it might stem from methodological distinctions, particularly the choice of plate material. The polypropylene plates with a neutral surface aimed to minimize non-specific binding—a critical aspect frequently overlooked in the realm of antibiotic resistance research, to ensure precise measurement of vancomycin activity (Singhal et al., 2018). Furthermore, our demonstration of detectable differences in the stationary growth phase allows us to suggest that SanA expression may occur in stress conditions, such as the late growth phase or elevated temperatures employed in prior studies.

In contrast, we observed an inverse effect with anionic bile salts, wherein the WT demonstrated higher resistance. This observation aligns with that of Langridge et al. (2009) who found that an *S.* Typhimurium *sanA* mutant exhibits increased bile sensitivity (Langridge et al., 2009). It suggests a distinct role of SanA on various chemical compounds, implying that the protein affects barrier function by altering properties of the envelope, rather than the antibiotic's mechanism of action, sequestration, modification, or target blocking (Langridge et al., 2009). Thus, we further explored this phenomenon using the PM, which analyzed the growth of strains in the presence of 240 different agents, simultaneously. The obtained data were then validated using the microbroth dilution assay, since the Biolog phenotype microarray is a screening method and results are not as accurate as using the classical approach (Dunkley et al., 2019). Moreover, the Biolog PM assay indirectly measures bacterial growth through colorimetric signals, which may not directly correlate with the bacterial growth inhibition caused by antibiotics (Dunkley et al., 2019). Our analysis highlighted a decreased resistance trend in the *ΔsanA* to phosphomycin, detergents, and polymyxin B. Additionally, the same strain showed lower resistance to protein synthesis-targeting

10.3389/fmicb.2023.1340143

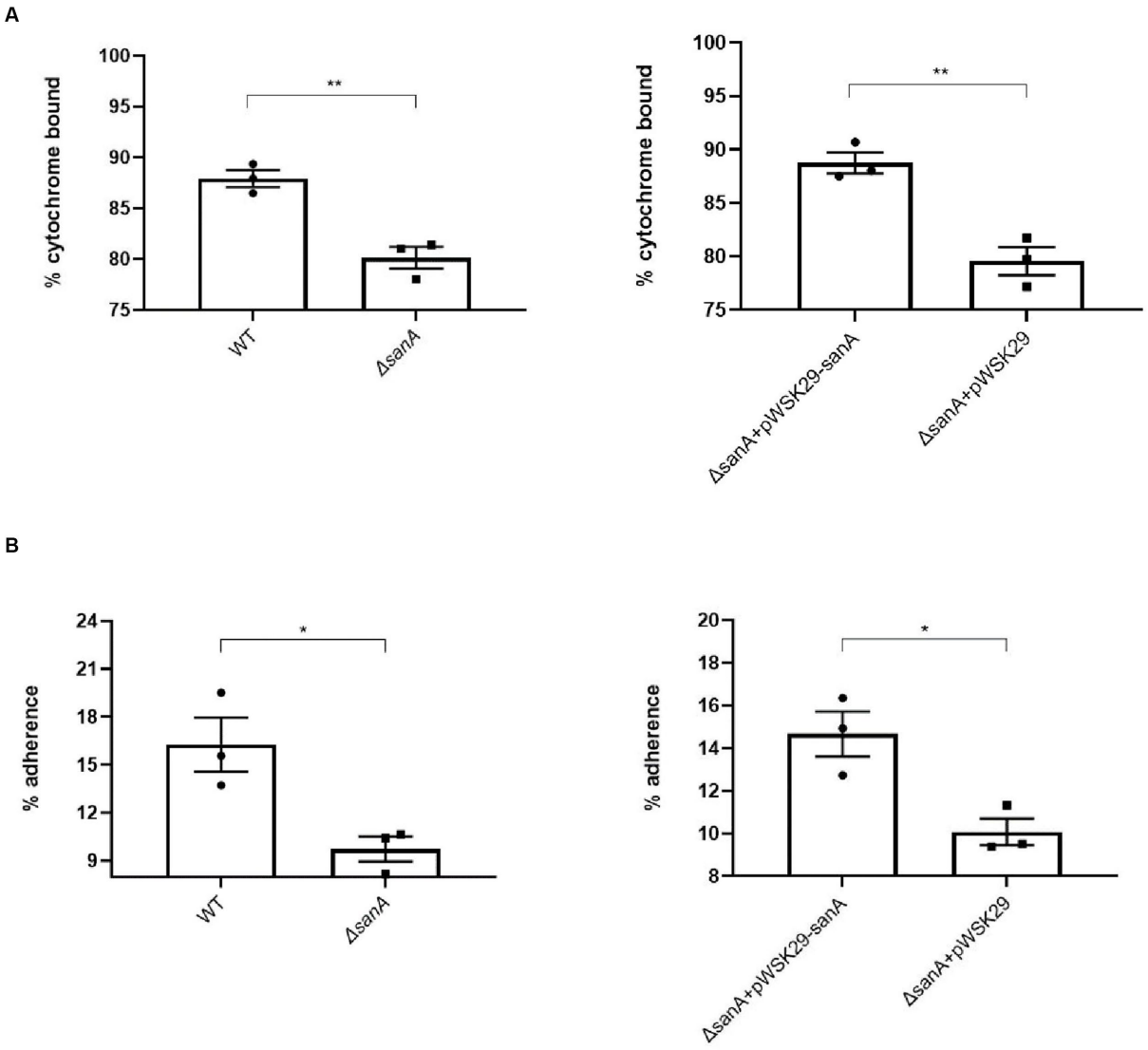

FIGURE 4
Physicochemical properties of the cell surfaces of *Salmonella* Typhimurium 4/74, its deletion mutant *ΔsanA*, and *ΔsanA* transformed with empty pWSK29 plasmid or vector with *sanA* **(A)** Surface charges were examined by a cytochrome c binding assay. **(B)** Hydrophobicities of cell surfaces were examined by a hexadecane adhesion assay. Data shown are means and SEM for at least three independent experiments. Statistical significance was determined by Student's *t* test (*$p < 0.05$; **$p < 0.01$).

antibiotics, such as aminoglycosides and aminocyclitoles, as well as to transcription-related compounds such as fluoroquinolones and quinolines. Conversely, enhanced resistance was noted toward cell wall synthesis and efflux pumps-associated xenobiotics as well as DNA targeting agents, such as glycopeptides and sulfonamides.

Previously published data did not determine the role of *sanA* unequivocally, but has suggested its role in peptidoglycan synthesis (Mouslim et al., 1998). The location of the C-terminus, containing DUF218 domain with charged amino acids in the periplasm, which is the site of the cell wall synthesis, may indicate that it plays a role in blocking the activity of vancomycin at its site of action (Mitchell et al., 2017). In contrast, the hydrophobic nature of the SanA protein, suggests that it participates in the barrier functions of bacterial cell envelopes, affecting the synthesis of murein, which is essential for cell wall function and maintenance. This role was indicated by the dual effect of the *sanA* mutation—induction of vancomycin sensitivity and suppression of cell division inhibition (Rida et al., 1996; Mouslim et al., 1998). Our data revealed that *sanA* deletion resulted in higher resistance to vancomycin as well as different classes of antibiotics associated with the cell wall synthesis—ceftriaxone and carbenicillin. In contrast, the same strain revealed higher susceptibility to phosphomycin, another murein synthesis-targeting antibiotic. Since all these agents hinder bacterial growth by inhibiting peptidoglycan synthesis, each of them targets another stage of this process. Carbenicillin, and ceftriaxone are beta-lactam antibiotics, which function by mimicking the D-alanyl-D-alanine structure and binding to Penicillin-binding proteins; this prevents them from cross-linking the peptidoglycan layers and causing cell death in the final, extracytoplasmic stage of peptidoglycan synthesis (Lima et al., 2020). Unlike beta-lactam antibiotics, vancomycin affects the second stage of creating bacterial cell membranes, by targeting the

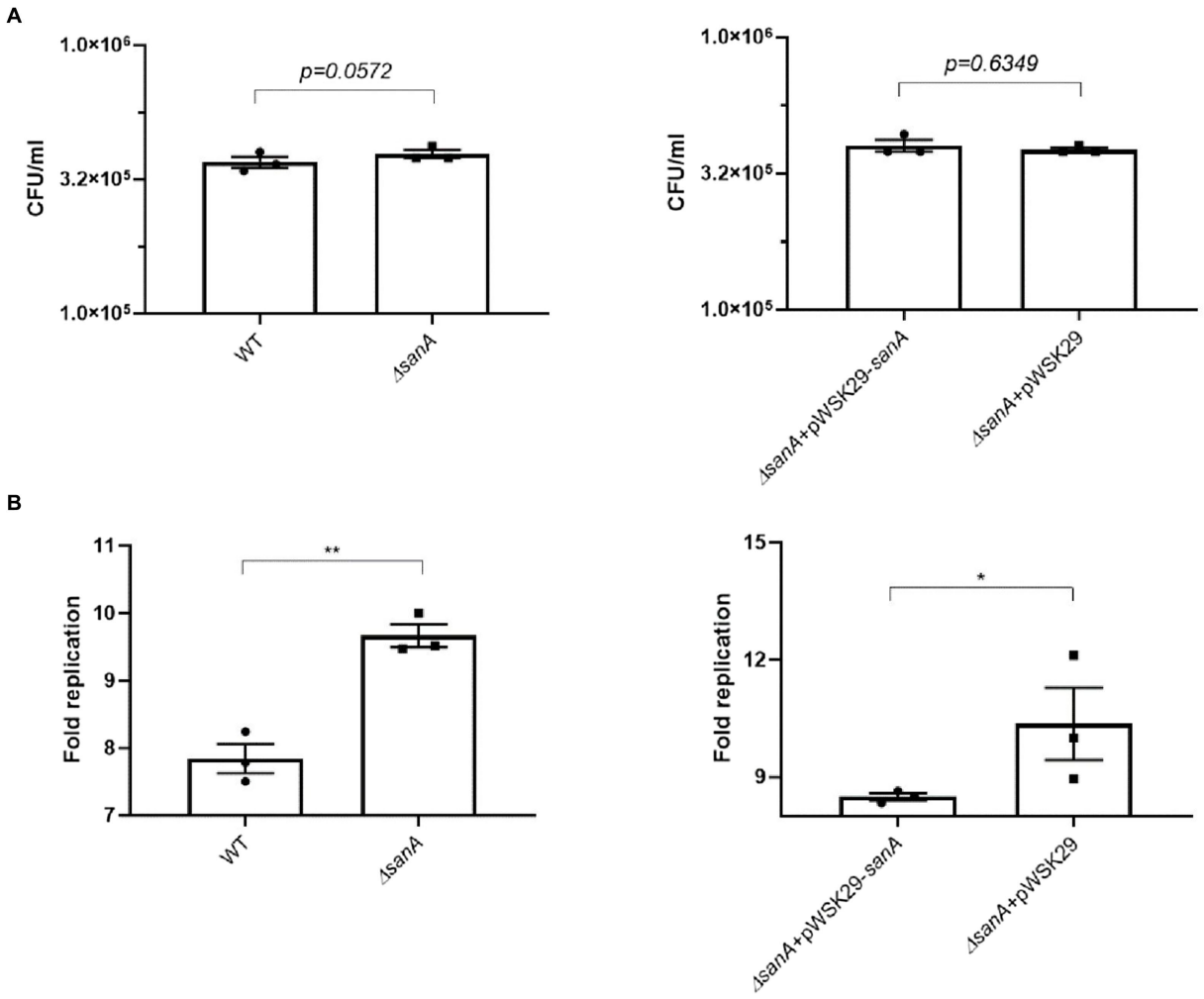

FIGURE 5
Salmonella infection of primary bone marrow macrophages (pBMDM). **(A)** invasion level of BMDM, **(B)** intracellular replication within BMDM isolated from C57BL/6 mice of *S. Typhimurium* 4/74, its deletion mutant *ΔsanA* and *ΔsanA* transformed with empty pWSK29 plasmid or vector with *sanA*. The fold replication was determined by comparing the bacterial population within macrophages after a 24 h incubation period to that after a 2 h initial incubation. The data are shown as mean values and SEM of three separate experiments of intracellular replication. Statistical differences were analyzed by Student's *t* test (*$p < 0.05$; **$p < 0.01$).

d-Ala-d-Ala terminus of peptidoglycan. In turn, phosphomycin has a unique mechanism of action. It inhibits the first step in peptidoglycan synthesis by targeting the enzyme MurA (UDP-N-acetylglucosamine enolpyruvyl transferase). This enzyme catalyzes the conversion of UDP-N-acetylglucosamine to UDP-N-acetylmuramic acid, the first committed step in peptidoglycan synthesis. By inhibiting this enzyme, phosphomycin disrupts the production of peptidoglycan precursors, repressing early cell wall synthesis (Falagas et al., 2016). Thus, the role of SanA in peptidoglycan synthesis, and hence in antibiotic resistance, may be more complex than expected. Based on our *in silico* predictions and considering SanA's putative role as a permease, its function might be similar to that of AmpG, an IM permease responsible for transporting anhydromuropeptides into the bacterial cytoplasm, contributing to peptidoglycan recycling (Jacobs et al., 1994). This would explain why the deletion of *sanA* does not confer resistance to all antibiotics targeting peptidoglycan synthesis, as demonstrated by reduced resistance to phosphomycin. It is worth noting however that the Panther database's classification of SanA as a potential permease may not align with biological reality, given that SanA has only one transmembrane helix (Thomas et al., 2003). The same database assigns a similar classification to YdcF, a cytoplasmic protein containing a DUF218 domain (Thomas et al., 2003).

Any changes in peptidoglycan synthesis can alter the bacterial envelope structure and composition, leading to modified interactions with xenobiotics (Nikolaidis et al., 2014; Yadav et al., 2018). Since peptidoglycan is critical for maintaining the shape and structural integrity of the cell wall, interference at any stage of its synthesis, assembly, or recycling can effectively inhibit cell growth (Typas et al., 2012). It correlates with previously published data demonstrating the role of *sanA* in the cell division of a defective mutant (Mouslim et al., 1998). Additionally, changes to the murein synthesis pathway could impact the overall cell wall structure and stability, bacterial membrane permeability, or transport mechanisms, which could impact the uptake or efflux of antibiotics. The stability of the OM is maintained through tethering of the OM to the sacculus, a process that is

facilitated by both covalent and non-covalent interactions between abundant OM proteins (such as Lpp, Pal, and OmpA) and peptidoglycan (Hantke and Braun, 1973; Parsons et al., 2006). Complex resistance effect, based on increased susceptibility to membrane-bound antibiotics–chlorhexidine acetate, cetylpyridinum chloride, umbelliferone, and polymyxin B confirmed this occurrence, suggesting a correlation between the IM protein, SanA, and OM, responsible for maintaining integrity of the envelope. This situation is reminiscent to that of TolA, wherein a defect in *tolA* leads to detergent sensitivities. This protein, being anchored in the IM by its hydrophobic amino-terminal 21-residue segment similar to SanA, presumably interacts through its carboxyl-terminal domain with components on the inner surface of the OM for maintaining its integrity (Levengood et al., 1991; Levengood-Freyermuth et al., 1993). Our data indicating significantly higher OM permeability of the *sanA* mutant corroborates this hypothesis.

Furthermore, the phenotype of *sanA* mutant correlates with an increased sensitivity for aminoglycosides—streptomycin, tobramycin, and aminocyclitole—spectinomycin, having the same target of action. Aminoglycoside resistance typically involves diminished uptake or decreased cellular permeability, modifications at the ribosomal binding sites, or the generation of aminoglycoside modifying enzymes (Garneau-Tsodikova and Labby, 2016). Thus, enhanced membrane permeability due to *sanA* knockout was the primary reason for the observed shifts in the resistance phenotype. Notably, we observed a reverse phenotype for all the agents tested, except tobramycin, further supporting that the resistance phenotype is more complex than initially assumed. Similarly, we demonstrated decreased resistance of the *ΔsanA* to transcription-associated antibiotics such as fluoroquinolones and quinolines. Nevertheless, the expression of *sanA* from a plasmid did not completely reverse the effects of the mutation, indicating that SanA plays only a partial role in this phenotype. Additionally, the absence of a specific SanA antibody prevents direct comparison of *sanA* expression in its plasmid and chromosomal forms. Therefore, variations in expression levels and regulatory elements could be responsible for the observed incomplete restoration of the phenotype.

Although WT bacteria exhibited resistance to a broader spectrum of xenobiotics, the mutant displayed increased resistance to replication-targeting antibiotics, bleomycin and sulfamonomethoxine. These two antibiotics have similar targets of action, but differ significantly in their physicochemical properties. Bleomycin, like vancomycin, has a notably high molecular weight (1,415 Da) and is classified as a cationic glycopeptide however, bleomycin and vancomycin have distinct mechanisms of action (Hecht, 2000). This finding further suggests that *sanA* is not directly associated with the specific action mechanisms of these xenobiotics. Instead, it seems to be linked, at least partially, with the membrane charge (Davlieva et al., 2013). As *sanA* contributes to a more positive membrane charge, it subsequently increased resistance to cationic antibiotics.

Bacterial resistance to bleomycin and sulfamonomethoxine, a derivative of sulfonamide, is mainly attributed to the Resistance-Nodulation-Division (RND) family of efflux pumps. The SanA structure does not resemble that of an RND transporter, suggesting that its absence, as observed in the mutant, may lead to the overexpression of another efflux pump that compensates for the transport of this antibiotic. Moreover, due to the neutral charge of sulfamonomethoxine, alterations in the phospholipid composition of the IM may hinder the passive diffusion of neutral antibiotics (Kadner, 1996).

Considering the distinct effects of *sanA* deletion on resistance to different classes of antibiotics, we decided to explore whether this genetic modification also affects the intracellular replication of *Salmonella* within macrophages. Macrophages are immune cells essential for host defense against bacterial infections, as they internalize and destroy them using various mechanisms, including the production of reactive oxygen and nitrogen species and antimicrobial peptides (Gordon, 1999). These substances possess bactericidal properties and disrupt bacterial cell envelope integrity and function, similar to antibiotics. Therefore, modifications affecting antibiotic resistance might also influence the bacterium's ability to tolerate the hostile intracellular environment of a macrophage. To further explore this phenomenon, we selected a C57BL/6 primary BMDM model for *Salmonella* replication, which provides a physiologically relevant environment for studying the interactions between *Salmonella* and host cells compared to cell lines As a result, *sanA* deletion resulted in higher replication rates of *Salmonella* within primary macrophages, suggesting that the absence of *sanA* may enhance the ability of the bacterium to resist the bactericidal actions of macrophages. We suggest it is linked to alterations in the bacterial cell envelope associated with *sanA* deletion as our data suggest that *sanA* knockout leads to increased membrane hydrophilicity and positive charge. As the outer layer of bacterial cells possesses an anionic charge, most antimicrobial peptides (AMPs) effective against bacteria are cationic, enabling them to bind to the negatively charged bacterial surface (Lei et al., 2019). Consequently, bacterial resistance to AMPs often involves surface modification to reduce the negative charge, which serves as an initial defense mechanism (Peschel, 2002). Also, previously published data revealed that the efficiency of phagocytosis increases with the hydrophobicity of bacterial cells and that hydrophilic bacteria resist ingestion by phagocytes (Matz and Jürgens, 2001). Surprisingly, we did not observe significant changes in the invasiveness of the analyzed strains in the conditions we used. To better elucidate the role of *sanA* in host-pathogen interactions, it is necessary to investigate changes occurring in the bacterial envelope due to *sanA* knockout. We hypothesize that *sanA* deletion and the subsequent increase in membrane permeability may be linked to an upregulation of SPI-II and/or SPI-I genes, which are responsible for intracellular replication and invasion, respectively. Currently, this hypothesis is under investigation.

In conclusion, our study offers a crucial understanding of the dynamics of antibiotic resistance, underscoring how alterations in membrane properties influence bacterial susceptibility to various xenobiotics. The insights regarding SanA's influence on membrane physicochemical properties shed new light on the role of membrane proteins in *Salmonella*'s resistance to environmental stressors. This highlights the importance of these proteins in comprehending bacterial pathogenicity and survival mechanisms.

Data availability statement

The original contributions presented in the study are included in the article/Supplementary material, further inquiries can be directed to the corresponding author.

Ethics statement

The animal study was approved by UK Home Office Project License in a Home Office designated facility. Imperial College Animal Welfare and Ethical Review Body (AWERB) granted approval for all mouse work. The study was conducted in accordance with the local legislation and institutional requirements.

Author contributions

AA: Conceptualization, Data curation, Investigation, Methodology, Validation, Visualization, Writing – original draft. RK: Conceptualization, Resources, Supervision, Writing – review & editing. KB: Investigation, Writing – review & editing. TLMT: Methodology, Resources, Writing – review & editing. JS: Investigation, Writing – review & editing. KG: Conceptualization, Data curation, Formal analysis, Funding acquisition, Project administration, Resources, Supervision, Writing – review & editing.

Funding

The author(s) declare financial support was received for the research, authorship, and/or publication of this article. AA and KG were supported by the Polish National Science Centre Research Grant PRELUDIUM BIS number 2019/35/O/NZ6/01590. TLMT was funded by a Biotechnology and Biological Sciences Research Council David Phillips Fellowship BB/R011834/1. The APC was co-financed by the Wrocław University of Environmental and Life Sciences.

Acknowledgments

The authors thank dr hab. Krzysztof Matkowski and Department of Plant Protection, Wroclaw University of Environmental and Life Sciences for giving us the access to Biolog Phenotype Microarrays instrument.

Conflict of interest

The authors declare that the research was conducted in the absence of any commercial or financial relationships that could be construed as a potential conflict of interest.

The author(s) declared that they were an editorial board member of Frontiers, at the time of submission. This had no impact on the peer review process and the final decision.

Publisher's note

Supplementary material

The Supplementary material for this article can be found online at: https://www.frontiersin.org/articles/10.3389/fmicb.2023.1340143/full#supplementary-material

References

Alenazy, R. (2022). Antibiotic resistance in Salmonella: targeting multidrug resistance by understanding efflux pumps, regulators and the inhibitors. *J King Saud Univ Sci.* 34:102275. doi: 10.1016/j.jksus.2022.102275

Asmar, A. T., and Collet, J. F. (2018). Lpp, the Braun lipoprotein, turns 50—major achievements and remaining issues. *FEMS Microbiol. Lett.* 365:fny199. doi: 10.1093/femsle/fny199

Ayukekbong, J. A., Ntemgwa, M., and Atabe, A. N. (2017). The threat of antimicrobial resistance in developing countries: causes and control strategies. *Antimicrob. Resist. Infect. Control* 6:47. doi: 10.1186/s13756-017-0208-x

Bailey, J. D., Shaw, A., McNeill, E., Nicol, T., Diotallevi, M., Chuaiphichai, S., et al. (2020). Isolation and culture of murine bone marrow-derived macrophages for nitric oxide and redox biology. *Nitric Oxide* 100-101, 17–29. doi: 10.1016/j.niox.2020.04.005

Boughner, L. A., and Doerrler, W. T. (2012). Multiple deletions reveal the essentiality of the DedA membrane protein family in *Escherichia coli*. *Microbiology* 158, 1162–1171. doi: 10.1099/mic.0.056325-0

Centers for Disease Control and Prevention (2019). *Antibiotic resistance threats in the United States*, Centers for Disease Control and Prevention (United States) 2019

Cherepanov, W. W. (1995). Gene disruption in *Escherichia coli*: Tc R and km R cassettes with the option of Flp-catalyzed excision of the antibiotic-resistance determinant. *Gene* 158, 9–14. doi: 10.1016/0378-1119(95)00193-a

Datsenko, K. A., and Wanner, B. L. (2000). One-step inactivation of chromosomal genes in *Escherichia coli* K-12 using PCR products. *Proc. Natl. Acad. Sci.* 97, 6640–6645. doi: 10.1073/pnas.120163297

Davlieva, M., Zhang, W., Arias, C. A., and Shamoo, Y. (2013). Biochemical characterization of cardiolipin synthase mutations associated with daptomycin resistance in enterococci. *Antimicrob. Agents Chemother.* 57, 289–296. doi: 10.1128/AAC.01743-12

Dunkley, E. J., Chalmers, J. D., Cho, S., Finn, T. J., and Patrick, W. M. (2019). Assessment of phenotype microarray plates for rapid and high-throughput analysis of collateral sensitivity networks. *PloS One* 14:e0219879. doi: 10.1371/journal.pone.0219879

Ernst, R. K., Guina, T., and Miller, S. I. (1999). How Intracellular Bacteria survive: surface modifications that promote resistance to host innate immune responses. *J Infect Dis* 179, S326–S330. doi: 10.1086/513850

Falagas, M. E., Vouloumanou, E. K., Samonis, G., and Vardakasa, K. Z. (2016). Fosfomycin. Clin Microbiol rev. American society for. *Microbiology* 29, 321–347. doi: 10.1128/CMR.00068-15

Finn, R. D., Bateman, A., Clements, J., Coggill, P., Eberhardt, R. Y., Eddy, S. R., et al. (2014). Pfam: the protein families database. *Nucleic Acids Res.* 42, D222–D230. doi: 10.1093/nar/gkt1223

Garneau-Tsodikova, S., and Labby, K. J. (2016). Mechanisms of resistance to aminoglycoside antibiotics: overview and perspectives. *Medchemcomm* 7, 11–27. doi: 10.1039/c5md00344j

Gordon, S. (1999). *Phagocytosis: The host*. Stamford, CT: JAI Press.

Guard-Bouldin, J., Morales, C. A., Frye, J. G., Gast, R. K., and Musgrove, M. (2007). Detection of *Salmonella enterica* subpopulations by phenotype microarray antibiotic resistance patterns. *Appl. Environ. Microbiol.* 73, 7753–7756. doi: 10.1128/AEM.01228-07

Hantke, K., and Braun, V. (1973). Covalent binding of lipid to protein diglyceride and amide-linked fatty acid at the N-terminal end of the Murein-lipoprotein of the *Escherichia coli* outer membrane Eur. *J. Biochem.* 34, 284–296. doi: 10.1111/j.1432-1033.1973.tb02757.x

Havelaar, A. H., Kirk, M. D., Torgerson, P. R., Gibb, H. J., Hald, T., Lake, R. J., et al. (2015). World Health Organization global estimates and regional comparisons of the burden of foodborne disease in 2010. *PLoS Med.* 12:e1001923. doi: 10.1371/journal.pmed.1001923

Hecht, S. M. (2000). Bleomycin: new perspectives on the mechanism of action. *J. Nat. Prod.* 63, 158–168. doi: 10.1021/np990549f

Huerta-Cepas, J., Szklarczyk, D., Heller, D., Hernández-Plaza, A., Forslund, S. K., Cook, H., et al. (2019). Egg NOG 5.0: a hierarchical, functionally and phylogenetically annotated orthology resource based on 5090 organisms and 2502 viruses. *Nucleic Acids Res.* 47, D309–D314. doi: 10.1093/nar/gky1085

Ize, B., Stanley, N. R., Buchanan, G., and Palmer, T. (2003). Role of the *Escherichia coli* tat pathway in outer membrane integrity. *Mol. Microbiol.* 48, 1183–1193. doi: 10.1046/j.1365-2958.2003.03504.x

Jacobs, C., Huang, L.-J., Bartowsky, E., Normark, S., and Park, J. T. (1994). Bacterial cell wall recycling provides cytosolic muropeptides as effectors for-lactamase induction. *EMBO J.* 13, 4684–4694. doi: 10.1002/j.1460-2075.1994.tb06792.x

Kadner, R. J. (1996). Cytoplasmic membrane. *Cell. Mol. Biol.* 1, 58–87.

Käll, L., Krogh, A., and Sonnhammer, E. L. L. (2007). Advantages of combined transmembrane topology and signal peptide prediction-the Phobius web server. *Nucleic Acids Res.* 35, W429–W432. doi: 10.1093/nar/gkm256

Kelley, L. A., Mezulis, S., Yates, C. M., Wass, M. N., and Sternberg, M. J. E. (2015). The Phyre2 web portal for protein modeling, prediction and analysis. *Nat. Protoc.* 10, 845–858. doi: 10.1038/nprot.2015.053

Kolenda, R., Burdukiewicz, M., Wimonc, M., Aleksandrowicz, A., Ali, A., Szabo, I., et al. (2021). Identification of natural mutations responsible for altered infection phenotypes of *Salmonella enterica* clinical isolates by using cell line infection screens. *Appl. Environ. Microbiol.* 87, e02177–e02120. doi: 10.1128/AEM.02177-20

Kristian, S. A., Datta, V., Weidenmaier, C., Kansal, R., Fedtke, I., Peschel, A., et al. (2005). D-alanylation of teichoic acids promotes group a Streptococcus antimicrobial peptide resistance, neutrophil survival, and epithelial cell invasion. *J. Bacteriol.* 187, 6719–6725. doi: 10.1128/JB.187.19.6719-6725.2005

Krogh, A., Larsson, B., Von Heijne, G., and Sonnhammer, E. L. L. (2001). Predicting transmembrane protein topology with a hidden Markov model: application to complete genomes. *J. Mol. Biol.* 305, 567–580. doi: 10.1006/jmbi.2000.4315

Langridge, G. C., Phan, M. D., Turner, D. J., Perkins, T. T., Parts, L., Haase, J., et al. (2009). Simultaneous assay of every *Salmonella Typhi* gene using one million transposon mutants. *Genome Res.* 19, 2308–2316. doi: 10.1101/gr.097097.109

Lei, J., Sun, L., Huang, S., Zhu, C., Li, P., He, J., et al. (2019). The antimicrobial peptides and their potential clinical applications. *Am. J. Transl. Res.* 11, 3919–3931.

Levengood, S. K., Beyer, W. F., and Webster, R. E. (1991). TolA: a membrane protein involved in colicin uptake contains an extended helical region. *Nati. Acad. Sci. USA.* 88, 5939–5943. doi: 10.1073/pnas.88.14.5939

Levengood-Freyermuth, S. K., Click, E. M., and Webster, R. E. (1993). Role of the carboxyl-terminal domain of TolA in protein import and integrity of the outer membrane. *J. Bacteriol.* 175, 222–228. doi: 10.1128/jb.175.1.222-228.1993

Lima, L. M., Silva, B. N. M., Barbosa, G., and Barreiro, E. J. (2020). β-Lactam antibiotics: an overview from a medicinal chemistry perspective. *Eur. J. Med. Chem.* 208:112829. doi: 10.1016/j.ejmech.2020.112829

Malinverni, J. C., and Silhavy, T. J. (2011). Assembly of outer membrane β-barrel proteins: the bam complex. *Eco Sal Plus.* 4, 16–23. doi: 10.1128/ecosalplus.4.3.8

Matz, C., and Jürgens, K. (2001). Effects of hydrophobic and electrostatic cell surface properties of bacteria on feeding rates of heterotrophic nanoflagellates. *Appl. Environ. Microbiol.* 67, 814–820. doi: 10.1128/AEM.67.2.814-820.2001

Mitchell, A. M., Wang, W., and Silhavy, T. J. (2017). Novel RpoS-dependent mechanisms strengthen the envelope permeability barrier during stationary phase. *J. Bacteriol.* 199, e00708–e00716. doi: 10.1128/JB.00708-16

Monack, D. M., Raupach, B., Hromockyj, A. E., and Falkow, S. (1996). *Salmonella typhimurium* invasion induces apoptosis in infected macrophages source. *Proc. Natl. Acad. Sci. U. S. A.* 93, 9833–9838. doi: 10.1073/pnas.93.18.9833

Mouslim, C., Cano, D. A., and Casadesús, J. (1998). The sfiX, rfe and metN genes of Salmonella typhimurium and their involvement in the his (c) pleiotropic response. *Mol. Gen. Genet.* 259, 46–53. doi: 10.1007/s004380050787

Murata, T., Tseng, W., Guina, T., Miller, S. I., and Nikaido, H. (2007). PhoPQ-mediated regulation produces a more robust permeability barrier in the outer membrane of *Salmonella enterica* serovar typhimurium. *J. Bacteriol.* 189, 7213–7222. doi: 10.1128/JB.00973-07

Nikaido, H. (2003). Molecular basis of bacterial outer membrane permeability revisited. *Microbiol. Mol. Biol. Rev.* 67, 593–656. doi: 10.1128/mmbr.67.4.593-656.2003

Nikolaidis, I., Favini-Stabile, S., and Dessen, A. (2014). Resistance to antibiotics targeted to the bacterial cell wall. *Protein Sci.* 23, 243–259. doi: 10.1002/pro.2414

O'Neil, J. (2016). *Antimicrobial resistance: Tackling a crisis for the health and wealth of nations*. London, United Kingdom: Antimicrobial Resistance.

Oguri, T., Yeo, W. S., Bae, T., and Lee, H. (2016). Identification of envC and its cognate amidases as novel determinants of intrinsic resistance to cationic antimicrobial peptides. *Antimicrob. Agents Chemother.* 60, 2222–2231. doi: 10.1128/AAC.02699-15

Papanastasiou, M., Orfanoudaki, G., Kountourakis, N., Koukaki, M., Sardis, M. F., Aivaliotis, M., et al. (2016). Rapid label-free quantitative analysis of the *E. coli* BL21(DE3) inner membrane proteome. *Proteomics* 16, 85–97. doi: 10.1002/pmic.201500304

Parsons, L. M., Lin, F., and Orban, J. (2006). Peptidoglycan recognition by pal, an outer membrane lipoprotein. *Biochemistry* 45, 2122–2128. doi: 10.1021/bi052227i

Peschel, A. (2002). How do bacteria resist human antimicrobial peptides? *Trends Microbiol.* 10, 179–186. doi: 10.1016/s0966-842x(02)02333-8

Petersen, T. N., Brunak, S., Von Heijne, G., and Nielsen, H. (2011). SignalP 4.0: discriminating signal peptides from transmembrane regions. *Nat. Methods* 8, 785–786. doi: 10.1038/nmeth.1701

Reygaert, C. (2018). An overview of the antimicrobial resistance mechanisms of bacteria. *AIMS Microbiol* 4, 482–501. doi: 10.3934/microbiol.2018.3.482

Rida, S., Caillet, J., and Alix, J. H. (1996). Amplification of a novel gene, sanA, abolishes a vancomycin-sensitive defect in *Escherichia coli*. *J. Bacteriol.* 178, 94–102. doi: 10.1128/jb.178.1.94-102.1996

Shea, A., Wolcott, M., Daefler, S., and Rozak, D. A. (2012). Biolog phenotype microarrays. *Methods Mol. Biol.* 881, 331–373. doi: 10.1007/978-1-61779-827-6_12

Silhavy, T. J., Kahne, D., and Walker, S. (2010). The bacterial cell envelope. *Cold Spring Harb. Perspect. Biol.* 2:a000414. doi: 10.1101/cshperspect.a000414

Singhal, L., Sharma, M., Verma, S., Kaur, R., Britto, X. B., Kumar, S. M., et al. (2018). Comparative evaluation of broth microdilution with polystyrene and glass-coated plates, agar dilution, E-test, vitek, and disk diffusion for susceptibility testing of colistin and polymyxin B on carbapenem-resistant clinical isolates of *acinetobacter baumannii*. *Microb. Drug Resist.* 24, 1082–1088. doi: 10.1089/mdr.2017.0251

Sun, J., Rutherford, S. T., Silhavy, T. J., and Huang, K. C. (2022). Physical properties of the bacterial outer membrane. *Nat. Rev. Microbiol.* 20, 236–248. doi: 10.1038/s41579-021-00638-0

Thomas, P. D., Campbell, M. J., Kejariwal, A., Mi, H., Karlak, B., Daverman, R., et al. (2003). PANTHER: a library of protein families and subfamilies indexed by function. *Genome Res.* 13, 2129–2141. doi: 10.1101/gr.772403

Thurston, T. L. M., Matthews, S. A., Jennings, E., Alix, E., Shao, F., Shenoy, A. R., et al. (2016). Growth inhibition of cytosolic Salmonella by caspase-1 and caspase-11 precedes host cell death. *Nat. Commun.* 7:13292. doi: 10.1038/ncomms13292

Typas, A., Banzhaf, M., Gross, C. A., and Vollmer, W. (2012). From the regulation of peptidoglycan synthesis to bacterial growth and morphology. *Nat. Rev. Microbiol.* 10, 123–136. doi: 10.1038/nrmicro2677

Viau, C., Le Sage, V., Ting, D. K., Gross, J., and Le Moual, H. (2011). Absence of PmrAB-mediated phosphoethanolamine modifications of *Citrobacter rodentium* lipopolysaccharide affects outer membrane integrity. *J. Bacteriol.* 193, 2168–2176. doi: 10.1128/JB.01449-10

Yadav, A. K., Espaillat, A., and Cava, F. (2018). Bacterial strategies to preserve cell wall integrity against environmental threats. *Front. Microbiol.* 9:2064. doi: 10.3389/fmicb.2018.02064

Yu, N. Y., Wagner, J. R., Laird, M. R., Melli, G., Rey, S., Lo, R., et al. (2010). PSORTb 3.0: improved protein subcellular localization prediction with refined localization subcategories and predictive capabilities for all prokaryotes. *Bioinformatics* 26, 1608–1615. doi: 10.1093/bioinformatics/btq249

5. 2nd manuscript

5.1. Foreword to the 2nd manuscript

A) Rationale of research objectives and hypotheses

Our previous study (**M1**) emphasized the significance of SanA in altering the physicochemical properties of the bacterial membrane, such as permeability, charge and hydrophobicity. According to the findings, these modifications play a crucial role in determining the antibiotic resistance and promoting the intracellular persistence of *S.* Typhimurium (**M1**). Moreover, the prior research revealed that a specific 10-nucleotide deletion in the *sanA* correlates with increased bacterial invasiveness in human cell line (**Chapter 1.5**). The mechanism underlying this phenotype, however, has not been identified to date.

In light of these findings, the **M2** aimed to conduct a thorough examination of SanA's expression during infection, its subcellular localization, and its interplay with one of the key *Salmonella* virulence factors– *Salmonella* Pathogenicity Island 1 (SPI-1). Furthermore, it delved into SanA's influence on the infection process of *Salmonella in vitro*. These research goals were designed to test **H3** and **H4**, which propose that SanA plays a role in the initial phases of *Salmonella* infection. The deletion of the *sanA* might result in increased invasiveness in mammalian cell models, which is linked to enhanced membrane permeability. This alternation is believed to facilitate better nutrient absorption, which is associated with a heightened expression of SPI-1 in the *sanA*-deficient strain, thereby further contributing to its elevated invasive capabilities.

B) Methodology and techniques

- Investigation of the subcellular localization of SanA utilizing fractionation and newly generated anti-SanA antibody,
- Preparation of the transcriptional fusion of *sanA* with luciferase (*sanA*$_{RBS}$*::luc*) and analysis of the environmental conditions that induce *sanA* expression,
- Determination of the *sanA* expression pattern during infection of a mouse bone marrow macrophages (iBMDMs),

- Quantification of bacterial invasion in mammalian cells using gentamycin protection assays with strains 4/74WT, 4/74*ΔsanA*, 4/74*ΔsanA*+pWSK29-*sanA* and 4/74*ΔsanA*+pWSK29, along with human intestinal epithelial cells (Caco-2) and iBMDMs,
- Investigation of the relationship between *sanA* and SPI-1 under varying nutrient levels (0 % representing low, 0.5 % as moderate, and 2 % as high), employing reporter systems with green fluorescent protein (GFP) and mCherry. These reporters were employed in both flow cytometry and Western blot analyses to explore this phenomenon at the levels of promoter activity and protein expression, respectively.

C) Results

Our key findings include that:

- SanA is localized in the inner membrane of *Salmonella* (**Fig. 1** in **M2**).
- SanA is expressed on the highest level in bacteria entering the late exponential and early stationary growth phases (**Fig. 2A** in **M2**). During infection, the highest expression is detected after 24 h, what is further associated with a significantly higher replication of the deletion mutant as compared to the WT within immortalized macrophages (**Fig. 2B** in **M2**).
- The number of invading WT bacteria is significantly lower than *ΔsanA*, which reveals more than 32 % and about 42 % higher invasiveness towards Caco-2 and iBMDM, respectively (**Fig. 3A** and **3B** in **M2**). This phenotype is observed only among bacteria growing until stationary growth phase.
- The *sicA* expression is significantly higher in *ΔsanA* on both, protein and promoter activity level, with the differences detect in the early stationary growth phase (**Fig. 4A** in **M2**).
- When bacteria grow in LB containing 2 % nutrients, we observe the highest (>86 %) population of cells where the *sicA* promoter is active for both, WT and *ΔsanA*, whereas the lowest percentage of on state population is showed with the absence of the nutrients (<66 %) (**Fig. 5**, **Fig. S4** in **M2**). Furthermore, in the presence of 0.5 % nutrients, there is a shift for *ΔsanA* as compared to WT, as the population of cells where the *sicA* promoter was active was 62 % and 83 %, respectively (**Fig. 5**, **Fig. S4** in **M2**).

D) Conclusions

We conclude that the inner membrane protein SanA is important for *Salmonella* stress environment response regulation, which is a significant aspect of both *Salmonella* entry and survival in macrophages and the hostile gastric tract. We also suggest that SanA is a mediator of virulence genes hosted in the SPI-1 genomic region, which in turn are modulated in a nutrient availability-dependent manner.

5.2. Copy of the 2nd manuscript

Aleksandrowicz A., Kolenda R., Thurston T., Grzymajło K. SanA is an inner membrane protein mediating early stages of *Salmonella* infection. 2024. bioRxiv preprint doi: https://doi.org/10.1101/2024.01.05.574334

SanA is an inner membrane protein mediating the early stages of Salmonella infection

Adrianna Aleksandrowicz[1], Rafał Kolenda[1], Teresa L M Thurston[2], Krzysztof Grzymajło[1*]

[1]Wrocław University of Environmental and Life Sciences; Faculty of Veterinary Medicine; Department of Biochemistry and Molecular Biology, Poland

[2]Centre for Bacterial Resistance Biology, Department of Infectious Disease, Imperial College London, SW7 2AZ, UK

*corresponding author:

Krzysztof Grzymajło; Mailing address: Wrocław University of Environmental and Life Sciences, Faculty of Veterinary Medicine, Department of Biochemistry and Molecular Biology, 50-375 Wrocław, Poland;

E-mail: krzysztof.grzymajlo@upwr.edu.pl

ORCID: https://orcid.org/0000-0002-1163-0679

Abstract

Bacterial membrane proteins, crucial for the interaction with the environment, encompass various functional molecules such as SanA. SanA is pivotal for the physicochemical properties of the bacterial membrane, influencing *Salmonella*'s antibiotic resistance and infection phenotype. Previous studies identified a link between *sanA* mutation and increased *Salmonella* invasiveness, but the mechanisms underlying this phenomenon remain largely unexplored. Therefore, our research investigates SanA's role during *Salmonella* infection, examining its expression pattern, localization within the cell, and association with *Salmonella* Pathogenicity Island I (SPI-I). Using subcellular fractionation and Western Blotting we revealed that SanA is predominantly located in the inner membrane. Additionally, we utilized transcriptional fusion to monitor SanA expression under various environmental conditions. We observed that SanA plays a significant role during the late exponential and early stationary growth phase and remains important 24 hours after the bacteria enter host cells. Moreover, our invasion assays demonstrated that deletion of *sanA* in bacteria grown to early stationary phase significantly enhances their invasiveness, partly due to increased SPI-I expression, which is regulated in a nutrient availability-dependent manner. Our results highlight SanA's essential role in *Salmonella*'s response to environmental stress, critical for its entry and survival in hostile environments. This research underscores the importance of inner membrane proteins in bacterial pathogenicity, particularly in the initial stages of infection.

Keywords: SanA, inner membrane, invasion, *Salmonella*, SPI-I, pathogenicity, infection

Introduction

Salmonella enterica stands out as one of the most prominent bacterial pathogens, causing food-borne diseases with significant morbidity and mortality in both humans and livestock (Ferrari et al., 2019). A critical stage in *Salmonella*'s pathogenicity depends on its ability to adhere to and invade host cells (Pizarro-Cerdá and Cossart, 2006). The bacterial structures employed in these processes vary widely, extending from monomeric proteins and multimeric macromolecules to intricate molecular machines. Notable for *Salmonella*, specialized type III secretion system (T3SS) encoded by genes of *Salmonella* Pathogenicity island I (SPI-I) and II (SPI-II) facilitate bacteria to invade and survive within phagocytic and non-phagocytic cells. It includes mechanisms that involve the translocation of the effector proteins into the host cell, thereby altering vesicular trafficking and cytoskeletal dynamics (Coburn et al., 2007).

Salmonella evades the host's intracellular immune responses and persists in adverse environments by developing a sophisticated and complex cell envelope, which not only offers protection but also facilitates the selective passage of nutrients from the outside and removal of waste products from the inside (Silhavy et al., 2010). The envelope bilayer, composed of an outer membrane (OM) and an inner membrane (IM), showcases complexity and versatility, highlighted by numerous embedded proteins, each playing a specialized role. The OM with tightly packed lipopolysaccharide (LPS), provides a range of outer membrane proteins (OMPs) and functions as both a selective barrier and a platform for contact with the external environment (Silhavy et al., 2010). OMPs, including porins and efflux pumps, balance nutrient uptake and toxin exclusion, thus ensuring cellular homeostasis and protecting against threats like xenobiotics by moderating their intracellular accumulation (Sun et al., 2022). On the other hand, the IM, although less directly exposed to extracellular environments, harbors inner membrane proteins (IMPs) that participate in vital cellular processes, such as ATP synthesis and nutrient translocation (Silhavy et al., 2010). The synergistic interplay between OMPs and IMPs complexes constitutes a key adaptive mechanism in bacterial response to environmental stressors. These interactions strengthen the bacterial cell's permeability barrier, enhancing resistance to xenobiotics and antimicrobial agents (Boughner and Doerrler, 2012).

Given the diverse functionalities of the bacterial envelope, Gram-negative pathogens utilize various modifications to the membranes, aiming to enhance their resilience to environmental stress and to successfully establish infections. For instance, it was shown that *Enterobacteriaceae* decrease porin expression as a quick response to toxic agents (Dam et al., 2018). Additionally, they modify lipopolysaccharides (LPS) to change the characteristics of the

outer membrane, which helps in avoiding recognition by the host's immune system and enhances their resilience to antimicrobial peptides. These modifications include altering lipid A phosphates, the core oligosaccharide phosphates, and lipid A acylation (Simpson and Trent, 2019). Adding to the complexity, other membrane attributes, like charge and hydrophobicity, modulate bacterial resistance to external stresses and were shown to affect pathogenicity indirectly. It was demonstrated that the efficiency of phagocytosis increases with the hydrophobicity of bacterial cells and that hydrophilic bacteria resist ingestion by phagocytes (Matz and Jürgens, 2001).

The link between membrane permeability and pathogenicity is further highlighted in *Salmonella*. Many of *Salmonella*'s invasion factors, such as T3SS-1, flagella, and chemotactic receptors, are integral components of its envelope. This association suggests a complex interplay between membrane permeability and the expression of virulence factors. Previous studies demonstrated that the expression of *hilD*, a principal regulator of the SPI-I, not only increases membrane permeability but also makes *Salmonella* more susceptible to membrane stress (Sobota et al., 2022). It highlights that the expression of virulence genes, while critical for pathogenesis, can also impose a significant fitness cost on pathogenic bacteria to maintain the balance between virulence and survival. Our current research has spotlighted the role of SanA in modulating the properties of the bacterial membrane, influencing its charge and hydrophobicity, which in turn affects antibiotic resistance and enhances the intracellular survival of *S.* Typhimurium (Aleksandrowicz et al., 2024). Additionally, our previous work demonstrated that a 10-nucleotide deletion in the *sanA* coding sequence is associated with enhanced invasive capabilities of bacteria (Kolenda et al., 2021). However, the mechanism underlying this phenotype has not yet been identified.

In light of these findings, this study aims to conduct a thorough examination of SanA's expression during infection, its subcellular localization, and its interplay with SPI-1. Furthermore, we delve into SanA's influence on the infection process of *Salmonella in vitro*.

Material and Methods

1. Bacteria, plasmids, and growth conditions

Tables 1, **2**, and **3** contain the complete list of bacterial strains, plasmids, and primers used in this study, respectively. All the *Salmonella* strains employed were derived from the *Salmonella* enterica serovar Typhimurium 4/74 wild type (WT). Unless specified otherwise, bacterial

cultures were typically cultivated at 37°C for 16 h (overnight) either in Lysogeny Broth (LB) under dynamic conditions with shaking (180 rpm), or on agar plates. For all invasion studies, *Salmonella* strains were grown under SPI-I-inducing conditions (early stationary growth phase in LB medium; OD_{600}=2.0). When activation of SPI-II was required, the bacterial strains were grown overnight in LB medium and then washed in Mg-MES minimal medium (consisted of: 170 mM 2-(Nmorpholino)ethanesulfonic acid (MES) at pH 5.0, 5 mM KCl, 7.5 mM $(NH_4)_2SO_4$, 0.5 mM K_2SO_4, 1 mM KH_2PO_4, 10 mM $MgCl_2$, 38 mM glycerol, and 0.1 % Casamino Acids), with the pH adjusted to 5.0. The bacteria were then grown for 6 h in the same medium.

If required, antibiotics were supplemented at specific concentrations: 100 µg/ml for Ampicillin (Amp); 50 µg/ml for Kanamycin (Km), and 500 µg/ml for Erythromycin (Ery). For inducing *lac* and *ara* promoters, isopropylthio-β-galactoside (IPTG) was added to a final concentration of 0.5 mM or arabinose to a final concentration of 0.2 %, respectively. Cell growth was analyzed using optical density readings at 600 nm.

Table 1 Bacterial strains used in this study

Strain	Relevant feature(s)	Reference
Salmonella enterica subsp. *enterica* serovar Typhimurium 4/74	wild type (WT)	(Aleksandrowicz et al., 2024)
S. Typhimurium *sanA*$_{RBS}$::*luc*	*sanA*$_{RBS}$::*luc*	This study
S. Typhimurium pFCcGi-p*sicA*	pFCcGi-p*sicA*	This study
S. Typhimurium pFPV25.1GFPmut3Kan-*sicA*-2xHA	pFPV25.1GFPmut3Kan-*sicA*-2xHA	This study
S. Typhimurium 4/74 *ΔsanA*	*S.* Typhimurium 4/74 with *sanA* gene knockout	(Aleksandrowicz et al., 2024)
S. Typhimurium *ΔsanA* pWSK29	pWSK29	(Aleksandrowicz et al., 2024)
S. Typhimurium *ΔsanA* pWSK29-*sanA*	pWSK29-*sanA*	(Aleksandrowicz et al., 2024)
S. Typhimurium *ΔsanA* pFCcGi-p*sicA*	pFCcGi-p*sicA*	This study
S. Typhimurium *ΔsanA* pFPV25.1GFPmut3Kan-*sicA*-2xHA	pFPV25.1GFPmut3Kan-*sicA*-2xHA	This study
E. coli XL1-Blue	*recA1 endA1 gyrA96 thi-1 hsdR17 supE44 relA1 lac [F′*	Wroclaw University of Environmental and

	proAB lacIq Z¨M15 Tn10 (Tetr)]	Life Sciences, Department of Biochemistry and Molecular Biology collection

Table 2 Plasmids used in this study

Plasmid	Relevant feature(s)	Reference
p3121	*luc* template vector, AmpR	(Gerlach et al., 2007)
pFCcGi	vector with arabinose-inducible expression of GFP and constitutive expression of mCherry, AmpR	(Figueira et al., 2013)
pFC-p*sicA*	based on pFCcGi; with constitutive mCherry expression and GFP expression under the control of *sicA* promoter, AmpR	This study
pFPV25.1GFPmut3Kan	plasmid with GFPmut3 under the constitutive *rpsM* promoter, multliple cloning site and hemagglutinin tag (HA), KanR	Dr Rafał Kolenda, Department of Biochemistry and Molecular Biology, Wroclaw University of Environmental and Life Sciences, Wroclaw, Poland
pFPV25.1GFPmut3Kan-*sicA*-2xHA	pFPV25.1GFPmut3Kan vector with *sicA* and its promoter insert, KanR	This study

Table 3 Primers used in this study

Name	Sequence (5'-3')	Reference
sanA-red-luc-for	CCGTTACGCCGGAACAATTGCTTGAACTGGA AAAGAAAAAAGGGAAATGAAGGAGGACAGC TATGGAAGACGCCAAAAACATAAGAA	this study
sanA-red-rev	AAGCGGGAGTAGCAGAAAGGCTAATATGACA AATATCGTCTGTACATCCACGTGTAGGCTGGA GCTGCTTC	this study

sanA-check-seq-for	AGTGTTACGCGGTACCTTCAC	this study
sanA-check-seq-rev	CAATATTGTACGGGATCGGCAT	this study
pFCcGi-sicA-for	ACATACGCGTGCGCCGCGTAAGGCAGTAGC	this study
pFCcGi-sicA-rev	ACATTCTAGATACTTACTCCTGTTATCTGTCACCG	this study
pFCcGi-seq-for	CATACTCCCGCCATTCAG	this study
pFCcGi-seq-rev	GTGTCTTGTAGTTCCCGTC	this study
sicA-2xHASac-for	ACAGAGCTCGCCGCGTAAGGCAGTAGC	this study
sicA-2xHABgl-rev	ACAGATCTTTCCTTTTCTTGTTCACTGTGCTG	this study

2. Cell culture

Human intestinal epithelial cell line Caco-2 (DMSZ, Germany) was grown at 37°C with 5 % CO_2 in Dulbecco's Modified Eagle's Medium (DMEM)/Ham's F-12 supplemented with 1 mM l-glutamine, 100 U/ml penicillin-streptomycin and 10 % fetal bovine serum (FBS) and passaged in the log phase of growth (at a confluency of 80-90 %) according to standard protocols. For infection assays cells were seeded in 24-well plates at a density of $1.2x10^5$ cells and used in experiments after five, six, or seven days.

Immortalized bone marrow-derived macrophages (iBMDM) were maintained in DMEM high glucose supplemented with 20 % (vol/vol) of L929-MCSF supernatant (LCM), 10 % (vol/vol) of FBS 10 mM of HEPES, 1 mM of sodium pyruvate, 0.05 mM of β-mercaptoethanol and 100 U/ml of penicillin/streptomycin and seeded at a concentration of $1x10^6$ or $2x10^5$ cells per well in a 6-well or 24-well plate, respectively 24 h prior infection.

3. Growth curves

To determine the growth curves, LB medium was inoculated with an individual bacterial colony and incubated overnight at 37°C with agitation at 180 rpm. The resulting cultures were then diluted to an optical density (OD_{600}) of 0.05 in LB medium and incubated until the early log-phase growth (OD_{600}=0.5) at 37°C, 220 rpm. Subsequently, cultures were centrifuged, rinsed with 0.9 % NaCl, and resuspended in the same solution. Optical density was assessed and cultures were further diluted in LB medium to achieve a bacterial concentration of $5x10^6$ CFU/ml. Optical density measurements were taken in Tecan Spark Control (Tecan) at 15-

minute intervals over a 16 h period, and the cultures were shaken 30 seconds before each measurement. The study was conducted with a minimum of three independent biological replicates, and dilution series were set up on LB agar plates for verification of the initial bacteria number.

4. Cloning of *sicA* and its promoter

All genes or their promoters were amplified from *S*. Typhimurium 4/74 strain. Amplification was carried out by PCR using Phusion polymerase (Thermo) with primers listed in **Table 3**. PCR products were purified by GeneJET PCR purification kit (Thermo) whereas plasmid DNA was isolated by GeneJET Plasmid Miniprep Kit (Thermo). For creating a dual reporter with constitutive mCherry expression and inducible GFP expression, *sicA* promoter was inserted into pFCcGi plasmid in MluI/XbaI digestion sites. For HA-based reporter, *sicA* with promoter sequences were cloned into pFPV25.1GFPmut3.1Kan-2xHA in SacI/BglII digestion sites. DNA sequence of all the inserts was confirmed by Sanger sequencing.

5. Infection assay

Bacteria were grown under conditions optimizing SPI-I-dependent invasion or SPI-II-dependent replication within macrophages. For SPI-I-inducing conditions, an overnight culture was subcultured in LB at 37°C until the early stationary growth phase (OD_{600}=2.0) (Peterson J. W, 1996). For SPI-II-inducing conditions bacteria were grown until the late stationary growth phase (overnight culture) (Martínez et al., 2014). iBMDM monolayers were infected with stationary phase bacteria opsonized in mouse serum for 20 min using a multiplicity of infection (MOI) of 10:1. To synchronize the infection, the plates were centrifuged for 5 min at 165 x g, followed by a 30-min incubation at 37°C (5 % CO_2). Fresh DMEM supplemented with 100 µg/ml of gentamicin (Gm) was added to kill extracellular bacteria, and the macrophage monolayers were incubated with added Gm for 90 minutes (Monack et al., 1996). After washing with DMEM, the monolayers were lysed in 1 % Triton X-100 and diluted with PBS. Dilutions of the suspension were then plated on LB agar medium to assess the number of viable bacteria. To evaluate intracellular growth, the medium containing 100 µg/ml Gm was replaced with DMEM supplemented with 10 µg/ml of Gm, and parallel cell cultures were examined for viable bacteria 24 h following infection. Similarly, for the Caco-2 invasion assay, early stationary phase bacteria were added to the monolayer until the final MOI=100, cells were treated as described above and CFU/ml of bacteria was determined by plating dilutions of the suspension on LB agar.

6. Determination of SanA expression during infection

Transcriptional fusion was created as described previously by Gerlach et al (Gerlach et al., 2007). Briefly, the p3121 plasmid, carrying luciferase was used as a template and amplified with target gene-specific primers. PCR products were then purified, and the residual template plasmid was removed by a DpnI restriction digest. The resulting PCR product was analyzed by agarose gel electrophoresis and used for electroporation into competent cells of *S.* Typhimurium, harboring pKD46. Proper integration of the reporter cassette was confirmed by colony PCR using sanA-check-seq-for and sanA-check-seq-rev primers and Sanger sequencing. To determine SanA expression during infection, the *S.* Typhimurium *sanA*$_{RBS}$*::luc* strain proceeded in infection assay with the use of iBMDM according to the protocol described above. After lysis with Triton X-100, an equal number of samples were used to determine CFU by dilutional plating, while the rest was collected by centrifugation 3 min, 13,000xg. The pellet was then resuspended in the lysis buffer (100 mM potassium phosphate buffer [pH 7.8], 2 mM EDTA, 1 % [wt/vol] Triton X-100, 5 mg/ml bovine serum albumin, 1 mM DTT, 5 mg/ml lysozyme), incubated 30 min on ice and sonicated. Lysates were then analyzed by the addition of luciferase reagent LAR (Promega) in white microtiter plates using a Tecan plate reader and represented as relative light units (RLU) per $2x10^6$ bacteria.

7. Hemagglutinin-based reporter gene assays and Western Blotting

S. Typhimurium WT and *ΔsanA* strains were transformed with pFPV25.1GFPmut3.1Kan-*sicA*-2xHA construct by electroporation according to Sambrook and Russell (Sambrook and Russell, 2006). For assays, transformants were grown O/N at 37°C, 180 rpm. The next day, cultures were diluted to an OD_{600}=0.05 and grown in SPI-I-inducing conditions, as described above. At indicated time points, the equivalent of bacteria to OD_{600}=0.4 was collected by centrifugation for 4 min at 4°C, 16,100xg (Westermann et al., 2019). For Western Blot analysis, pellets were suspended in 100 µl of loading dye, incubated for 5 min at 95°C, and proceeded with SDS PAGE in a 15 % gel. The separated proteins were transferred using semi-dry transfer (Biorad) onto nitrocellulose and blocked for 1 h at RT with 5 % fat-free dry milk in PBST (PBS supplemented with 0.1 % Tween-20). A 1:1000 dilution of HA-Tag Rabbit mAb (Cell Signalling, C29F4) in PBST was used as a primary antibody, whereas the secondary antibody was Anti-rabbit peroxidase diluted 1:5000 in PBST (Sigma, A6154). The blots were developed with Clarity Western ECL Substrate (BioRad). After the first blotting, the membrane was incubated with 30 % H_2O_2 for 20 min at 37°C to inactivate peroxidase activity (Sennepin et al., 2009). Then, the membrane was washed two times with PBST and processed with Western Blot

as described above, however with GFP Mouse mAb as a primary antibody diluted 1:1000 in PBST (Cell Signalling, 4B10) and Anti-mouse peroxidase (Dako, P0447) as a secondary antibody diluted 1:5000. The Western Blots were developed with the use of Chemidoc XRS+ and analyzed using Image Lab software (BioRad).

8. GFP-based reporter gene assays

The pFC-p*sicA* plasmid, which allows for the detection of GFP under the control of the *sicA* promoter and constitutive expression of mCherry, was constructed by cloning as described above. *S.* Typhimurium WT and *ΔsanA* strains were transformed with constructs by electroporation according to the Sambrook and Russell protocol (Sambrook and Russell, 2006). For assays, transformants were grown O/N at 37°C, 180 rpm. The next day, cultures were diluted to an OD_{600}=0.05 and grown in SPI-I-inducing conditions as described above. At the indicated time points, OD_{600} was measured, equivalent to $3x10^8$ bacteria was collected by centrifugation (6000xg, 5 min, room temperature), and washed with PBS. Next, bacteria were resuspended in PBS, fixed for 30 min in 4 % PFA in the dark, and washed 3 times with PBS. Prior to analysis, bacteria were resuspended in PBS and filtered. Bacteria carrying pFCcGi empty plasmid (mCherry constitutive expression; GFP no expression) or empty plasmid induced by arabinose (mCherry constitutive expression; GFP induced expression) were used as negative and positive GFP controls, respectively. A cellular fluorescence was measured on the BD Fortessa II cell analyzer with Diva 8 software (Becton Dickinson, Franklin Lakes, NJ, USA) with a total of 10,000 events of the bacterial population (gated on Forward Scatter (FSC)-H versus Side Scatter (SSC)-H dot plots). GFP-positive cells were gated on mCherry-positive bacteria and double-positive populations were further analyzed using FlowJo.

9. Generation of an antibody against SanA

The peptide DHRFKHLYGLHRDHHHD, corresponding to amino acid residues 165–184 of SanA, was synthesized and coupled to keyhole limpet hemocyanin (KLH) by Davids Biotechnologie GmbH, Regensburg, Germany. The KLH-coupled peptide was used as immunogen for the generation of rabbit antiserum which was further purified according to protocol used by the company. The optimal concentration of antibody determined for Western Blotting application was 20 µg/ml.

10. Bacteria fractionation

Bacterial cultures were separated at the early stationary growth phase into soluble and membrane fractions by a lysozyme-EDTA-osmotic shock and further, the inner and outer membranes were selectively extracted with Triton X-100 as described previously (Russel and Kazmierczak, 1993). Fractions were resuspended in 30 % SDS with Laemmli buffer (50 mM Tris-HCl pH 6.8, 2 % SDS, 10 % glycerol, 1 % β-mercaptoethanol, 12.5 mM EDTA, 0.02 % bromophenol blue) and proceeded with Western Blotting. Briefly, samples were normalized according to Bicinchoninic acid (BCA) assay (Thermo), separated by SDS-PAGE on 12 % gel, and transferred onto PVDF membrane using a semidry transblot system (Bio-Rad). Next, the membranes were blocked for 1 h at room temperature with 5 % fat-free dry milk in PBST. They were then incubated overnight with a 1:100 dilution of OmpA Rabbit antiserum (as a marker of the outer membrane) and LepB Rabbit antiserum (as a marker of the inner membrane), both of which were gifts from Prof. R. Dalbey, Ohio State University. Additionally, a 1:500 dilution of SanA Rabbit polyclonal antibody in PBST was used. The blots were developed with Clarity Western ECL Substrate (BioRad) with the use of Chemidoc XRS+ and analyzed using Image Lab software (BioRad).

Results

SanA is located in the inner membrane

The subcellular localisation of the SanA has not been determined so far, and our knowledge about its location within bacterial compartments is based solely on bioinformatic prediction tools. Furthermore, the results of these analysis are not consistent, indicating that SanA can be an outer or an inner membrane protein (Aleksandrowicz et al., 2024). To explore this aspect, we aimed to analyze the subcellular localisation of SanA in *Salmonella*.

SanA was identified solely in the inner membrane fraction, co-located in this compartment with the control protein OmpA (**Fig. 1**). The absence of SanA expression in the *ΔsanA* deletion mutant confirmed the specificity of the newly created SanA antibody, evidenced by the absence of non-specific binding. Furthermore, the membrane marker proteins LepB (inner membrane) and OmpA (outer membrane) were detected predominantly in their respective fractions (**Fig. 1**). This observation suggests that the cytoplasmic membrane integrity was maintained without significant disruption during the process of fractionation, ensuring the reliability of the experiment results.

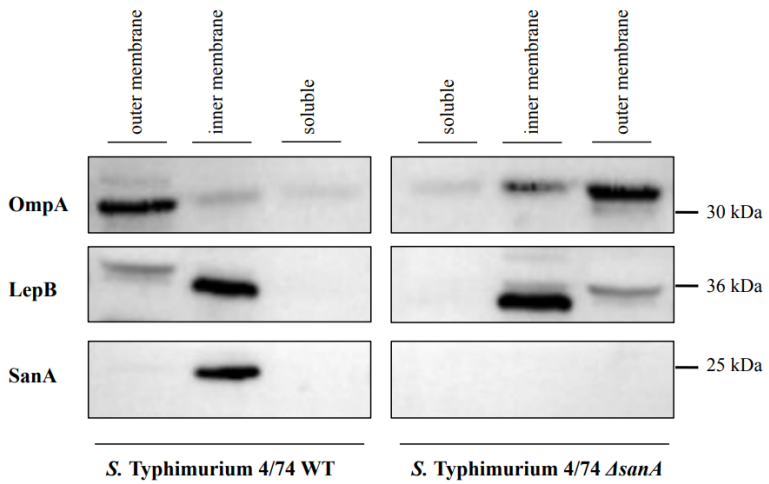

Figure 1 Fractionation of *S.* Typhimurium 4/74 WT and its deletion mutant *ΔsanA* by lysozyme–EDTA method. After fractionation, proteins were subjected to SDS-PAGE. Then, the proteins were blotted onto a PVDF membrane and were probed with the indicated antisera. Proteins from the same number of cells were electrophoresed on each lane. Lane 1, outer membrane fraction; Lane 2, inner membrane fraction; Lane 3, soluble fraction of WT; Lane 4, soluble fraction; Lane 5, inner membrane fraction; Lane 6, outer membrane fraction of *ΔsanA*.

SanA expression is growth-phase dependent and correlates with intracellular survival within macrophages

To examine the impact of diverse *in vitro* conditions on *sanA* expression, an analysis employing transcriptional fusion was carried out. Addition of transcriptional *luc* reporter had no effect on growth kinetics of the bacteria (**Fig. S1**). We observed strong induction of the reporter in bacteria entering the late exponential and early stationary growth phases (**Fig. 2A**). Only a low level of reporter activity was detected in bacteria during the late stationary growth phase (**Fig. 2A**). Upon culturing bacteria in Mg-MES pH 5.0 medium, resembling conditions in infected macrophages, the activity level was comparable to that in the early exponential growth phase (**Fig. 2A**).

Similarly, to determine whether *sanA* is significantly expressed at a specific stage following entry into host cells, macrophages were infected with the reporter strain. Subsequently, cells were lysed at different intervals post-infection for the quantification of luciferase activity. The *sanA* expression was low and comparable between 2 h and 8 h post-infection (**Fig. 2B**). The highest expression was detected after 24 h, what was further associated with the differences in intracellular survival of *Salmonella* within immortalized macrophages.

Indeed, we showed no differences in the intracellular bacteria 8 h post-infection and significantly higher replication of the deletion mutant as compared to the WT strain (**Fig. 2C**).

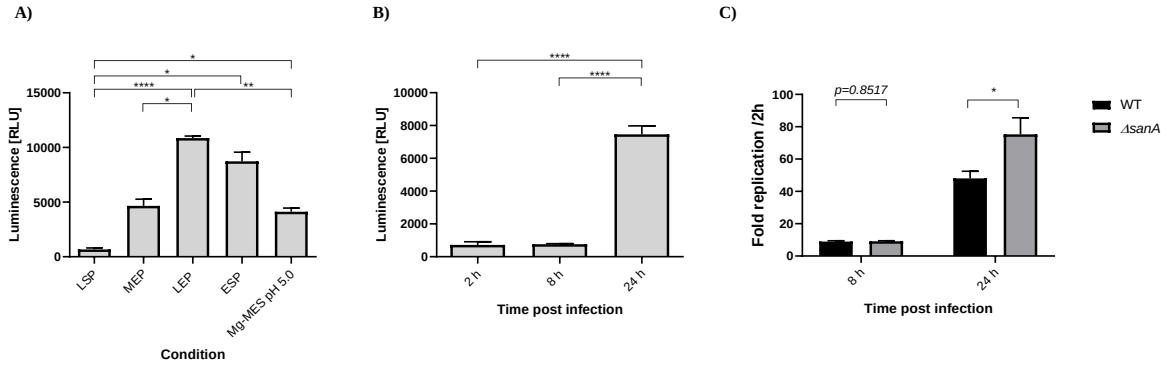

Figure 2 A) *In vitro* expression of a *luc* reporter fused to the *sanA* (*sanA*$_{RBS}$*::luc*) in different growth phases; LSP – late stationary phase (16 h culture); MEP – early exponential phase (OD_{600}=0.5); LEP – late exponential phase (OD_{600}=1.0); ESP – early stationary phase (OD_{600}=2.0); Mg-MES pH 5.0 – SPI-II inducing conditions, mimicking environment of infected macrophages. **B)** *In vitro* expression of a *luc* reporter fused to the *sanA* (*sanA*$_{RBS}$*::luc*) during the infection of immortalized BMDM isolated from C57BL/6 mice. C) Intracellular survival within immortalized BMDM isolated from C57BL/6 mice of *S*. Typhimurium 4/74 and its deletion mutant. The data are shown as mean values and SEM of at least three separate experiments. Statistical differences were analyzed by one-way ANOVA with Tukey's correction (*, $p<0.05$; **, $p < 0.01$; ***, $p<0.001$; ****, $p<0.0001$).

SanA deletion increases the invasion of intestinal epithelial cells and macrophages

Given prior studies indicating a possible involvement of SanA in the initial stages of infection, we utilized invasion assays to examine this phenomenon (Kolenda et al., 2021). Human epithelial cell line Caco-2 and immortalized bone marrow mice macrophages (iBMDM) were infected with SPI-I-induced *Salmonella* strains at the multiplicity of infection (MOI)=100, and MOI=10, respectively. We noticed that the number of invading WT bacteria was significantly lower than *ΔsanA*, which revealed more than 32 % and about 42 % higher invasiveness towards Caco-2 and iBMDM, respectively (**Fig. 3A** and **3B**). Moreover, the complementation of mutation *in trans* restored the WT phenotype, as *ΔsanA*-pWSK29 invaded both cells type significantly better than *ΔsanA*-pWSK29-*sanA* (**Fig. 3A** and **3B**). Invasiveness

towards the Caco-2 cell line was about 16 % higher, whereas in the case of iBMDM 18 % more bacteria invaded the cells.

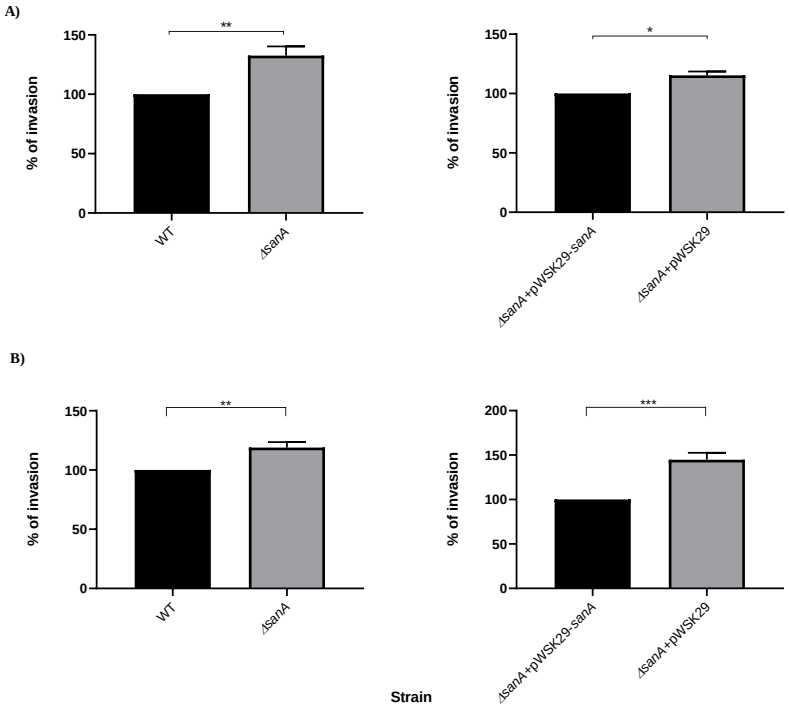

Figure 3. Invasion assay of **A)** Caco-2 cell line and **B)** immortalized bone marrow macrophages isolated from C57BL/6 mice infected by *S.* Typhimurium 4/74, its deletion mutant *ΔsanA* and *ΔsanA* transformed with empty pWSK29 plasmid or vector with *sanA*. The data are shown as mean values and SEM of at least three separate experiments of invasion assay statistical differences were analyzed by Student's t-test (*, $p<0.05$; **, $p < 0.01$).

SanA deletion correlates with enhanced expression of SicA

As we observed higher invasiveness of *Salmonella* because of a SanA knockout, we decided to analyze the molecular basis responsible for this phenotype. Keeping in mind that SPI-I is the main determinant responsible for the invasion of host cells, our examination included a comparative analysis of type III secretion-associated chaperone SicA promoter activity across populations, and protein expression in the WT and *ΔsanA*. For SicA, the differences were detected in the early stationary growth phase, whereas a very low expression with no differences between analyzed strains was shown in the early exponential growth phase (**Fig. 4A**). These results were examined quantitatively in densitometric analysis, where the average relative density of SicA was assessed against the relative density of GFP, used as a protein load control in the bacterial lysates (**Fig. S2**).

These findings are consistent with our FACS analysis of the reporter system based on the GFP under the control of the promoter of interest and constitutive expression of mCherry. This examination showed a greater proportion of the *ΔsanA* population expressed *sicA*, particularly noticeable during the early stationary growth phase (**Fig. 4B, Fig. S3**). In this phase, approximately 72 % of the WT population and about 95 % of the *ΔsanA* population expressed *sicA* (**Fig. 4B, Fig. S3**).

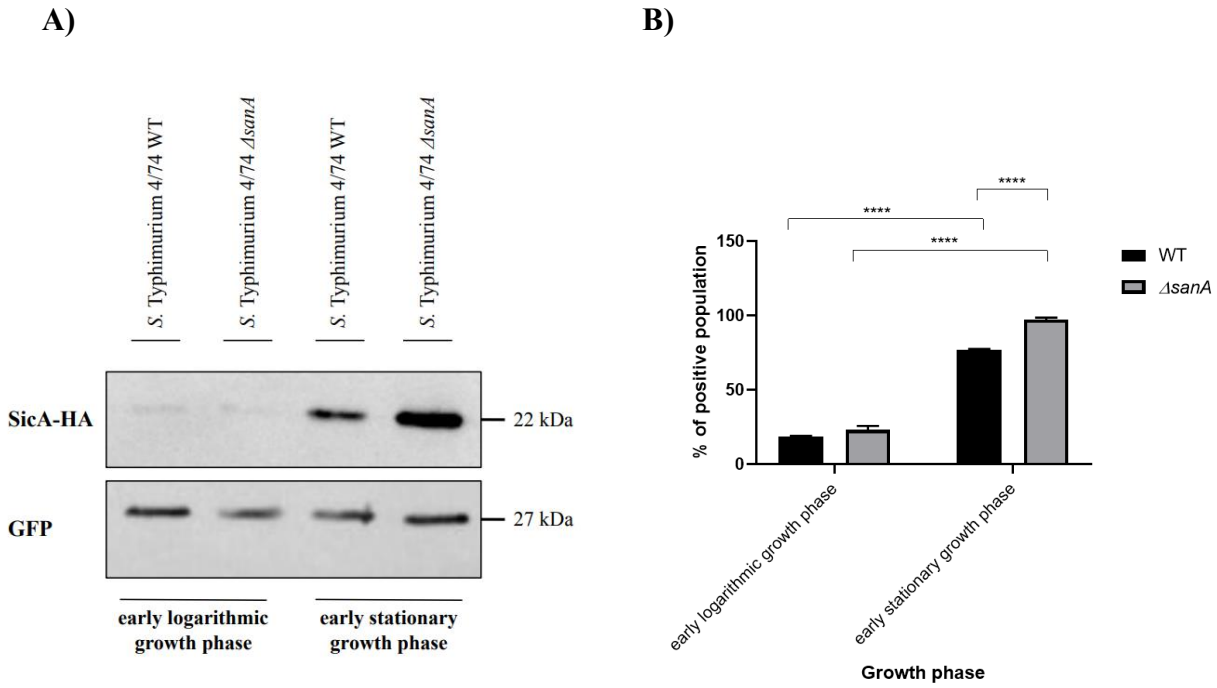

Figure 4 A) Determination of SicA expression by Western Blotting; depending on growth conditions in *S*. Typhimurium 4/74, its deletion mutant *ΔsanA*. Early exponential growth phase corresponding to OD_{600}=0.5; early stationary growth phase corresponding to OD_{600}=2.0; **B)** Fraction of cells expressing *sicA* (on state) during growth in LB medium until early exponential or early stationary growth phase. The fraction of cells in the on state was determined relative to the negative control (100% in the off state), which consisted of the measured fluorescence of cells not expressing the GFP. The data are shown as mean values and SEM of at least three separate experiments. Statistical differences were analyzed by ANOVA (*, $p<0.05$; **, $p < 0.01$).

SPI-I expression in *ΔsanA* is regulated in a nutrient accessibility dependent manner

The observation of a higher expression of SicA in the *sanA* deletion mutant raised a question of what was responsible for this molecular pattern. As previously demonstrated, high

levels of nutrients, resulting from improved accessibility or enhanced transport to bacteria, are associated with heightened virulence in pathogens (Penttinen et al., 2016; Hamed et al., 2019). To address this issue, we employed the abovementioned reporter system to analyse if similar regulation occurs in *S*. Typhimurium. When we grew cells in LB containing 2 % Yeast Extract (YE), we observed the highest (>86 %) population of cells where the *sicA* promoter was active for both, WT and *ΔsanA,* whereas the lowest percentage of on state population was shown with the absence of the yeast extract (<66 %) (**Fig. 5, Fig. S4**). Furthermore, in the presence of 0.5 % YE, there was a shift for *ΔsanA* as compared to WT, as the population of cells where the *sicA* promoter was active was 62 % and 83 %, respectively (**Fig. 5, Fig. S4**).

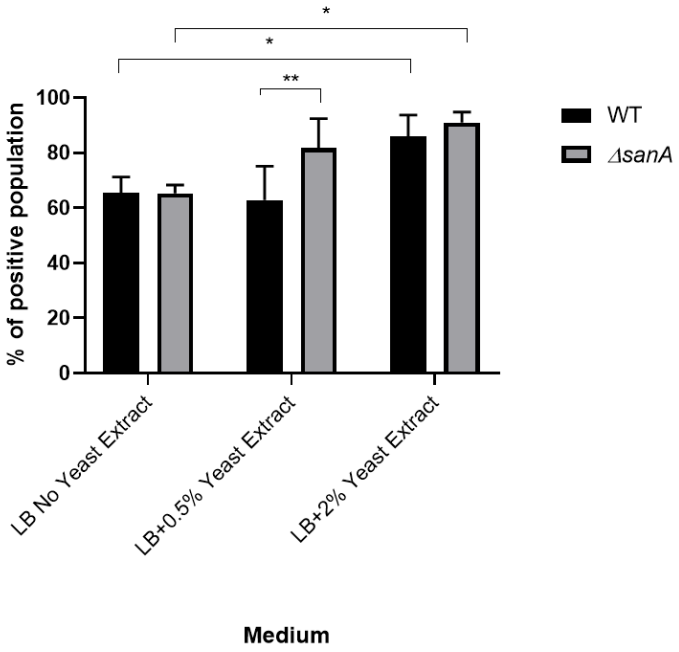

Figure 5 Fraction of cells expressing *sicA* (on state) during growth in LB medium with different concentrations of the yeast extract. The fraction of cells in the on state was determined relative to the negative control (100% in the off state), which consisted of the measured fluorescence of cells not expressing the GFP (without *sicA* promoter). The data are shown as mean values and SEM of at least three separate experiments. Statistical differences were analyzed by ANOVA (*, $p<0.05$; **, $p < 0.01$).

Discussion

Bacterial membranes are composed of numerous proteins that are crucial in the interaction between the pathogen and both the environment and the host (Delcour, 2009; van der Heijden et al., 2016). Among these molecules is SanA, which was first described by Rida et al. in 1996, who identified it as a protein contributing to vancomycin resistance. Specifically, they noted that increased overexpression of SanA reduced the vancomycin sensitivity of *E. coli* mutant with an unidentified envelope permeability defect (Rida et al., 1996). Similarly, *S.* Typhimurium's SfiX, an ortholog of SanA, was found to mitigate the cell division defect caused by HisHF overproduction (Mouslim et al., 1998).

In our previous studies, we confirmed that SanA is a key player in antibiotic resistance and suggested the association of this phenotype with the physicochemical properties of the bacterial membrane (Aleksandrowicz et al., 2024). Furthermore, we showed that a 10-nucleotide mutation in the *sanA*-encoding sequence results in an enhanced invasion of intestinal epithelial cells of human origin (Kolenda et al., 2021). However, the mechanisms underlying this phenotype remain unexplored. Given the current gaps in understanding SanA's role in pathogenicity, our objective was to investigate the impact of SanA on the infection phenotype of *S.* Typhimurium 4/74 and explore the correlation between SanA-dependent membrane permeability and host-pathogen interaction.

Although SanA affects the physicochemical properties of the bacterial membrane its subcellular localization remains unverified (Aleksandrowicz et al., 2024). To address this issue, we investigated whether SanA is anchored in the inner membrane and interacts with the components of the outer membrane, thereby inducing specific modifications in this compartment. Alternatively, we considered whether SanA is an outer membrane protein and independently maintains the integrity of the cell envelope. By employing subcellular fractionation and Western blotting techniques, we unequivocally demonstrated that SanA is indeed an inner membrane protein, which aligns with our initial hypothesis. This situation parallels that of TolA, where a mutation in the *tolA* gene results in heightened permeability of the outer membrane. Similar to SanA, TolA is embedded in the inner membrane through its hydrophobic N-terminal segment, which comprises 21 amino acid residues. It is believed that it interacts with components on the inner surface of the outer membrane through its carboxyl-terminal domain to maintain its integrity (Levengood et al., 1991; Levengood-Freyermuth et al., 1993).

To investigate the role of SanA in *Salmonella* infection, we employed two distinct models: human intestinal epithelial cells and immortalized mouse macrophages. These models allowed us to assess invasiveness and intracellular survival, shedding light on SanA's multifaceted function. Notably, when *Salmonella* was cultured under conditions conducive to the expression of SPI-I, the deletion of *sanA* led to an increase in bacterial invasion of both epithelial cells and macrophages. This finding aligns with our earlier investigation, where we observed enhanced invasiveness due to a 10-nucleotide deletion in *sanA* within a human cell model (Kolenda et al., 2021). Furthermore, this phenomenon correlates with the level of *sanA* expression, as we demonstrated that the protein reached its peak in SPI-I-inducing conditions, particularly during the early stationary growth phase. This observation is consistent with the findings of Kroger et al., who reported a similar expression pattern at the RNA level (Kröger et al., 2013). We propose that the pronounced level of SanA under these conditions is sufficient for the observation of the phenotype, given the substantial difference in expression between the WT and *ΔsanA*. Additionally, in our prior research, we established that the invasiveness level of bacteria remains unchanged when cultivated under conditions that induce the SPI-II (late stationary growth phase), in which the SanA amount is noticeably lower. It suggests a specific association between the phenotype we observed and the correlation between *sanA* expression level and SPI-I (Aleksandrowicz et al., 2024).

Similarly, within the macrophage model, we observed a higher replication rate of *sanA*-deleted bacteria compared to the WT strain after 24 hours of the assay, mirroring the observed pattern of SanA expression during infection. SanA levels increased steadily throughout the assay and were significantly higher after 24 h compared to the 8 h. Moreover, this observation is consistent with outcomes from our previous research, where we demonstrated an analogous pattern in primary bone marrow-derived macrophages. This finding prompted us to hypothesize a correlation between this phenotype, membrane permeability, and the bacterium's resistance toward host immune response (Aleksandrowicz et al., 2024). The dynamic expression levels of bacterial proteins are known to be influenced by the growth phase and environmental conditions. Significantly, inner membrane proteins like RpoS, AcrAB, FtsH, or SecA are typically expressed at relatively high levels during the early stationary growth phase. These proteins play pivotal roles in adapting to stress, nutrient limitations, and the transition from exponential growth to the stationary phase (Fischer et al., 2002; Hsieh et al., 2011; Mitchell et al., 2017; Kapach et al., 2020). Coupled with earlier research from 1998, which indicated that *sanA* deletion inhibits cell division only at temperatures of 43°C or higher, it becomes increasingly plausible that SanA is vital for bacterial adaptation to harsh environments and is

significantly expressed in the stress conditions (Mouslim et al., 1998). The multifaceted role of SanA in *Salmonella* infection emphasizes its significance in the pathogenicity and adaptive response of these bacteria.

Keeping in mind the observed phenotype, our subsequent aim was to elucidate the regulatory dynamics of virulence genes following the host cells invasion. Importantly, our previous genome sequencing data revealed that strain harboring a mutated *sanA* gene displays the gene expression profiles characteristic of highly infectious strains (Kolenda et al., 2021). Therefore, our focus shifts to *sicA*, a crucial component of the *sic-sip* secreted-effector operon within SPI-I known for its essential role in initiating infection. SicA's expression pattern is expected to closely mirror that of *hilA*, a central regulator of SPI-1 genes (Hensel et al., 1998; Deiwick and Hensel, 1999; Chakravortty et al., 2002). To delve into this, we utilized a GFP transcriptional reporter and investigated its expression patterns in the presence or absence of *sanA*. Remarkably, our findings revealed that SPI-1 gene expression was notably up-regulated in *ΔsanA* during the early stationary growth phase, the SPI-I inducing conditions, under which our infection assays were conducted. This observation strongly suggests a direct link between these regulatory dynamics and the presence of SanA. Intriguingly, a similar outcome was reported in 2020 by Kirthinka et al., who highlighted the role of the Lon protease in controlling SPI-1 genes across a range of stress conditions (Kirthika et al., 2020). As previously hypothesized, a high expression of virulence factors may disrupt the integrity of the bacterial membrane (Bustamante et al., 2008). This observation raises an intriguing possibility: the overexpression of T3SS, resulting from *sanA* deletion, may lead to higher membrane permeability. This scenario is consistent with antibiotic resistance mechanisms and the overall infection phenotype, where membrane permeability can significantly influence bacterial survival and virulence. Virulence gene expression can impose a significant fitness cost on pathogenic bacteria (Sobota et al., 2022). Importantly, Sobota et al. discovered that the expression of *hilD*, a key regulator of *Salmonella* virulence genes, can increase membrane permeability and render bacteria more susceptible to stresses that disrupt the bacterial envelope (Sobota et al., 2022). Therefore, it is compelling to conclude that the heightened membrane permeability observed in the mutant strain, coupled with the overexpression of SPI-I in *ΔsanA* is a direct consequence of these interrelated events. This tight regulation of bimodal virulence gene expression serves to hinder the fixation of attenuated mutants during infection, ensuring the transmission of the virulent genotype, and being an example of bacterial adaptation and survival strategies (Sobota et al., 2022).

As the cell envelope plays a crucial role in the interaction between bacteria and their host, any changes within this compartment can significantly impact the infection phenotype. One notable alteration in the cell envelope is enhanced permeability, which allows for more efficient transport of essential nutrients and ions, supporting bacteria survival and proliferation within host cells (Shimizu, 2013; Hamed et al., 2019). Recent research unveiled intriguing connections between nutrient availability and gene expression in bacteria. For example, it has been observed that nutrients such as yeast extract can induce the expression of the SPI-I gene in *Salmonella* (Hamed et al., 2019, 2021). The yeast extract has been found to induce flagellar gene expression via RflP (also known as YdiV) (Wada et al., 2011). Interestingly, this induction does not appear to be driven by a specific metabolite but rather results from the improved growth facilitated by these nutrients. Although yeast extract's exact role in invasion remains unknown, it serves as a chemical signal that modulates both SPI-I and flagellar gene expression. This suggests that yeast extract likely acts as a surrogate for other metabolites present in the distal small intestine (Hamed et al., 2021). With these insights in mind, our research aimed to investigate the correlation between enhanced membrane permeability, increased nutrient transport across membranes, and the expression of *sicA* in *Salmonella*. Our findings demonstrated that *sicA* expression was dependent on the level of yeast extract present in the LB medium for both analyzed *Salmonella* strains. Moreover, we observed a significantly higher content of GFP-positive *ΔsanA* cells when 0.5 % yeast extract was present, a condition like the environment where bacteria grew for infection assays in our experimental setup. Based on these results, we can conclude that increased invasiveness is at least partly a consequence of enhanced SPI-I expression, which, in turn, is regulated in a nutrient-accessibility dependent manner.

Taken together, we conclude that the inner membrane protein SanA is of significance for *Salmonella* stress environment response regulation, which is an important aspect of both *Salmonella* entry and survival in macrophages and the gastrointestinal tract. We suggest that SanA is a mediator of virulence genes hosted in the SPI-1 genomic region. This study adds insight into the fate of *Salmonella* in the absence of SanA and highlights the importance of inner membrane proteins in the context of bacteria pathogenicity, especially in the early stages of infection.

Bibliography

Aleksandrowicz, A., Kolenda, R., Baraniewicz, K., Thurston, T. L. M., Suchański, J., and Grzymajlo, K. (2024). Membrane properties modulation by SanA: implications for xenobiotic resistance in Salmonella Typhimurium. *Front Microbiol* 14. doi: 10.3389/fmicb.2023.1340143.

Boughner, L. A., and Doerrler, W. T. (2012). Multiple deletions reveal the essentiality of the DedA membrane protein family in Escherichia coli. *Microbiology (N Y)* 158, 1162–1171. doi: 10.1099/mic.0.056325-0.

Bustamante, V. H., Martínez, L. C., Santana, F. J., Knodler, L. A., Steele-Mortimer, O., and Puente, J. L. (2008). HilD-mediated transcriptional cross-talk between SPI-1 and SPI-2. Proc Natl Acad Sci U S A, 105(38): 14591–14596. doi: 10.1073/pnas.0801205105

Chakravortty, D., Hansen-Wester, I., and Hensel, M. (2002). Salmonella pathogenicity island 2 mediates protection of intracellular Salmonella from reactive nitrogen intermediates. *Journal of Experimental Medicine*. 195(9):1155-66. doi: 10.1084/jem.20011547.

Coburn, B., Sekirov, I., and Finlay, B. B. (2007). Type III secretion systems and disease. *Clin Microbiol Rev* 20, 535–549. doi: 10.1128/CMR.00013-07.

Dam, S., Pagès, J. M., and Masi, M. (2018). Stress responses, outer membrane permeability control and antimicrobial resistance in enterobacteriaceae. *Microbiology (United Kingdom)* 164, 260–267. doi: 10.1099/mic.0.000613.

Deiwick, J., and Hensel, M. (1999). Regulation of virulence genes by environmental signals in Salmonella typhimurium. in *Electrophoresis* (Wiley-VCH Verlag), 813–817. doi: 10.1002/(SICI)1522-2683(19990101)20:4/5<813::AID-ELPS813>3.0.CO;2-Q.

Delcour, A. H. (2009). Outer membrane permeability and antibiotic resistance. *Biochim Biophys Acta Proteins Proteom* 1794, 808–816. doi: 10.1016/j.bbapap.2008.11.005.

Ferrari, R. G., Rosario, D. K. A., Cunha-Neto, A., Mano, S. B., Figueiredo, E. E. S., and Conte-Juniora, C. A. (2019). Worldwide epidemiology of Salmonella serovars in animal-based foods: A meta-analysis. *Appl Environ Microbiol* 85. doi: 10.1128/AEM.00591-19.

Figueira, R., Watson, K. G., Holden, D. W., and Helaine, S. (2013). Identification of Salmonella pathogenicity island-2 type III secretion system effectors involved in intramacrophage

replication of S. enterica serovar typhimurium: Implications for rational vaccine design. *mBio* 4. doi: 10.1128/mBio.00065-13.

Fischer, B., Rummel, G., Aldridge, P., and Jenal, U. (2002). The FtsH protease is involved in development, stress response and heat shock control in Caulobacter crescentus. *Mol Microbiol* 44, 461–478. doi: 10.1046/j.1365-2958.2002.02887.x.

Gerlach, R. G., Hölzer, S. U., Jäckel, D., and Hensel, M. (2007). Rapid engineering of bacterial reporter gene fusions by using red recombination. *Appl Environ Microbiol*. 73(13):4234-42. doi: 10.1128/AEM.00509-07.

Hamed, S., Shawky, R. M., Emara, M., Slauch, J. M., and Rao, C. V. (2021). HilE is required for synergistic activation of SPI-1 gene expression in Salmonella enterica serovar Typhimurium. *BMC Microbiol* 21. doi: 10.1186/s12866-021-02110-8.

Hamed, S., Wang, X., Shawky, R. M., Emara, M., Aldridge, P. D., and Rao, C. V. (2019). Synergistic action of SPI-1 gene expression in Salmonella enterica serovar typhimurium through transcriptional crosstalk with the flagellar system. *BMC Microbiol* 19, 211. doi: 10.1186/s12866-019-1583-7.

Hensel, M., Shea, J. E., Waterman, S. R., Mundy, R., Nikolaus, T., Banks, G., et al. (1998). Genes encoding putative effector proteins of the type III secretion system of Salmonella pathogenicity island 2 are required for bacterial virulence and proliferation in macrophages. *Mol Microbiol* 30, 163–174. doi: 10.1046/j.1365-2958.1998.01047.x.

Hsieh, Y. H., Zhang, H., Lin, B. R., Cui, N., Na, B., Yang, H., et al. (2011). SecA alone can promote protein translocation and ion channel activity: SecYEG increases efficiency and signal peptide specificity. *Journal of Biological Chemistry* 286, 44702–44709. doi: 10.1074/jbc.M111.300111.

Kapach, G., Nuri, R., Schmidt, C., Danin, A., Ferrera, S., Savidor, A., et al. (2020). Loss of the Periplasmic Chaperone Skp and Mutations in the Efflux Pump AcrAB-TolC Play a Role in Acquired Resistance to Antimicrobial Peptides in Salmonella typhimurium. *Front Microbiol* 11. doi: 10.3389/fmicb.2020.00189.

Kirthika, P., Senevirathne, A., Jawalagatti, V., Park, S. W., and Lee, J. H. (2020). Deletion of the lon gene augments expression of Salmonella Pathogenicity Island (SPI)-1 and metal ion uptake genes leading to the accumulation of bactericidal hydroxyl radicals and host pro-inflammatory

cytokine-mediated rapid intracellular clearance. *Gut Microbes* 11, 1695–1712. doi: 10.1080/19490976.2020.1777923.

Kolenda, R., Burdukiewicz, M., Wimonc, M., Aleksandrowicz, A., Ali, A., Szabo, I., et al. (2021). Identification of Natural Mutations Responsible for Altered Infection Phenotypes of Salmonella enterica Clinical Isolates by Using Cell Line Infection Screens. *Appl Environ Microbiol,* 87(2):e02177-20. doi: 10.1128/AEM.

Kröger, C., Colgan, A., Srikumar, S., Händler, K., Sivasankaran, S. K., Hammarlöf, D. L., et al. (2013). An infection-relevant transcriptomic compendium for salmonella enterica serovar typhimurium. *Cell Host Microbe* 14, 683–695. doi: 10.1016/j.chom.2013.11.010.

Levengood SK, Beyer WF, Webster RE. 1991. TolA: A membrane protein involved in colicin uptake contains an extended helical region. *National Academy of Sciences*. USA. 88(14): 5939–5943. doi: 10.1073/pnas.88.14.5939

Levengood-Freyermuth SK, Click EM, Webster RE. 1993. Role of the Carboxyl-Terminal Domain of TolA in Protein Import and Integrity of the Outer Membrane. *Journal of Bacteriology*. 175(1):222-8. doi: 10.1128/jb.175.1.222-228.1993

Martínez, L. C., Banda, M. M., Fernández-Mora, M., Santana, F. J., and Bustamante, V. H. (2014). HilD induces expression of Salmonella pathogenicity Island 2 genes by displacing the global negative regulator H-NS from ssrAB. *J Bacteriol* 196, 3746–3755. doi: 10.1128/JB.01799-14.

Matz, C., and Jürgens, K. (2001). Effects of hydrophobic and electrostatic cell surface properties of bacteria on feeding rates of heterotrophic nanoflagellates. *Appl Environ Microbiol,* 67, 814–820. doi: 10.1128/AEM.67.2.814-820.2001.

Mitchell, A. M., Wang, W., and Silhavy, T. J. (2017). Novel RpoS-dependent mechanisms strengthen the envelope permeability barrier during stationary phase. *J Bacteriol* 199. doi: 10.1128/JB.00708-16.

Monack DM, Raupach B, Hromockyj AE, Falkow S. 1996. Salmonella typhimurium Invasion Induces Apoptosis in Infected Macrophages Source. *Proc Natl Acad Sci U S A*. 93(18):9833–9838. doi: 10.1073/pnas.93.18.9833

Mouslim, C., Cano, D. A., and Casadesús, J. (1998). The sfiX, rfe and metN genes of Salmonella typhimurium and their involvement in the His(c) pleiotropic response. *Molecular and General Genetics*, 259(1):46-53. doi: 10.1007/s004380050787.

Penttinen, R., Kinnula, H., Lipponen, A., Bamford, J. K. H., and Sundberg, L. R. (2016). High Nutrient Concentration Can Induce Virulence Factor Expression and Cause Higher Virulence in an Environmentally Transmitted Pathogen. *Microb Ecol* 72, 955–964. doi: 10.1007/s00248-016-0781-1.

Peterson J. W (1996). Bacterial Pathogenesis in Medical Microbiology. 4th edition.

Pizarro-Cerdá, J., and Cossart, P. (2006). Bacterial adhesion and entry into host cells. *Cell* 124, 715–727. doi: 10.1016/j.cell.2006.02.012.

Rida, S., Caillet, J., and Alix, J. H. (1996). Amplification of a novel gene, sanA, abolishes a vancomycin-sensitive defect in Escherichia coli. *J Bacteriol*, 178(1):94-102. doi: 10.1128/jb.178.1.94-102.1996.

Russel, M., and Kazmierczak, B. (1993). Analysis of the Structure and Subcellular Location of Filamentous Phage pIV. J Bacteriol, 175(13): 3998–4007. doi: 10.1128/jb.175.13.3998-4007.1993.

Sambrook, J., and Russell, D. W. (2006). Transformation of E. coli by Electroporation . *Cold Spring Harb Protoc*. CSH Protoc, 2006(1):pdb.prot3933. doi: 10.1101/pdb.prot3933.

Sennepin, A. D., Charpentier, S., Normand, T., Sarré, C., Legrand, A., and Mollet, L. M. (2009). Multiple reprobing of Western blots after inactivation of peroxidase activity by its substrate, hydrogen peroxide. *Anal Biochem* 393, 129–131. doi: 10.1016/j.ab.2009.06.004.

Shimizu, K. (2013). Regulation Systems of Bacteria such as Escherichia coli in Response to Nutrient Limitation and Environmental Stresses. *Metabolites* 4, 1–35. doi: 10.3390/metabo4010001.

Silhavy, T. J., Kahne, D., and Walker, S. (2010). The bacterial cell envelope. *Cold Spring Harb Perspect Biol*, 2(5):a000414. doi: 10.1101/cshperspect.a000414.

Simpson, B. W., and Trent, M. S. (2019). Pushing the envelope: LPS modifications and their consequences. *Nat Rev Microbiol* 17, 403–416. doi: 10.1038/s41579-019-0201-x.

Sobota, M., Ramirez, P. N. R., Cambré, A., Rocker, A., Mortier, J., Gervais, T., et al. (2022). The expression of virulence genes increases membrane permeability and sensitivity to envelope stress in Salmonella Typhimurium. *PLoS Biol* 20. doi: 10.1371/journal.pbio.3001608.

Sun, J., Rutherford, S. T., Silhavy, T. J., and Huang, K. C. (2022). Physical properties of the bacterial outer membrane. *Nat Rev Microbiol* 20, 236–248. doi: 10.1038/s41579-021-00638-0.

van der Heijden, J., Reynolds, L. A., Deng, W., Mills, A., Scholz, R., Imami, K., et al. (2016). Salmonella rapidly regulates membrane permeability to survive oxidative stress. *mBio* 7. doi: 10.1128/mBio.01238-16.

Wada, T., Morizane, T., Abo, T., Tominaga, A., Inoue-Tanaka, K., and Kutsukake, K. (2011). EAL domain protein YdiV acts as an anti-FlhD4C2 factor responsible for nutritional control of the flagellar regulon in Salmonella enterica serovar typhimurium. *J Bacteriol* 193, 1600–1611. doi: 10.1128/JB.01494-10.

Westermann, A. J., Venturini, E., Sellin, M. E., Förstner, K. U., Hardt, W. D., and Vogel, J. (2019). The major RNA-binding protein ProQ impacts virulence gene expression in salmonella enterica serovar typhimurium. *mBio* 10. doi: 10.1128/mBio.02504-18.

6. Summary and future prospects

This doctoral thesis significantly advances our understanding of inner membrane proteins and their role in bacterial pathogenicity, contributing to the development of more effective strategies to combat antibiotic resistance. The growing challenge of multidrug resistance in bacteria, especially in key species such as *Salmonella*, *Pseudomonas*, and *Campylobacter*, poses a major public health concern (**Chapter 1.2**). These pathogens employ various mechanisms, including enzymatic barriers and membrane composition modifications, to reduce the efficacy of surface disinfectants and antibiotic treatments, thus thriving in hostile environments. The complex cell envelopes of Gram-negative bacteria, particularly the OM, act as an additional defense line (**Chapter 1.4**). The permeability of this membrane is crucial in determining bacterial susceptibility to antibiotics. Proteins in the IM, although less studied, play a vital role in survival under extreme environmental conditions. Gene variations encoding these proteins can increase membrane permeability, thereby boosting bacterial resilience to environmental stressors. Other membrane characteristics, like charge and hydrophobicity, also influence bacterial resistance to external stresses and indirectly affect pathogenicity (**Chapter 1.4**).

In this context, the protein SanA, predominantly found by our research group in the IM, emerges as a significant factor. However, its specific mechanisms and roles in antibiotic resistance and pathogenicity have remained largely unexplored until now (**Chapter 1.5**). This thesis comprises a series of publications dedicated to unravel SanA's complex role in *Salmonella*. The initial publication paved the way by elucidating the basic functions of SanA in antibiotic resistance, describing how changes in the physicochemical properties of bacterial membranes, influenced by SanA, modify the bacterium's resistance profile to different drugs. Subsequent research further delved into the pathogenic role of SanA, examining its impact on *Salmonella*'s ability to invade and survive within host cells, thereby establishing a link between membrane composition and pathogenic behavior.

Our findings demonstrate that SanA, mainly located in the IM and featuring an unknown DUF218 domain, is pivotal in modifying membrane properties. The absence of *sanA* leads to increased membrane permeability, hydrophilicity, and positive charge. This aligns with our initial hypothesis (**H1**) and lays the foundation for future multidisciplinary research into bacterial membrane biophysics. Techniques like fluorescence spectroscopy, isothermal titration calorimetry, cryo-electron microscopy, and X-ray crystallography could anticipate crucial insights into membrane dynamics and organization, providing high-resolution structural information. The investigation of the lipid profile of *Salmonella* also offers an interesting perspective. Although it is a relatively underexplored area in

bacterial examination, this approach could provide significant information about changes in lipid composition resulting from *sanA* knockout and how these changes affect the homeostasis of bacterial membranes.

Our second hypothesis (**H2**) was confirmed by showing that membrane alterations lead to a changed resistance profile towards various xenobiotics, especially increased sensitivity to membrane-targeting antibiotics. The deletion of *sanA* also resulted in a higher *Salmonella* replication rate within macrophages, suggesting an enhanced ability to resist host immune responses due to increased membrane hydrophilicity, thereby highlighting SanA's role in bacterial survival in hostile environments (**H2**). Keeping all the abovementioned in mind, our second manuscript aimed to correlate increased membrane permeability with enhanced invasiveness resulting from *sanA* knockout. We confirmed that *sanA* deletion and the consequent increase in membrane permeability were linked to the upregulation of other virulence factors responsible for *Salmonella* invasion (**H3** and **H4**). However, it is worth mentioning that our study was limited to a chaperone of SPI-1 – SicA, which served as a determinant of the expression of other genes in this genomic region. Undoubtedly, high-throughput methods like proteomic and transcriptomic analysis, or next-generation sequencing (NGS), would provide a comprehensive overview of the proteome/transcriptome alterations following *sanA* deletion, leading to further functional assays. Due to the complexity of processes involved in *Salmonella* pathogenesis, precise determination of *sanA* function requires in-depth analysis. Considering the simplified research model using cell lines and the significant role of animal reservoirs, extending the research to an *in vivo* model is a crucial direction. Moreover, the role of *sanA* in biofilm formation, particularly in relation to long-term *Salmonella* carriage, should also be of interest (**Chapter 1.2**). A multi-aspect analysis could provide valuable insights, potentially applicable in preventing biofilm formation on either biotic or abiotic surfaces, thereby significantly limiting *Salmonella* spread.

In conclusion, the series of publications offers a detailed analysis of SanA's role in *Salmonella*, shedding light on the complex relationship between bacterial resistance mechanisms and pathogenic behavior. By integrating genetic, biochemical, and infection model studies, we have shown that SanA's impact extends beyond antibiotic resistance, influencing the bacterium's adaptation to stressful environments and interaction with the host immune system. This is particularly relevant given *Salmonella*'s adaptability to various environments, its facultative intracellular lifestyle, and the challenges posed by multidrug-resistant strains in treatment. Therefore, a deep understanding of *Salmonella* is crucial for developing new therapeutic strategies, including those targeting protein-protein interactions or inhibiting the biosynthesis of these molecules, to limit the spread of the pathogens in high-risk areas.

7. Conclusions

The key findings derived from the research carried out in this thesis are as follows:

1. SanA is an inner membrane protein, playing a role in maintaining the integrity of the bacterial membrane.
2. SanA is responsible for the membrane hydrophobicity and negative charge, affecting the bacterium's xenobiotic resistance profile.
3. Alterations in the membrane's physicochemical properties correlate with the bacteria's enhanced ability to resist host immune defense, thereby increasing their intracellular replication
4. SanA is of significance in the regulation of virulence genes, particularly those in the SPI-1 genomic region. This regulation plays a significant role in *Salmonella*'s invasion, linking changes in membrane integrity and nutrient transport to the overexpression of the *sicA* gene.
5. The SanA-depending changes found in *Salmonella* highlights the importance of inner membrane proteins in the context of bacteria pathogenicity and may indicate the potential use of these molecules as new therapeutic targets.

8. Bibliography

1. Evangelopolou G, Bourriel A, Spyrou V. 2018. A concise history of *Salmonella* spp. nomenclature. Journal of the Hellenic Veterinary Medical Society. 61:323.

2. Andino A, Hanning I. 2015. *Salmonella enterica*: Survival, colonization, and virulence differences among serovars. Scientific World Journal. Hindawi Publishing Corporation. 2015:520179

3. Brenner FW, Villar RG, Angulo FJ, Tauxe R, Swaminathan B. 2000. Guest Commentary. *Salmonella* Nomenclature. Journal of Clinical Microbiology. J Clin Microbiol. 38(7):2465–2467

4. Popoff MY, Bockemühl J, Brenner FW, Gheesling LL. 2001. Supplement 2000 (no. 44) to the Kauffmann-White scheme. Res. Microbiol. 152(10):907-9

5. Crouse A, Schramm C, Emond-Rheault J-G, Herod A, Kerhoas M, Rohde J, Gruenheid S, Kukavica-Ibrulj I, Boyle B, T Greenwood CM, Goodridge LD, Garduno R, Levesque RC, Malo D, Daigle F, Crouse CA, J-g E-R. 2020. Combining Whole-Genome Sequencing and Multimodel Phenotyping To Identify Genetic Predictors of *Salmonella* Virulence. 5(3):e00293-20

6. Uzzau S, Brown DJ, Wallis T, Rubino S, Leori G, Bernard S, Casadesu SJ, Platt DJ, Olsen JE. 2000. Host adapted serotypes of *Salmonella enterica*. Epidemiol. Infect. 125(2):229-55

7. European Food Safety Authority. 2022. The European Union One Health 2021 Zoonoses Report. EFSA Journal 20. 20(12):7666

8. Gal-Mor O, Boyle EC, Grassl GA. 2014. Same species, different diseases: How and why typhoidal and non-typhoidal *Salmonella enterica* serovars differ. Front Microbiol. Frontiers Research Foundation. 5:391

9. Feasey NA, Hadfield J, Keddy KH, Dallman TJ, Jacobs J, Deng X, Wigley P, Barquist Barquist L, Langridge GC, Feltwell T, Harris SR, Mather AE, Fookes M, Aslett M, Msefula C, Kariuki S, Maclennan CA, Onsare RS, Weill FX, Le Hello S, Smith AM, McClelland M, Desai P, Parry CM, Cheesbrough J, French N, Campos J, Chabalgoity JA, Betancor L, Hopkins KL, Nair S, Humphrey TJ, Lunguya O, Cogan TA, Tapia MD, Sow SO, Tennant SM, Bornstein K, Levine MM, Lacharme-Lora L, Everett DB, Kingsley RA, Parkhill J, Heyderman RS, Dougan G, Gordon MA, Thomson NR. 2016. Distinct *Salmonella* Enteritidis lineages associated with enterocolitis in high-income settings and invasive disease in low-income settings. Nat Genet. 48:1211–1217.

10. Ward LR, De JDH, Rowe B. 1987. A phage-typing scheme for *Salmonella enteritidis*. Epidem. Inf. 99(2):291-4

11. Ngogo FA, Joachim A, Abade AM, Rumisha SF, Mizinduko MM, Majigo M V. 2020. Factors associated with *Salmonella* infection in patients with gastrointestinal complaints seeking health care at Regional Hospital in Southern Highland of Tanzania. BMC Infect Dis. 20(1):135

12. Motladiile TW, Tumbo JM, Malumba A, Adeoti B, Masekwane NJ, Mokate OMR, Sebekedi OC. 2019. *Salmonella* food-poisoning outbreak linked to the National School Nutrition Programme, North West province, South Africa. S Afr J Infect Dis. 34(1):124

13. Dewey-Mattia D, Manikonda K, Hall AJ, Wise ME, Crowe SJ. 2018. Surveillance for Foodborne Disease Outbreaks — United States, 2009–2015. MMWR Surveill Summ. 67(10):1–11.

14. Ehuwa O, Jaiswal AK, Jaiswal S. 2021. *Salmonella*, food safety and food handling practices. Foods. 10(5): 907

15. Mkangara M. 2023. Prevention and Control of Human *Salmonella enterica* Infections: An Implication in Food Safety. Int J Food Sci. Hindawi Limited. 11:2023:8899596

16. Shaji S, Selvaraj RK, Shanmugasundaram R. 2023. *Salmonella* Infection in Poultry: A Review on the Pathogen and Control Strategies. Microorganisms. Multidisciplinary Digital Publishing Institute (MDPI). 11(11), 2814

17. de Kraker MEA, Stewardson AJ, Harbarth S. 2016. Will 10 Million People Die a Year due to Antimicrobial Resistance by 2050? PLoS Med. 13(11): e1002184

18. Ma F, Xu S, Tang Z, Li Z, Zhang L. 2021. Use of antimicrobials in food animals and impact of transmission of antimicrobial resistance on humans. Biosaf Health. Elsevier B.V. 3:32-38

19. Alenazy R. 2022. Antibiotic resistance in *Salmonella*: Targeting multidrug resistance by understanding efflux pumps, regulators and the inhibitors. J King Saud Univ Sci. Elsevier B.V. 34(7):102275

20. Chen W, Fang T, Zhou X, Zhang D, Shi X, Shi C. 2016. IncHI2 plasmids are predominant in antibiotic-resistant *Salmonella* isolates. Front Microbiol. 7:1566

21. Jacob JJ, Solaimalai D, Rachel T, Pragasam AK, Sugumar S, Jeslin P, Anandan S, Veeraraghavan B. 2022. A secular trend in invasive non-typhoidal *Salmonella* in South India, 2000–2020: Identification challenges and antibiogram. Indian J Med Microbiol. 40:536–540

22. Nadi ZR, Salehi TZ, Tamai IA, Foroushani AR, Sillanpaa M, Dallal MMS. 2020. Evaluation of antibiotic resistance and prevalence of common *Salmonella enterica* serovars isolated from foodborne outbreaks. Microchemical Journal. 155:104660

23. Kariuki S, Gordon MA, Feasey N, Parry CM. 2015. Antimicrobial resistance and management of invasive *Salmonella* disease. Vaccine. Elsevier. 33 Suppl 3(03):C21-9

24. He J, Sun F, Sun D, Wang Z, Jin S, Pan Z, Xu Z, Chen X, Jiao X. 2020. Multidrug resistance and prevalence of quinolone resistance genes of *Salmonella enterica* serotypes in China. Int J Food Microbiol. 2:330:108692

25. Qiao J, Zhang Q, Alali WQ, Wang J, Meng L, Xiao Y, Yang H, Chen S, Cui S, Yang B. 2017. Characterization of extended-spectrum β-lactamases (ESBLs)-producing *Salmonella* in retail raw chicken carcasses. Int J Food Microbiol. 248:72–81

26. Yukawa S, Tamura Y, Tanaka K, Uchida I. 2015. Rapid detection of *Salmonella enterica* serovar Typhimurium DT104 strains by the polymerase chain reaction. Acta Vet Scand. 25:57:59

27. Rice LB. 2012. Mechanisms of resistance and clinical relevance of resistance to β-lactams, glycopeptides, and fluoroquinolones, p. 198–208. In Mayo Clinic Proceedings. Elsevier Ltd. 87(2):198–208

28. Leclercq R. 2002. Mechanisms of Resistance to Macrolides and Lincosamides: Nature of the Resistance Elements and Their Clinical Implications. Clin Infect Dis. 15;34(4):482-92

29. Alexander KA, Warnick LD, Wiedmann M. 2009. Antimicrobial resistant *Salmonella* in dairy cattle in the United States. Vet Res Commun. 33(3):191-209

30. Lima LM, Silva BNM da, Barbosa G, Barreiro EJ. 2020. β-lactam antibiotics: An overview from a medicinal chemistry perspective. Eur J Med Chem. Elsevier Masson. 15:208:112829

31. Garneau-Tsodikova S, Labby KJ. 2016. Mechanisms of resistance to aminoglycoside antibiotics: Overview and perspectives. Medchemcomm. Royal Society of Chemistry. 7, 11-27

32. Wallinga D, Smit LAM, Davis MF, Casey JA, Nachman KE. 2022. A Review of the Effectiveness of Current US Policies on Antimicrobial Use in Meat and Poultry Production. Curr Environ Health Rep. Springer Science and Business Media Deutschland GmbH. 9(2):339–354

33. Gupta R, Sharma S. 2022. Role of alternatives to antibiotics in mitigating the antimicrobial resistance crisis. Indian J Med Res. NLM (Medline). 156(3):464–477

34. Khan CMA. 2014. The Dynamic Interactions between *Salmonella* and the Microbiota, within the Challenging Niche of the Gastrointestinal Tract . Int Sch Res Notices. 2014:1–23

35. Wallis TS, Galyov EE. 2000. Molecular basis of *Salmonella*-induced enteritis. Mol Microbiol. 36(5):997-1005

36. Andres Vazquez-Torres. 2000. Cellular routes of invasion by enteropathogens Vazquez-Torres and Fang. 3(1):54-9

37. Steve Yan S, Pendrak ML, Abela-Ridder B, Punderson JW, Fedorko DP, Foley SL. 2003. An overview of *Salmonella* typing: Public health perspectives. Clin Appl Immunol Rev. 4(3):189-204

38. Velge P, Wiedemann A, Rosselin M, Abed N, Boumart Z, Chaussé AM, Grépinet O, Namdari F, Roche SM, Rossignol A, Virlogeux-Payant I. 2012. Multiplicity of *Salmonella* entry mechanisms, a new paradigm for *Salmonella* pathogenesis. Microbiology open. 1:243–258

39. Dickson K, Lehmann C. 2019. Inflammatory response to different toxins in experimental sepsis models. Int J Mol Sci. MDPI. 20(18):4341

40. Levine MM, Robins-Browne RM. 2012. Factors that explain excretion of enteric pathogens by persons without diarrhea. Clinical Infectious Diseases. 55(Suppl 4):S303–S311

41. Sévellec Y, Vignaud ML, Granier SA, Lailler R, Feurer C, Hello S Le, Mistou MY, Cadel-Six S. 2018. Polyphyletic nature of *Salmonella enterica* serotype derby and lineage-specific host-association revealed by genome-wide analysis. Front Microbiol. 9:891

42. Sabbagh SC, Forest CG, Lepage C, Leclerc JM, Daigle F. 2010. So similar, yet so different: Uncovering distinctive features in the genomes of *Salmonella enterica* serovars Typhimurium and Typhi. FEMS Microbiol Lett. 305(1):1-13

43. Wang M, Qazi IH, Wang L, Zhou G, Han H. 2020. *Salmonella* virulence and immune escape. Microorganisms. MDPI. 8(3):407

44. Hautefort I, Thompson A, Eriksson-Ygberg S, Parker ML, Lucchini S, Danino V, Bongaerts RJM, Ahmad N, Rhen M, Hinton JCD. 2008. During infection of epithelial cells *Salmonella enterica* serovar Typhimurium undergoes a time-dependent transcriptional adaptation that results in simultaneous expression of three type 3 secretion systems. Cell Microbiol. 10:958–984

45. Haraga A, Ohlson MB, Miller SI. 2008. *Salmonellae* interplay with host cells. Nat Rev Microbiol. 6:53-66

46. Coburn B, Sekirov I, Finlay BB. 2007. Type III secretion systems and disease. Clin Microbiol Rev. 20(4):535-49

47. Cornelis GR. 2006. The type III secretion injectisome. Nat Rev Microbiol. 4(11):811-25

48. Watson PR, Paulin SM, Bland AP, Jones PW, Wallis TS. 1995. Characterization of Intestinal Invasion by *Salmonella* typhimurium and *Salmonella* dublin and Effect of a Mutation in the invH Gene. Infection and Immunity. 63(7):2743-54

49. Lou L, Zhang P, Piao R, Wang Y. 2019. *Salmonella* Pathogenicity Island 1 (SPI-1) and Its Complex Regulatory Network. Front Cell Infect Microbiol. Frontiers Media S.A. 31:9:270

50. Friebel A, Ilchmann H, Aepfelbacher M, Ehrbar K, Machleidt W, Hardt WD. 2001. SopE and SopE2 from *Salmonella* typhimurium Activate Different Sets of RhoGTPases of the Host Cell. Journal of Biological Chemistry. 276:34035–34040

51. McGhie E. J, Hayward R. D, Koronakis V. 2001. Cooperation between actin-binding proteins of invasive *Salmonella*: SipA potentiates SipC nucleation and bundling of actin. EMBO J. 20(9): 2131–2139

52. Ahmer BMM, Van Reeuwijk J, Watson PR, Wallis TS, Heffron F. 1999. Salmonella SirA is a global regulator of genes mediating enteropathogenesis. Mol Microbiol. 31:971–982

53. Bajaj V, Lucas R. L, Hwang C, Lee C. A. 1996. Co-ordinate regulation of *Salmonella* typhimurium invasion genes by environmental and regulatory factors is mediated by control of hilA expression. Mol Biol. 22(4):703-14

54. Kato A, Groisman EA. 2008. The PhoQlPhoP Regulatory Network of *Salmonella enterica*. Adv Exp Med Biol. 2008: 631:7-21

55. Lucas RL, Lee CA. 2001. Roles of hilC and hilD in regulation of hilA expression in *Salmonella enterica* serovar typhimurium. J Bacteriol. 183:2733–2745

56. Baxter MA, Fahlen TF, Wilson RL, Jones BD. 2003. HilE interacts with hilD and negatively regulates hilA transcription and expression of the *Salmonella enterica* serovar typhimurium invasive phenotype. Infect Immun. 71:1295–1305.

57. Ellermeier CD, Ellermeier JR, Slauch JM. 2005. HilD, HilC and RtsA constitute a feed forward loop that controls expression of the SPI1 type three secretion system regulator hilA in *Salmonella enterica* serovar Typhimurium. Mol Microbiol. 57:691–705

58. Darwin KH, Miller VL. 2000. The putative invasion protein chaperone SicA acts together with InvF to activate the expression of *Salmonella* typhimurium virulence genes. Mol Microbiol. 35:949–960

59. Dieye Y, Dyszel JL, Kader R, Ahmer BMM. 2007. Systematic analysis of the regulation of type three secreted effectors in *Salmonella enterica* serovar Typhimurium. BMC Microbiol. 18:7:3

60. Hamed S, Wang X, Shawky RM, Emara M, Aldridge PD, Rao C V. 2019. Synergistic action of SPI-1 gene expression in *Salmonella enterica* serovar typhimurium through transcriptional crosstalk with the flagellar system. BMC Microbiol. 19:211

61. Chilcott GS, Hughes KT. 2000. Coupling of Flagellar Gene Expression to Flagellar Assembly in *Salmonella enterica* Serovar Typhimurium and *Escherichia coli.* Microbiol Mol Biol Rev. 64(4):694-708

62. Saini S, Brown JD, Aldridge PD, Rao C V. 2008. FliZ is a posttranslational activator of FlhD4C 2-dependent flagellar gene expression. J Bacteriol. 190:4979–4988

63. Wada T, Tanabe Y, Kutsukake K. 2011. FliZ acts as a repressor of the ydiV Gene, which encodes an Anti-FlhD 4C 2 Factor of the flagellar regulon in *Salmonella* Enterica Serovar Typhimurium. J Bacteriol. 193:5191–5198

64. Cott Chubiz JE, Golubeva YA, Lin D, Miller LD, Slauch JM. 2010. FliZ regulates expression of the *Salmonella* pathogenicity island 1 invasion locus by controlling HilD protein activity in *Salmonella enterica* serovar typhimurium. J Bacteriol. 192:6261–6270

65. Ellermeier CD, Slauch JM. 2003. RtsA and RtsB coordinately regulate expression of the invasion and flagellar genes in *Salmonella enterica* serovar typhimurium. J Bacteriol. 185:5096–5108

66. Hamed S, Shawky RM, Emara M, Slauch JM, Rao C V. 2021. HilE is required for synergistic activation of SPI-1 gene expression in *Salmonella enterica* serovar Typhimurium. BMC Microbiol. 21(1):49

67. Koirala S, Mears P, Sim M, Golding I, Chemla YR, Aldridge PD, Rao C V. 2014. A nutrient-tunable bistable switch controls motility in *Salmonella enterica* serovar Typhimurium. mBio. 5(5):e01611-14

68. Waterman SR, Holden DW. 2003. Functions and effectors of the *Salmonella* pathogenicity island 2 type III secretion system. Cell Microbiol. 5(8):501-11

69. Kuhle V, Hensel M. 2004. Cellular microbiology of intracellular *Salmonella enterica:* Functions of the type III secretion system encoded by *Salmonella* pathogenicity island 2. Cellular and Molecular Life Sciences. 61(22):2812-26

70. Uchiya K-I, Barbieri MA, Funato K, Shah AH, Stahl PD, Groisman EA. 1999. A *Salmonella* virulence protein that inhibits cellular trafficking. The EMBO Journal. 18(14): 3924–3933

71. Garmendia J, Beuzón CR, Ruiz-Albert J, Holden DW. 2003. The roles of SsrA-SsrB and OmpR-EnvZ in the regulation of genes encoding the *Salmonella* typhimurium SPI-2 type III secretion system. Microbiology (N Y). 149:2385–2396

72. Bustamante VH, Martínez LC, Santana FJ, Knodler LA, Steele-Mortimer O, Puente JL. 2008. HilD-mediated transcriptional cross-talk between SPI-1 and SPI-2. PNAS. 105 (38) 14591-14596

73. Silhavy TJ, Kahne D, Walker S. 2010. The bacterial cell envelope. Cold Spring Harb Perspect Biol. 2(5): a000414

74. Dam S, Pagès JM, Masi M. 2018. Stress responses, outer membrane permeability control and antimicrobial resistance in *enterobacteriaceae*. Microbiology (United Kingdom). Microbiology Society. 164(3):260-267

75. Simpson BW, Trent MS. 2019. Pushing the envelope: LPS modifications and their consequences. Nat Rev Microbiol. Nature Publishing Group. 17(7):403-416

76. Matz C, Jürgens K. 2001. Effects of hydrophobic and electrostatic cell surface properties of bacteria on feeding rates of heterotrophic nanoflagellates. Appl Environ Microbiol. 67:814–820

77. Glauert A. M, Thornley M. J. 1969. The topography of the bacterial cell wall. Annu Rev Microbiol. 23:159–198

78. Delcour AH. 2009. Outer membrane permeability and antibiotic resistance. Biochim Biophys Acta Proteins Proteom. 1794(5): 808–816

79. Kamio Y, Nikaido H. 1976. Outer membrane of *Salmonella* typhimurium: accessibility of phospholipid head groups to phospholipase c and cyanogen bromide activated dextran in the external medium. Biochemistry. 15:2561–2570

80. Raetz CRH, Whitfield C. 2002. Lipopolysaccharide Endotoxins. Annu Rev Biochem. 2002:71:635-700

81. Kuhn Editor A. 2019. Subcellular Biochemistry 92. Bacterial Cell Walls and Membranes. 9-77; 127-168

82. Noinaj N, Guillier M, Barnard TJ, Buchanan SK. 2010. TonB-dependent transporters: Regulation, structure, and function. Annu Rev Microbiol. 2010:64:43-60

83. Sun J, Rutherford ST, Silhavy TJ, Huang KC. 2022. Physical properties of the bacterial outer membrane. Nat Rev Microbiol. Nature Research. 20(4):236-248

84. Nakae T, Nikaido H. 1975. Outer membrane as a diffusion barrier in *Salmonella* typhimurium. Penetration of oligo and polysaccharides into isolated outer membrane vesicles and cells with degraded peptidoglycan layer. Journal of Biological Chemistry. 250:7359–7365

85. Zgurskaya HI, López CA, Gnanakaran S. 2016. Permeability Barrier of Gram-Negative Cell Envelopes and Approaches to Bypass It. ACS Infect Dis. 1:512–522

86. Braun V, Wolff H. 1970. The Murein-Lipoprotein Linkage in the Cell Wall of *Escherichia coli*. Eur J Biochem. 14:387–391

87. Vollmer W. 2008. Structural variation in the glycan strands of bacterial peptidoglycan. FEMS Microbiol Rev. 32(2):287-306

88. Lovering AL, Safadi SS, Strynadka NCJ. 2012. Structural perspective of peptidoglycan biosynthesis and assembly. Annu Rev Biochem. 81:451-78

89. Garde S, Chodisetti PK, Reddy M. 2021. Peptidoglycan: Structure, Synthesis, and Regulation. EcoSal Plus. 9(2)

90. Lovering AL, Safadi SS, Strynadka NCJ. 2012. Structural perspective of peptidoglycan biosynthesis and assembly. Annu Rev Biochem. 81:451-78

91. Yu CS, Chen YC, Lu CH, Hwang JK. 2006. Prediction of protein subcellular localization. Proteins: Structure, Function and Genetics. 64(3):643-51

92. Miller SI, Salama NR. 2018. The gram-negative bacterial periplasm: Size matters. PLoS Biol. Public Library of Science. 16(1): e2004935

93. Raetz CRH, Dowhan W. 1990. Biosynthesis and function of phospholipids in Escherichia coli. Journal of Biological Chemistry. American Society for Biochemistry and Molecular Biology Inc. 265(3):1235-8

94. Douglass M V, Cléon F, Stephen Trent M. 2021. Cardiolipin aids in lipopolysaccharide transport to the gram-negative outer membrane. Proc Natl Acad Sci U S A. 13;118(15):e2018329118

95. López GA, Heredia RM, Boeris PS, Lucchesi GI. 2016. Content of cardiolipin of the membrane and sensitivity to cationic surfactants in *Pseudomonas putida*. J Appl Microbiol. 121:1004–1014

96. Lopez-Campistrous A, Semchuk P, Burke L, Palmer-Stone T, Brokx SJ, Broderick G, Bottorff D, Bolch S, Weiner JH, Ellison MJ. 2005. Localization, annotation and comparison of the *Escherichia coli* K-12 proteome under two states of growth. Molecular and Cellular Proteomics. 4:1205–1209

97. Garmory HS, Titball RW. 2004. ATP-binding cassette transporters are targets for the development of antibacterial vaccines and therapies. Infect Immun. 72(12): 6757–6763

98. Chepuri V, Brooker RJ. 1999. Structural features of the uniporter/symporter/ antiporter superfamily. Protein Science. Cambridge University Press. 4(3): 534–537

99. Du D, Wang-Kan X, Neuberger A, van Veen HW, Pos KM, Piddock LJV, Luisi BF. 2018. Multidrug efflux pumps: structure, function and regulation. Nat Rev Microbiol. Nature Publishing Group. 16(9):523-539

100. Nishino K, Yamaguchi A. 2008. Role of xenobiotic transporters in bacterial drug resistance and virulence. IUBMB Life. 60(9):569-74

101. Mouslim C, Cano DA, Casadesús J. 1998. The sfiX, rfe and metN genes of *Salmonella* typhimurium and their involvement in the His(c) pleiotropic response. Molecular and General Genetics. 259(1):46-53

102. Rida S, Caillet J, Alix JH. 1996. Amplification of a novel gene, sanA, abolishes a vancomycin-sensitive defect in *Escherichia coli*. J Bacteriol. 178(1):94-102

103. Finn RD, Bateman A, Clements J, Coggill P, Eberhardt RY, Eddy SR, Heger A, Hetherington K, Holm L, Mistry J, Sonnhammer ELL, Tate J, Punta M. 2014. Pfam: The protein families database. Nucleic Acids Res. 42(Database issue): D222–D230

104. Mitchell AM, Wang W, Silhavy TJ. 2017. Novel RpoS-dependent mechanisms strengthen the envelope permeability barrier during stationary phase. J Bacteriol. 199(2):e00708-16

105. Levengood SK, Beyer WF, Webster RE. 1991. TolA: A membrane protein involved in colicin uptake contains an extended helical region. Proc Natl Acad Sci U S A. 88(14): 5939–5943

106. Levengood-Freyermuth SK, Click EM, Webster RE. 1993. Role of the Carboxyl-Terminal Domain of TolA in Protein Import and Integrity of the Outer Membrane. Journal of Bacteriology. 175(1):222-8

107. Thomas PD, Campbell MJ, Kejariwal A, Mi H, Karlak B, Daverman R, Diemer K, Muruganujan A, Narechania A. 2003. PANTHER: A library of protein families and subfamilies indexed by function. Genome Res. 13:2129–2141

108. Paradis-Bleau C, Kritikos G, Orlova K, Typas A, Bernhardt TG. 2014. A Genome-Wide Screen for Bacterial Envelope Biogenesis Mutants Identifies a Novel Factor Involved in Cell Wall Precursor Metabolism. PLoS Genet. 10(1):e1004056

109. Kolenda R, Burdukiewicz M, Wimonc M, Aleksandrowicz A, Ali A, Szabo I, Tedin K, Bartholdson Scott J, Pickard D, Schierack P, Kolenda CR, Scott BJ. 2021. Identification of Natural Mutations Responsible for Altered Infection Phenotypes of *Salmonella enterica* Clinical Isolates by Using Cell Line Infection Screens. 87(2):e02177-20

9. Supplementary material

9.1. Supplementary material for the 1st manuscript

Table S1 Antibiotic resistance patterns of *S* . Typhimurium 4/74 obtained by Biolog Phenotype MicroArray™

			S. Typhimurium 4/74 WT			S. Typhimurium 4/74 *ΔsanA*			*Probability (P) of similarity to S. Typhimurium 4/74 WT*
Compound name	**Plate**	**Well**	**i**	**ii**	**iii**	**i**	**ii**	**iii**	
Amikacin	PM11C	A01	292	290	302	302	298	296	0.206
Amikacin	PM11C	A02	303	302	306	305	301	296	
Amikacin	PM11C	A03	305	299	301	305	298	300	
Amikacin	PM11C	A04	309	311	307	299	300	295	
Chlortetracycline	PM11C	A05	292	300	303	298	297	298	0.694
Chlortetracycline	PM11C	A06	291	288	297	283	280	280	
Chlortetracycline	PM11C	A07	275	273	269	266	251	263	
Chlortetracycline	PM11C	A08	242	270	268	278	278	264	
Lincomycin	PM11C	A09	301	292	296	298	293	294	0.356
Lincomycin	PM11C	A10	298	296	296	311	301	306	
Lincomycin	PM11C	A11	291	285	292	305	300	300	
Lincomycin	PM11C	A12	272	261	300	279	283	267	
Amoxicillin	PM11C	B01	290	297	295	294	290	283	1.000
Amoxicillin	PM11C	B02	298	292	298	297	297	290	
Amoxicillin	PM11C	B03							
Amoxicillin	PM11C	B04	12	17	13	21	23	17	
Cloxacillin	PM11C	B05	307	303	308	304	299	296	0.916
Cloxacillin	PM11C	B06	315	312	317	313	308	310	
Cloxacillin	PM11C	B07	289	310	307	293	293	289	
Cloxacillin	PM11C	B08	27	14	15	17	18	16	
Lomefloxacin	PM11C	B09	299	301	296	292	286	285	0.856
Lomefloxacin	PM11C	B10	301	301	298	288	288	285	
Lomefloxacin	PM11C	B11	288	274	291	263	263	263	
Lomefloxacin	PM11C	B12	20	20	21	28	33	29	
Bleomycin	PM11C	C01	294	306	289	288	290	288	0.000
Bleomycin	PM11C	C02	292	297	300	285	282	280	

Bleomycin	PM11C	C03	291	299	298	285	283	282	
Bleomycin	PM11C	C04	292	297	298	284	282	280	
Colistin	PM11C	C05	301	306	304	302	298	297	0.944
Colistin	PM11C	C06	304	303	306	304	299	294	
Colistin	PM11C	C07	286	273		286	271		
Colistin	PM11C	C08	15	17	18	15	12	11	
Minocycline	PM11C	C09	287	291	295	282	273	275	0.820
Minocycline	PM11C	C10	281	288	291	270	265	259	
Minocycline	PM11C	C11	64	23	29	23	28	27	
Minocycline	PM11C	C12	34	32	29	35	29	32	
Capreomycin	PM11C	D01	294	301	299	307	298	308	0.842
Capreomycin	PM11C	D02	289	291	296	290	290	280	
Capreomycin	PM11C	D03	294	293	302	297	288	287	
Capreomycin	PM11C	D04	278	246	285	282	283	271	
Demeclocyline	PM11C	D05	301	295	300	295	290	287	0.360
Demeclocyline	PM11C	D06	301	291	297	292	286	276	
Demeclocyline	PM11C	D07	303	289	308	277	257	270	
Demeclocyline	PM11C	D08		67	86	24	37	14	
Nafcillin	PM11C	D09	295	289	298	288	285	285	0.241
Nafcillin	PM11C	D10	289	293	296	290	285	279	
Nafcillin	PM11C	D11	303	298	296	290	283	282	
Nafcillin	PM11C	D12	141	157		20	55	21	
Cefazolin	PM11C	E01	287	286	288	290	285	299	0.128
Cefazolin	PM11C	E02	285	290	295	295	302	292	
Cefazolin	PM11C	E03	290	291	293	301	295	290	
Cefazolin	PM11C	E04	299	299	298	297	299	295	
Enoxacin	PM11C	E05	301	299	303	291	289	291	0.430
Enoxacin	PM11C	E06	297	295	297	303	298	296	
Enoxacin	PM11C	E07	287		277	19	59		
Enoxacin	PM11C	E08	19	21	22	25	22	20	
Nalidixic acid	PM11C	E09	289	288	293	292	283	284	0.988
Nalidixic acid	PM11C	E10	262	262	272	274	267	265	
Nalidixic acid	PM11C	E11	17	12	22	14	18	17	
Nalidixic acid	PM11C	E12	24	18	26	22	17	22	
Chloramphenicol	PM11C	F01	273	275	276	290	278	287	0.874
Chloramphenicol	PM11C	F02	270	240	265	263	278	255	

Chloramphenicol	PM11C	F03	49	40	48	20		18	
Chloramphenicol	PM11C	F04	16	15	21	14	19	12	
Erythromycin	PM11C	F05	301	300	304	294	291	292	0.969
Erythromycin	PM11C	F06	308	310	309	319	301	310	
Erythromycin	PM11C	F07	280	284	291	284	283	279	
Erythromycin	PM11C	F08	271	265	267	284	279	271	
Neomycin	PM11C	F09	284	283	276	281	287	282	0.937
Neomycin	PM11C	F10	271	272	269	278	269	271	
Neomycin	PM11C	F11	270	266	273	287	286	283	
Neomycin	PM11C	F12	238		258		216	212	
Ceftriaxone	PM11C	G01	282	280	281	296	290	293	0.008
Ceftriaxone	PM11C	G02	275	285	296	294	301	296	
Ceftriaxone	PM11C	G03	291	284	294	302	299	294	
Ceftriaxone	PM11C	G04	296	299	296	297	297	290	
Gentamicin	PM11C	G05	304	282	293	280	289	289	0.977
Gentamicin	PM11C	G06	301	293	289	290	299	298	
Gentamicin	PM11C	G07	296	297	304	310	298	296	
Gentamicin	PM11C	G08	295	299	299	303	300	299	
Potassium tellurite	PM11C	G09	281	274	277	282	283	277	0.088
Potassium tellurite	PM11C	G10	273	293	268	277	281	284	
Potassium tellurite	PM11C	G11	286	278	284	300	300	295	
Potassium tellurite	PM11C	G12	293	296	299	304	309	307	
Cephalothin	PM11C	H01	310	296	297	298	293	291	0.824
Cephalothin	PM11C	H02	288	306	288	282	303	272	
Cephalothin	PM11C	H03	294		290		242	286	
Cephalothin	PM11C	H04	24	22	24	15	11	11	
Kanamycin	PM11C	H05	293	295	299	291	295	292	0.930
Kanamycin	PM11C	H06	295	293	290	297	292	282	
Kanamycin	PM11C	H07	292	290	307	290	293	298	
Kanamycin	PM11C	H08	289	277	276	293	286	284	
Ofloxacin	PM11C	H09	290	287	295	282	286	278	0.850
Ofloxacin	PM11C	H10	304	299	293	288	293	281	
Ofloxacin	PM11C	H11	295	284	302	288	286	288	
Ofloxacin	PM11C	H12	38	36	35	23	29	26	
Penicillin G	PM12B	A01	265	303	304	306	301	278	0.908
Penicillin G	PM12B	A02							

Penicillin G	PM12B	A03	14	24	12	29	21	20	
Penicillin G	PM12B	A04	14	15	11	28	29	18	
Tetracycline	PM12B	A05	306	305	299	304	299	301	0.111
Tetracycline	PM12B	A06	306	305	301	301	295	298	
Tetracycline	PM12B	A07	297	296	298	299	290	297	
Tetracycline	PM12B	A08	308	321	323	312	298	310	
Carbenicillin	PM12B	A09	303	296	298	296	293	292	0.220
Carbenicillin	PM12B	A10	296	296	299	302	304	299	
Carbenicillin	PM12B	A11	295	299	303	299	296	305	
Carbenicillin	PM12B	A12		83	24	246	290	268	
Oxacillin	PM12B	B01	302	301	291	294	290	291	0.936
Oxacillin	PM12B	B02	306	302	307	293	287	293	
Oxacillin	PM12B	B03	282	269	266	272	261	259	
Oxacillin	PM12B	B04	11	16	14	30	28	21	
Penimepicycline	PM12B	B05	302	298	304	294	292	289	0.003
Penimepicycline	PM12B	B06	301	309	311	300	301	299	
Penimepicycline	PM12B	B07	296	304	307	294	274	299	
Penimepicycline	PM12B	B08		299	304	296		297	
Polymyxin B	PM12B	B09	304	305	301	288	290	284	0.039
Polymyxin B	PM12B	B10	299	297	307	288	286	285	
Polymyxin B	PM12B	B11	293	293	293	275	273	270	
Polymyxin B	PM12B	B12		244	277	234		260	
Paromomycin	PM12B	C01	291	289	288	293	283	285	0.992
Paromomycin	PM12B	C02							
Paromomycin	PM12B	C03	18	35	21	17	35	14	
Paromomycin	PM12B	C04	16	14	17	20	22	14	
Vancomycin	PM12B	C05	305	302	302	297	290	296	0.046
Vancomycin	PM12B	C06	308	306	305	297	299	295	
Vancomycin	PM12B	C07	307	300	302	294	293	287	
Vancomycin	PM12B	C08	274	292	282	276	279	287	
D,L-Serine Hydroxamate	PM12B	C09	303	301	300	288	288	283	0.001
D,L-Serine Hydroxamate	PM12B	C10	294	289	294	270	273	268	
D,L-Serine Hydroxamate	PM12B	C11	283	283	290	261	263	260	
D,L-Serine Hydroxamate	PM12B	C12	275	270	274	270	267	253	
Sisomicin	PM12B	D01	292	289	299	306	291	299	0.098
Sisomicin	PM12B	D02	291	290	279	283	285	278	

Sisomicin	PM12B	D03	298	301	293	292	294	289	
Sisomicin	PM12B	D04	306	301	296	286	283	286	
Sulfamethazine	PM12B	D05	305	301	294	293	294	289	0.000
Sulfamethazine	PM12B	D06	306	311	300	298	297	300	
Sulfamethazine	PM12B	D07	309	304	299	293	287	287	
Sulfamethazine	PM12B	D08	305	302	300	288	290	291	
Novobiocin	PM12B	D09	294	301	288	291	284	262	0.447
Novobiocin	PM12B	D10	296	298	292	280	285	286	
Novobiocin	PM12B	D11	282	279	281	281	272	277	
Novobiocin	PM12B	D12	227	246	215	215	239	222	
2,4-Diamino-6,7-Diisopropylpteridine	PM12B	E01	295	284	299	303	297	305	0.202
2,4-Diamino-6,7-Diisopropylpteridine	PM12B	E02	290	288	291	291	303	292	
2,4-Diamino-6,7-Diisopropylpteridine	PM12B	E03	278	295	281	290	295	291	
2,4-Diamino-6,7-Diisopropylpteridine	PM12B	E04	279	275	269	280	278	266	
Sulfadiazine	PM12B	E05	303	305	304	295	290	291	0.000
Sulfadiazine	PM12B	E06	303	296	295	294	299	300	
Sulfadiazine	PM12B	E07	299	297	299	288	290	287	
Sulfadiazine	PM12B	E08	304	300	298	294	292	291	
Benzethonium Chloride	PM12B	E09	303	297	292	289	286	277	0.753
Benzethonium Chloride	PM12B	E10	292	294	292	287	295	291	
Benzethonium Chloride	PM12B	E11		18	15	13	18	19	
Benzethonium Chloride	PM12B	E12	54	27	24	30	27	27	
Tobramycin	PM12B	F01	283	281	277	299	290	290	0.011
Tobramycin	PM12B	F02	262	290	290	282	290	278	
Tobramycin	PM12B	F03	293	276	279	298	297	300	
Tobramycin	PM12B	F04	271	291			286	295	
Sulfathiazole	PM12B	F05	293	300	286	290	288	276	0.898
Sulfathiazole	PM12B	F06	310	296	299	301	299	301	
Sulfathiazole	PM12B	F07	298	292	283	296	294	290	
Sulfathiazole	PM12B	F08	295	298	253	290	294	291	
5-Fluoroorotic Acid	PM12B	F09	302	289	264	275	290	289	0.452
5-Fluoroorotic Acid	PM12B	F10	255	265	272	260	262	263	
5-Fluoroorotic Acid	PM12B	F11	251	255	258	273	270	268	
5-Fluoroorotic Acid	PM12B	F12	265	271	260	266	268	270	

Spectinomycin	PM12B	G01	273	279	273	285	288	290	0.021
Spectinomycin	PM12B	G02	267	269	274	286	275	261	
Spectinomycin	PM12B	G03	276	269	263	277	287	279	
Spectinomycin	PM12B	G04	277	276	275	271	280	275	
Sulfamethoxazole	PM12B	G05	285	309	299	303	303	279	0.965
Sulfamethoxazole	PM12B	G06	312	292	296	309	304	293	
Sulfamethoxazole	PM12B	G07	306	302	301	307	296	295	
Sulfamethoxazole	PM12B	G08	308	310	304	316	304	317	
L-Aspartic-b-Hydroxamate	PM12B	G09	304	291	288	290	295	291	0.146
L-Aspartic-b-Hydroxamate	PM12B	G10	279	284	280	288	291	285	
L-Aspartic-b-Hydroxamate	PM12B	G11	259	262	259	283	280	279	
L-Aspartic-b-Hydroxamate	PM12B	G12							
Spiramycin	PM12B	H01	288	302	304	296	291	294	0.738
Spiramycin	PM12B	H02	292	300	292	300	295	300	
Spiramycin	PM12B	H03	266	260	257	264	275	227	
Spiramycin	PM12B	H04	25	47	24	46		19	
Rifampicin	PM12B	H05	311	299	286	309	305	305	0.306
Rifampicin	PM12B	H06	309	292	308	313	298	292	
Rifampicin	PM12B	H07	317	313	300	315	312	316	
Rifampicin	PM12B	H08	293	301	303	307	303	300	
Dodecyltrimethyl Ammonium Bromide	PM12B	H09	296	300	300	295	294	280	0.551
Dodecyltrimethyl Ammonium Bromide	PM12B	H10	306	290	297	287	284	273	
Dodecyltrimethyl Ammonium Bromide	PM12B	H11	308	312	307	304	302	295	
Dodecyltrimethyl Ammonium Bromide	PM12B	H12	45		39	26	51	26	
Ampicillin	PM13B	A01	287	290	293	305	298	299	0.750
Ampicillin	PM13B	A02	298	305	301	304	306	296	
Ampicillin	PM13B	A03	305	299	304	307	307	299	
Ampicillin	PM13B	A04	307	309	313	303	302	295	
Dequalinium	PM13B	A05	306	303	307	311	309	304	0.430
Dequalinium	PM13B	A06	311	304	311	309	308	304	
Dequalinium	PM13B	A07	298	303	307	314	307	304	
Dequalinium	PM13B	A08	306	305	311	307	305	304	
Nickel chloride	PM13B	A09	291	297	295	300	296	294	0.823

Nickel chloride	PM13B	A10	287	292	292	305	306	295	
Nickel chloride	PM13B	A11	292	280	287	293	295	294	
Nickel chloride	PM13B	A12		33	30	34	32	49	
Azlocillin	PM13B	B01	298	297	293	286	283	288	0.119
Azlocillin	PM13B	B02	299	304	300	294	299	286	
Azlocillin	PM13B	B03	315	306	313	288	305	292	
Azlocillin	PM13B	B04	287	261	274	277	272	274	
2,2`-Dipyridyl	PM13B	B05	302	275	306	320	322	280	0.905
2,2`-Dipyridyl	PM13B	B06	24	17	18	26	34	24	
2,2`-Dipyridyl	PM13B	B07	24	14	18	18	32	17	
2,2`-Dipyridyl	PM13B	B08	24	21	18	19	20	24	
Oxolinic acid	PM13B	B09	301	305	307	297	303	290	0.876
Oxolinic acid	PM13B	B10	299	302	304	294	292	283	
Oxolinic acid	PM13B	B11	279	265	270	255	257	248	
Oxolinic acid	PM13B	B12	23	22	21	26	27	34	
6-Mercaptopurine	PM13B	C01	282	274	281	275	274	277	0.356
6-Mercaptopurine	PM13B	C02	265	265	264	263	259	251	
6-Mercaptopurine	PM13B	C03	258	268	267	270	265	255	
6-Mercaptopurine	PM13B	C04							
Doxycycline	PM13B	C05	301	293	303	299	294	296	0.751
Doxycycline	PM13B	C06	298	297	304	292	296	288	
Doxycycline	PM13B	C07	295	263	287	223	225	249	
Doxycycline	PM13B	C08	24	23	21	22	19	16	
Potassium chromate	PM13B	C09	287	279	284	280	280	278	0.261
Potassium chromate	PM13B	C10	271	266	271	262	260	260	
Potassium chromate	PM13B	C11	248	259	270	22		22	
Potassium chromate	PM13B	C12	83	36	36	41	34	37	
Cefuroxime	PM13B	D01	293	292	286	292	296	304	0.983
Cefuroxime	PM13B	D02	302	301	307	292	298	279	
Cefuroxime	PM13B	D03	264	267	265	287	276	282	
Cefuroxime	PM13B	D04	29	24	25	23	24	15	
5-Fluorouracil	PM13B	D05	303	295	301	298	300	291	0.006
5-Fluorouracil	PM13B	D06	308	303	308	302	301	299	
5-Fluorouracil	PM13B	D07	302	299	305	298	301	289	
5-Fluorouracil	PM13B	D08	301	300	301	298	292	282	
Rolitetracycline	PM13B	D09	301	284	296	287	288	292	0.439

Rolitetracycline	PM13B	D10	278	289	292	270	283	271	
Rolitetracycline	PM13B	D11	258	268	296	242	255	237	
Rolitetracycline	PM13B	D12	99	101	144	29	57	37	
Cytosine arabinoside	PM13B	E01	287	286	290	290	285	299	0.021
Cytosine arabinoside	PM13B	E02	270	284	280	287	297	283	
Cytosine arabinoside	PM13B	E03	289	281	284	296	290	286	
Cytosine arabinoside	PM13B	E04	284	287	289	295	289	282	
Geneticin (G418)	PM13B	E05	306	302	308	302	301	288	0.330
Geneticin (G418)	PM13B	E06	296	297	302	303	302	307	
Geneticin (G418)	PM13B	E07	301	295	298	294	294	289	
Geneticin (G418)	PM13B	E08	292	296	298	301	295	287	
Ruthenium red	PM13B	E09	298	299	296	291	290	295	0.013
Ruthenium red	PM13B	E10	290	294	296	295	294	289	
Ruthenium red	PM13B	E11	295	295	295	289	298	284	
Ruthenium red	PM13B	E12	301	300	302	291	300	293	
Cesium chloride	PM13B	F01	284	281	280	288	286	292	0.003
Cesium chloride	PM13B	F02	278	280	283	290	293	287	
Cesium chloride	PM13B	F03	282	284	294	305	299	304	
Cesium chloride	PM13B	F04	277	292	279	291	281	285	
Glycine	PM13B	F05	306	301	299	298	300	291	0.450
Glycine	PM13B	F06	281	292	304	301	302	297	
Glycine	PM13B	F07	295	291	273	282	291	296	
Glycine	PM13B	F08	272	275	284	291	288	275	
Thallium (I) acetate	PM13B	F09	301	287	288	299	299	300	0.139
Thallium (I) acetate	PM13B	F10	267	263	266	265	272	272	
Thallium (I) acetate	PM13B	F11	261	262	269	283	285	280	
Thallium (I) acetate	PM13B	F12							
Cobalt chloride	PM13B	G01	287	292	294	305	295	311	0.893
Cobalt chloride	PM13B	G02	289	288	284	295	303	294	
Cobalt chloride	PM13B	G03	301	272	293	305	296	288	
Cobalt chloride	PM13B	G04	86	63	74	60	87	52	
Manganese (II) chloride	PM13B	G05	294	279	316	305	311	299	0.970
Manganese (II) chloride	PM13B	G06	298	287	288	291	294	297	
Manganese (II) chloride	PM13B	G07	298	289	297	300	295	290	
Manganese (II) chloride	PM13B	G08	152	134	156	134	157	128	
Trifluoperazine	PM13B	G09	295	294	296	292	293	290	0.139

Trifluoperazine	PM13B	G10	289	281	284	286	292	291	
Trifluoperazine	PM13B	G11	282	291	291	304	308	310	
Trifluoperazine	PM13B	G12	309	307	310	313	323	309	
Cupric chloride	PM13B	H01	304	315	290	303	304	305	0.995
Cupric chloride	PM13B	H02	266	288	301	286	287	285	
Cupric chloride	PM13B	H03	130	148	151	129	146	134	
Cupric chloride	PM13B	H04	60	65	65	80	56	65	
Moxalactam	PM13B	H05	299	292	293	306	306	311	0.876
Moxalactam	PM13B	H06	290	310	306	314	313	302	
Moxalactam	PM13B	H07		19	18	11	60	11	
Moxalactam	PM13B	H08	56	20	18	13	13	19	
Tylosin	PM13B	H09	301	295	298	292	291	286	0.467
Tylosin	PM13B	H10	299	310	297	292	291	286	
Tylosin	PM13B	H11	270	286	298	291	289	286	
Tylosin	PM13B	H12	254	254	237	235	245	228	
Acriflavine	PM14A	A01	293	271	272	305	307	308	0.733
Acriflavine	PM14A	A02	291	303	305	310	299	303	
Acriflavine	PM14A	A03	318	323	324	315	309	313	
Acriflavine	PM14A	A04	336	341	337	326	326	324	
Furaltadone	PM14A	A05	299	306	308	307	302	303	0.490
Furaltadone	PM14A	A06	299	308	309	305	297	301	
Furaltadone	PM14A	A07	300	296	304	299	294	293	
Furaltadone	PM14A	A08	289	284	290	290	289	286	
Sanguinarine	PM14A	A09	302	302	301	303	302	293	0.879
Sanguinarine	PM14A	A10	291	290	288	302	301	301	
Sanguinarine	PM14A	A11	295	291	293	303	302	299	
Sanguinarine	PM14A	A12		83	80	95	88	114	
9-Aminoacridine	PM14A	B01	308	311	310	296	292	293	0.197
9-Aminoacridine	PM14A	B02	308	311	308	302	296	291	
9-Aminoacridine	PM14A	B03	317	317	314	300	297	299	
9-Aminoacridine	PM14A	B04	238	224		232	234	216	
Fusaric Acid	PM14A	B05	312	312	307	298	290	282	0.004
Fusaric Acid	PM14A	B06	298	289	297	298	299	288	
Fusaric Acid	PM14A	B07	304	311	310	300	296	293	
Fusaric Acid	PM14A	B08		295	311	293	252	284	
Sodium Arsenate	PM14A	B09	278	269	277	282	279	270	0.960

Sodium Arsenate	PM14A	B10	195	150	186	166	207	180	
Sodium Arsenate	PM14A	B11	62		68	51	63	54	
Sodium Arsenate	PM14A	B12	21	26	24	33	43	43	
Boric Acid	PM14A	C01	285	290	289	284	281	282	0.892
Boric Acid	PM14A	C02	286	292	297	275	274	267	
Boric Acid	PM14A	C03	273	269	282	267	264	267	
Boric Acid	PM14A	C04	14	13	15	14	27	23	
1-Hydroxy-Pyridine-2-thione	PM14A	C05	297	300	302	294	291	288	0.007
1-Hydroxy-Pyridine-2-thione	PM14A	C06	305	305	304	296	298	289	
1-Hydroxy-Pyridine-2-thione	PM14A	C07	306	301	304	294	288	288	
1-Hydroxy-Pyridine-2-thione	PM14A	C08	289	285	281	282	286	278	
Sodium Cyanate	PM14A	C09	293	304	302	283	287	283	0.770
Sodium Cyanate	PM14A	C10	295	290	285	265	272	265	
Sodium Cyanate	PM14A	C11	265	270	281	256	246	247	
Sodium Cyanate	PM14A	C12	33	36	34	42	44	40	
Cadmium Chloride	PM14A	D01	299	292	294	296	296	289	0.957
Cadmium Chloride	PM14A	D02	280	273	277	278	273	267	
Cadmium Chloride	PM14A	D03		26	26	23		16	
Cadmium Chloride	PM14A	D04	35	61	51	56	44	43	
Iodoacetate	PM14A	D05	303	291	302	292	290	289	0.955
Iodoacetate	PM14A	D06	311	289	307	307	283	293	
Iodoacetate	PM14A	D07	243	276	266	237	286	283	
Iodoacetate	PM14A	D08	20	19	17	16	19	15	
Sodium Dichromate	PM14A	D09	290	286	298	294	288	285	0.262
Sodium Dichromate	PM14A	D10	277	280	274	273	276	272	
Sodium Dichromate	PM14A	D11	275	266	279	268	267	256	
Sodium Dichromate	PM14A	D12	276	256	248		235	215	
Cefoxitin	PM14A	E01	288	285	289	285	288	285	0.429
Cefoxitin	PM14A	E02	290	286	284	300	284	295	
Cefoxitin	PM14A	E03	287	292	283	280	289	291	
Cefoxitin	PM14A	E04		290	298		277	275	
Nitrofurantoin	PM14A	E05	292	301	300	286	284	282	0.002
Nitrofurantoin	PM14A	E06	297	296	295	302	295	303	
Nitrofurantoin	PM14A	E07	303	298	298	291	289	283	
Nitrofurantoin	PM14A	E08	298	298	298	291	289	292	
Sodium Metaborate	PM14A	E09	275	289	283	285	275	286	0.965

Sodium Metaborate	PM14A	E10	264	272	269	265	279	267	
Sodium Metaborate	PM14A	E11	247	231	248	258	243	238	
Sodium Metaborate	PM14A	E12	19	21	21	23	22	22	
Chloramphenicol	PM14A	F01	276	274	279	283	283	286	0.501
Chloramphenicol	PM14A	F02	273	266	263	287	280	263	
Chloramphenicol	PM14A	F03	272	249	271	250	264	276	
Chloramphenicol	PM14A	F04	113	92		20	31	17	
Piperacillin	PM14A	F05	292	293	302	279	281	283	0.103
Piperacillin	PM14A	F06	305	301	296	303	292	294	
Piperacillin	PM14A	F07	286	289	276	291	282	296	
Piperacillin	PM14A	F08	290	296	294	284	289	283	
Sodium Metavanadate	PM14A	F09	17	17	14	11	14	11	0.595
Sodium Metavanadate	PM14A	F10	17	15	13	19	18	20	
Sodium Metavanadate	PM14A	F11	19	19	21	12	20	16	
Sodium Metavanadate	PM14A	F12	27	20	25	23	25	23	
Chelerythrine	PM14A	G01	283	289	288	304	303	305	0.018
Chelerythrine	PM14A	G02	299	292	282	294	310	303	
Chelerythrine	PM14A	G03	297	296	301	296	293	295	
Chelerythrine	PM14A	G04	298	302	302	304	303	298	
Carbenicillin	PM14A	G05							0.001
Carbenicillin	PM14A	G06	20	19	18	13		11	
Carbenicillin	PM14A	G07	18	17	17	11	11	11	
Carbenicillin	PM14A	G08	12	14	11	11	13	11	
Sodium Nitrite	PM14A	G09	282	288	278	294	283	283	0.794
Sodium Nitrite	PM14A	G10	265	271	273	275	277	271	
Sodium Nitrite	PM14A	G11	240	231	240	264	255	281	
Sodium Nitrite	PM14A	G12	34	34	34	45	43	36	
EGTA	PM14A	H01	297	295	296	290	283	292	0.868
EGTA	PM14A	H02	287	282	291	289	288	279	
EGTA	PM14A	H03	284	289	291	291	292	290	
EGTA	PM14A	H04	284	283	286	296	288	291	
Promethazine	PM14A	H05	283	287	288	299	302	286	0.958
Promethazine	PM14A	H06	293	291	289	291	296	305	
Promethazine	PM14A	H07	305	311	305	299	304	300	
Promethazine	PM14A	H08	18	19	21	14	27	20	
Sodium Orthovanadate	PM14A	H09	21	19	22	11	25	13	0.363

Sodium Orthovanadate	PM14A	H10	19	24	18	13	25	17	
Sodium Orthovanadate	PM14A	H11	27	30	25	17	28	20	
Sodium Orthovanadate	PM14A	H12	32	37	31	26	35	40	
Procaine	PM15B	A01	291	292	302	308	308	305	0.771
Procaine	PM15B	A02	295	299	300	305	303	298	
Procaine	PM15B	A03	292	294	297	294	287	285	
Procaine	PM15B	A04	272	251	257	263	265	248	
Guanidine hydrochloride	PM15B	A05	285	290	291	297	292	291	0.966
Guanidine hydrochloride	PM15B	A06	294	289	291	293	292	294	
Guanidine hydrochloride	PM15B	A07	277	285	287	286	284	277	
Guanidine hydrochloride	PM15B	A08	20	15	13	19	20	18	
Cefmetazole	PM15B	A09	281	275	284	289	287	285	0.191
Cefmetazole	PM15B	A10	284	294	296	297	304	295	
Cefmetazole	PM15B	A11	290	292	299	297	288	306	
Cefmetazole	PM15B	A12	297	286	300		288	299	
D-Cycloserine	PM15B	B01	288	302	292	288	285	280	0.625
D-Cycloserine	PM15B	B02	293	294	291	287	288	285	
D-Cycloserine	PM15B	B03	294	286	293	290	288	287	
D-Cycloserine	PM15B	B04		252	233	290	287	283	
EDTA	PM15B	B05	294	288	293	295	290	294	0.951
EDTA	PM15B	B06	302	300	307	304	293	296	
EDTA	PM15B	B07	302	301	312	301	299	293	
EDTA	PM15B	B08		24	26	28		24	
quinaldine	PM15B	B09	304	305	303	288	291	281	0.0000042
quinaldine	PM15B	B10	296	299	306	292	289	287	
quinaldine	PM15B	B11	292	297	294	276	272	280	
quinaldine	PM15B	B12	289	297	293	283	275	280	
5,7-Dichloro-8-hydroxyquinoline	PM15B	C01	288	307	296	286	278	286	0.257
5,7-Dichloro-8-hydroxyquinoline	PM15B	C02	296	300	299	280	282	283	
5,7-Dichloro-8-hydroxyquinoline	PM15B	C03	295	298	300	295	291	288	
5,7-Dichloro-8-hydroxyquinoline	PM15B	C04		77	60	307	301		
Fusidic acid	PM15B	C05	284	280	287	288	287	280	0.809
Fusidic acid	PM15B	C06	302	293	294	293	294	284	
Fusidic acid	PM15B	C07	294	293	299	296	289	287	
Fusidic acid	PM15B	C08	252	229	231	255	266	245	
1,10-Phenanthroline	PM15B	C09	309	307	307	298	295	290	0.904

1,10-Phenanthroline	PM15B	C10	293	284	287	277	279	266	
1,10-Phenanthroline	PM15B	C11	34	44	37	33	37	60	
1,10-Phenanthroline	PM15B	C12	30	40	33	31	34	25	
Phleomycin	PM15B	D01	291	291	296	294	289	285	0.896
Phleomycin	PM15B	D02	286		301	279	287	280	
Phleomycin	PM15B	D03	29	22	22	23	23	18	
Phleomycin	PM15B	D04	23	21	20	22	20	20	
Domiphen bromide	PM15B	D05	283	287	292	288	291	287	0.972
Domiphen bromide	PM15B	D06	296	300	295	298	296	293	
Domiphen bromide	PM15B	D07	296	304	306	300	306	291	
Domiphen bromide	PM15B	D08	25	22	20	20	18	16	
Nordihydroguaiaretic acid	PM15B	D09	293	281	298	291	299	284	0.301
Nordihydroguaiaretic acid	PM15B	D10	296	302	300	289	292	293	
Nordihydroguaiaretic acid	PM15B	D11	306	306	312	293	297	295	
Nordihydroguaiaretic acid	PM15B	D12	318	316	319	315	324	314	
Alexidine	PM15B	E01	282	282	284	286	281	278	0.876
Alexidine	PM15B	E02	289	287	280	279	273	281	
Alexidine	PM15B	E03	249	241	284	296	297	289	
Alexidine	PM15B	E04	15	18	14	18	27	12	
Nitrofurazone	PM15B	E05	286	304	301	295	302	281	0.226
Nitrofurazone	PM15B	E06	301	300	300	302	302	308	
Nitrofurazone	PM15B	E07	300	301	307	295	297	289	
Nitrofurazone	PM15B	E08	279	289	291	278	276	270	
Methyl viologen	PM15B	E09	283	288	273	278	279	276	0.847
Methyl viologen	PM15B	E10	275	286	292	293	293	290	
Methyl viologen	PM15B	E11	272	275	273	274	273	278	
Methyl viologen	PM15B	E12	282	274	279	280	275	270	
3, 4-Dimethoxybenzyl alcohol	PM15B	F01	285	292	288	293	286	291	0.862
3, 4-Dimethoxybenzyl alcohol	PM15B	F02	267	265	262	269	268	266	
3, 4-Dimethoxybenzyl alcohol	PM15B	F03	244	231	251	263	240	253	
3, 4-Dimethoxybenzyl alcohol	PM15B	F04	22	17	19	67	21	21	
Oleandomycin	PM15B	F05	287	285	291	294	284	278	0.771
Oleandomycin	PM15B	F06	302	304	305	297	293	298	
Oleandomycin	PM15B	F07	280	274	282	281	284	280	
Oleandomycin	PM15B	F08	262	277	279	285	284	285	
Puromycin	PM15B	F09	280	268	292	287	285	277	0.467

Puromycin	PM15B	F10	277	280	267	276	279	273	
Puromycin	PM15B	F11	279	273	281	294	294	290	
Puromycin	PM15B	F12	314	313	309	313	315	307	
CCCP	PM15B	G01	280	296	293	311	297	306	0.853
CCCP	PM15B	G02	295	298	297	299	291	307	
CCCP	PM15B	G03		178	196	196	189		
CCCP	PM15B	G04	132	158	174	150	169	143	
Sodium azide	PM15B	G05	292	309	296	292	293	293	0.928
Sodium azide	PM15B	G06	292	281	291	287	271	285	
Sodium azide	PM15B	G07	22	23	20	11	14	11	
Sodium azide	PM15B	G08	17	19	18	22	23	14	
Menadione	PM15B	G09	304	295	299	309	307	304	0.005
Menadione	PM15B	G10	305	304	308	308	312	307	
Menadione	PM15B	G11	300	292	300	312	313	311	
Menadione	PM15B	G12	311	305	309	300	311	316	
2-Nitroimidazole	PM15B	H01	291	287	300	288	283	283	0.466
2-Nitroimidazole	PM15B	H02	291	286	291	290	287	288	
2-Nitroimidazole	PM15B	H03	305	297	306	313	308	306	
2-Nitroimidazole	PM15B	H04	112		67	210	247	221	
Hydroxyurea	PM15B	H05	295	295	299	300	295	293	0.757
Hydroxyurea	PM15B	H06	297	304	301	313	315	295	
Hydroxyurea	PM15B	H07	290	279	273	282	280	280	
Hydroxyurea	PM15B	H08		26	22	13	15	63	
Zinc chloride	PM15B	H09	293	288	290	291	284	280	0.207
Zinc chloride	PM15B	H10	298	291	295	281	288	280	
Zinc chloride	PM15B	H11	293	290	298	293	284	284	
Zinc chloride	PM15B	H12	297	300	307	308	306	307	
Cefotaxime	PM16A	A01	305	302	311	333	328	316	0.941
Cefotaxime	PM16A	A02	280	316	305	298	285	292	
Cefotaxime	PM16A	A03	36	20	16	26	26	24	
Cefotaxime	PM16A	A04	25	13	18	24	29	20	
Phosphomycin	PM16A	A05	308	305	313	308	304	298	0.007
Phosphomycin	PM16A	A06	311	313	317	307	301	299	
Phosphomycin	PM16A	A07	308	308	312	308	305	303	
Phosphomycin	PM16A	A08	303	299	305	295	307	295	
5-Chloro-7-Iodo-8-Hydroxyquinoline	PM16A	A09	303	302	306	297	302	293	0.098

5-Chloro-7-Iodo-8-Hydroxyquinoline	PM16A	A10	280	267	269	302	291	307	
5-Chloro-7-Iodo-8-Hydroxyquinoline	PM16A	A11		264	275	283	279	276	
5-Chloro-7-Iodo-8-Hydroxyquinoline	PM16A	A12	266		276		287	285	
Norfloxacin	PM16A	B01	307	308	307	298	293	288	0.000
Norfloxacin	PM16A	B02	300	303	303	292	292	286	
Norfloxacin	PM16A	B03	304	301	309	288	295	285	
Norfloxacin	PM16A	B04	306	302	310	297	296	292	
Sulfanilamide	PM16A	B05	315	311	315	306	303	297	0.000
Sulfanilamide	PM16A	B06	316	312	314	311	302	303	
Sulfanilamide	PM16A	B07	313	309	314	308	298	300	
Sulfanilamide	PM16A	B08	308	298	306	286	293	291	
Trimethoprim	PM16A	B09	300	299	301	284	289	283	0.595
Trimethoprim	PM16A	B10	300	292	298	283	288	283	
Trimethoprim	PM16A	B11	288	271	279	282	265	259	
Trimethoprim	PM16A	B12		19	22	32	36	26	
Dichlofluanid	PM16A	C01	302	303	299	309	290	299	0.096
Dichlofluanid	PM16A	C02	296	303	304	294	294	293	
Dichlofluanid	PM16A	C03	308	296	310	312	289	289	
Dichlofluanid	PM16A	C04							
Protamine Sulfate	PM16A	C05	302	297	306	292	303	292	0.983
Protamine Sulfate	PM16A	C06	301	295	292	299	299	293	
Protamine Sulfate	PM16A	C07	48	22	28	26	57	22	
Protamine Sulfate	PM16A	C08	26	21	22	22	24	16	
Cetylpyridinium Chloride	PM16A	C09	301	308	309	289	291	282	0.000
Cetylpyridinium Chloride	PM16A	C10	295	291	297	272	281	280	
Cetylpyridinium Chloride	PM16A	C11	290	293	280	264	261	249	
Cetylpyridinium Chloride	PM16A	C12	293	295	292	279	275	272	
1-Chloro-2,4-Dinitrobenzene	PM16A	D01	315	315	312	313	316	315	0.905
1-Chloro-2,4-Dinitrobenzene	PM16A	D02	305	299	304	298	300	292	
1-Chloro-2,4-Dinitrobenzene	PM16A	D03	308	296	314	307	306	297	
1-Chloro-2,4-Dinitrobenzene	PM16A	D04	93	83	81	70	84	66	
Diamide	PM16A	D05	313	310	314	308	313	303	0.000
Diamide	PM16A	D06	313	309	310	307	302	297	
Diamide	PM16A	D07	308	306	314	302	296	301	

Diamide	PM16A	D08	313	315	320	309	290	302	
Cinoxacin	PM16A	D09	300	293	300	288	294	290	0.761
Cinoxacin	PM16A	D10	290	285	275	273	273	266	
Cinoxacin	PM16A	D11		18	21	22	23	20	
Cinoxacin	PM16A	D12	28	26	28	23	27	23	
Streptomycin	PM16A	E01	293	312	296	307	310	310	0.020
Streptomycin	PM16A	E02	298	298	307	310	304	300	
Streptomycin	PM16A	E03	299	299	306	311	313	300	
Streptomycin	PM16A	E04	307	304	309	314	308	306	
5-Azacytidine	PM16A	E05	312	310	314	303	307	299	0.029
5-Azacytidine	PM16A	E06	306	305	309	306	307	292	
5-Azacytidine	PM16A	E07	308	299	307	291	295	299	
5-Azacytidine	PM16A	E08	296	299	305	308	299	299	
Rifamycin SV	PM16A	E09	299	302	307	293	294	290	0.085
Rifamycin SV	PM16A	E10	299	299	298	304	286	291	
Rifamycin SV	PM16A	E11	307	309	313	304	306	301	
Rifamycin SV	PM16A	E12	317	316	319	317	313	308	
Potassium Tellurite	PM16A	F01	301	293	301	303	301	299	0.817
Potassium Tellurite	PM16A	F02	290	295	299	316	318	310	
Potassium Tellurite	PM16A	F03	310		273	286		287	
Potassium Tellurite	PM16A	F04	133	126			129	146	
Sodium Selenite	PM16A	F05	306	287	299	307	304	291	0.303
Sodium Selenite	PM16A	F06	308	301	304	305	299	297	
Sodium Selenite	PM16A	F07	301	302	310	306	310	305	
Sodium Selenite	PM16A	F08	302	308	306	324	315	309	
Aluminum Sulfate	PM16A	F09	301	298	308	304	310	304	0.126
Aluminum Sulfate	PM16A	F10	287	283	287	285	288	278	
Aluminum Sulfate	PM16A	F11	282	274	281	300	299	299	
Aluminum Sulfate	PM16A	F12	289	288	297	297	294	290	
Chromium Chloride	PM16A	G01	299	285	290	297	297	307	0.021
Chromium Chloride	PM16A	G02	295	282	287	299	308	287	
Chromium Chloride	PM16A	G03	301	296	296	304	299	296	
Chromium Chloride	PM16A	G04	296	301	304	303	307	310	
Ferric Chloride	PM16A	G05	319	313	314	317	320	290	0.641
Ferric Chloride	PM16A	G06	314	313	318	314	321	321	
Ferric Chloride	PM16A	G07	316	304	317	313	310	308	

Ferric Chloride	PM16A	G08	307	291	287	314	298	310	
L-Glutamic-g-Hydroxamate	PM16A	G09	303	299	309	304	304	298	0.192
L-Glutamic-g-Hydroxamate	PM16A	G10	294	294	297	299	294	296	
L-Glutamic-g-Hydroxamate	PM16A	G11	269	285	275	293	289	293	
L-Glutamic-g-Hydroxamate	PM16A	G12	291	289	293	296	295	293	
Glycine Hydroxamate	PM16A	H01	293	286	299	286	287	286	0.850
Glycine Hydroxamate	PM16A	H02	289	285	289	296	287	288	
Glycine Hydroxamate	PM16A	H03	291	290	292	295	289	290	
Glycine Hydroxamate	PM16A	H04	295	298	301	310	300	300	
Chloroxylenol	PM16A	H05	323	307	325	320	325	318	0.135
Chloroxylenol	PM16A	H06	322	328	323	325	328	322	
Chloroxylenol	PM16A	H07	326	301	315	324	324	319	
Chloroxylenol	PM16A	H08	320	317	276	319	323	317	
Sorbic Acid	PM16A	H09	321	317	322	310	308	305	0.000
Sorbic Acid	PM16A	H10	326	321	319	304	304	304	
Sorbic Acid	PM16A	H11	316	306	309	313	311	303	
Sorbic Acid	PM16A	H12	314	313	311	311	294	313	
D-Serine	PM17A	A01	292	284	301	297	303	301	0.964
D-Serine	PM17A	A02	310	309	308	308	311	312	
D-Serine	PM17A	A03	313	310	317	314	292	309	
D-Serine	PM17A	A04	16	16	15	34	21	18	
b-Chloro-L-Alanine	PM17A	A05	289	287	292	294	288	281	0.808
b-Chloro-L-Alanine	PM17A	A06	300	297	297	301	296	298	
b-Chloro-L-Alanine	PM17A	A07	297	294	299	303	299	295	
b-Chloro-L-Alanine	PM17A	A08	305	299	302	304	296	296	
Thiosalicylate	PM17A	A09	295	295	296	292	296	292	0.038
Thiosalicylate	PM17A	A10	292	297	299	297	303	305	
Thiosalicylate	PM17A	A11	296	297	299	303	308	301	
Thiosalicylate	PM17A	A12	300	298	298	303	305	300	
Salicylate	PM17A	B01	284	287	284	286	275	276	0.879
Salicylate	PM17A	B02	257	258	253	271	255	253	
Salicylate	PM17A	B03	212		204	223	237	215	
Salicylate	PM17A	B04	13	17	13	26	20	20	
Hygromycin B	PM17A	B05	307	302	302	289	296	295	0.954
Hygromycin B	PM17A	B06	304	301	304	297	300	300	
Hygromycin B	PM17A	B07							

Hygromycin B	PM17A	B08	21	18	20	21	24	22	
Ethionamide	PM17A	B09	299	294	306	284	291	279	0.012
Ethionamide	PM17A	B10	298	300	311	279	285	290	
Ethionamide	PM17A	B11	272	287	272	262	255	256	
Ethionamide	PM17A	B12	275	285	265	270	259	264	
4-Aminopyridine	PM17A	C01	298	309	293	295	290	292	0.912
4-Aminopyridine	PM17A	C02	302	301	302	279	284	291	
4-Aminopyridine	PM17A	C03	303	303	302	290	289	292	
4-Aminopyridine	PM17A	C04	11	13	18	20	45	20	
Sulfachloropyridazine	PM17A	C05	300	302	307	306	304	304	0.003
Sulfachloropyridazine	PM17A	C06	307	307	309	303	305	302	
Sulfachloropyridazine	PM17A	C07	302	302	306	296	288	288	
Sulfachloropyridazine	PM17A	C08	309	302	310	289	294	294	
Sulfamonomethoxine	PM17A	C09	301	300	308	286	287	286	0.000
Sulfamonomethoxine	PM17A	C10	288	299	301	277	274	276	
Sulfamonomethoxine	PM17A	C11	293	291	299	262	264	273	
Sulfamonomethoxine	PM17A	C12	295	290	288	287	287	286	
Oxycarboxin	PM17A	D01	304	300	299	299	298	301	0.924
Oxycarboxin	PM17A	D02	278	272	289	284	284	277	
Oxycarboxin	PM17A	D03	136		155	185	182		
Oxycarboxin	PM17A	D04	26	23	18	15	15	16	
Aminotriazole	PM17A	D05	302	300	309	297	293	292	0.479
Aminotriazole	PM17A	D06	297	298	301	296	301	293	
Aminotriazole	PM17A	D07	288	294	292	292	292	283	
Aminotriazole	PM17A	D08	282	272	269	279	276	272	
Chlorpromazine	PM17A	D09	289	295	298	282	283	277	0.076
Chlorpromazine	PM17A	D10	293	297	300	286	282	296	
Chlorpromazine	PM17A	D11	311	309	317	300	297	294	
Chlorpromazine	PM17A	D12	317		286	30		27	
Niaproof	PM17A	E01	302	300	302	305	301	300	0.407
Niaproof	PM17A	E02	298	296	305	301	307	302	
Niaproof	PM17A	E03	274	270	256	287	281	274	
Niaproof	PM17A	E04	171	207	175	213	197		
Compound 48/80	PM17A	E05	299	299	308	279	289	291	0.581
Compound 48/80	PM17A	E06	298	300	302	297	302	291	
Compound 48/80	PM17A	E07	275	291	292	293	283	279	

Compound 48/80	PM17A	E08		60	21	23	25	26	
Sodium Tungstate	PM17A	E09	283	276	281	282	271	272	0.169
Sodium Tungstate	PM17A	E10	293	282	286	289	288	285	
Sodium Tungstate	PM17A	E11	296	281	283	281	296	282	
Sodium Tungstate	PM17A	E12	254		297	244	246	251	
Lithium Chloride	PM17A	F01	281	290	274	291	289	278	0.900
Lithium Chloride	PM17A	F02	254	246	259	268	264	261	
Lithium Chloride	PM17A	F03	225		200		229	190	
Lithium Chloride	PM17A	F04	34	57	36	41	63	43	
D,L-Methionine Hydroxamate	PM17A	F05	295	296	283	289	281	291	0.810
D,L-Methionine Hydroxamate	PM17A	F06	290	296	297	298	302	293	
D,L-Methionine Hydroxamate	PM17A	F07	16		23	15	13	20	
D,L-Methionine Hydroxamate	PM17A	F08	19	21	16	11	14	18	
Tannic acid	PM17A	F09	312	308	308	312	319	313	0.157
Tannic acid	PM17A	F10	304	305	307	306	310	309	
Tannic acid	PM17A	F11	318	315	314	341	339	342	
Tannic acid	PM17A	F12	339	342	338	344	343	340	
Chlorambucil	PM17A	G01	289	273	282	308	302	288	0.119
Chlorambucil	PM17A	G02	284	291	285	287	291	289	
Chlorambucil	PM17A	G03	283	274	284	303	291	285	
Chlorambucil	PM17A	G04	293	274	272	277	280	263	
Cefamandole	PM17A	G05	304	311	313	296	296	300	0.458
Cefamandole	PM17A	G06	298	293	294	308	296	298	
Cefamandole	PM17A	G07	295	302	307	294	302	280	
Cefamandole	PM17A	G08	300	298	303	307	310	304	
Cetoperazone	PM17A	G09	298	300	285	290	295	291	0.713
Cetoperazone	PM17A	G10	289	287	285	291	288	291	
Cetoperazone	PM17A	G11	279	280	288	288	286	295	
Cetoperazone	PM17A	G12	259	269	264	256	231	249	
Cefsulodin	PM17A	H01	300	290	301	297	291	286	0.766
Cefsulodin	PM17A	H02	299	290	290	293	295	290	
Cefsulodin	PM17A	H03	296	292	295	297	300	297	
Cefsulodin	PM17A	H04	301	296	301	307	306	300	
Caffeine	PM17A	H05	311	303	297	310	308	308	0.941
Caffeine	PM17A	H06	315	314	323	310	315	313	
Caffeine	PM17A	H07	314	306	313	310	311	310	

Caffeine	PM17A	H08		102	100		113	119	
Phenylarsine Oxide	PM17A	H09	298	291	295	286	294	290	0.789
Phenylarsine Oxide	PM17A	H10	304	295	304	287	280	291	
Phenylarsine Oxide	PM17A	H11	291	296	299	296		291	
Phenylarsine Oxide	PM17A	H12	43	42	40	43	22	39	
Ketoprofen	PM18C	A01	293	275	292	311	304	306	0.884
Ketoprofen	PM18C	A02	310	313	315	310	313	303	
Ketoprofen	PM18C	A03	299	296	296	295	298	292	
Ketoprofen	PM18C	A04	195		212	166		164	
Sodium pyrophosphate decahydrate	PM18C	A05	323	319	327	314	318	313	0.356
Sodium pyrophosphate decahydrate	PM18C	A06	307	290	311	304	296	304	
Sodium pyrophosphate decahydrate	PM18C	A07	310	308	300	311	301	307	
Sodium pyrophosphate decahydrate	PM18C	A08	315	305	309	312	302	303	
Thiamphenicol	PM18C	A09	291	281	288	293	289	285	0.705
Thiamphenicol	PM18C	A10	279	268	271	290	289	287	
Thiamphenicol	PM18C	A11	83	43	60	101	136	95	
Thiamphenicol	PM18C	A12	26	21	28	37	30	34	
Trifluorothymidine	PM18C	B01	290	289	288	285	277	279	0.006
Trifluorothymidine	PM18C	B02	288	292	302	291	287	283	
Trifluorothymidine	PM18C	B03	292	302	298	290	293	292	
Trifluorothymidine	PM18C	B04	302	308	307	292	297	290	
Pipemidic Acid	PM18C	B05	304	302	302	297	299	304	0.914
Pipemidic Acid	PM18C	B06	308	307	312	311	306	302	
Pipemidic Acid	PM18C	B07	278		240	278	276	269	
Pipemidic Acid	PM18C	B08	21	20	18	18	21	20	
Azathioprine	PM18C	B09	285	286	291	289	287	282	0.051
Azathioprine	PM18C	B10	286	279	288	286	282	277	
Azathioprine	PM18C	B11	288	290	287	281	271	273	
Azathioprine	PM18C	B12	301	296	306	300	286	291	
Poly-L-lysine	PM18C	C01	281	281	287	275	278	275	0.004
Poly-L-lysine	PM18C	C02	286	277	285	262	269	266	
Poly-L-lysine	PM18C	C03	286	288	298	282	285	279	
Poly-L-lysine	PM18C	C04							
Sulfisoxazole	PM18C	C05	303	307	308	304	302	301	0.005

Sulfisoxazole	PM18C	C06	312	310	314	313	312	301	
Sulfisoxazole	PM18C	C07	312	309	312	306	310	301	
Sulfisoxazole	PM18C	C08	320	322	320	310	309	296	
Pentachlorophenol (PCP)	PM18C	C09	308	313	313	295	296	292	0.002
Pentachlorophenol (PCP)	PM18C	C10	304	309	305	292	288	292	
Pentachlorophenol (PCP)	PM18C	C11	289	285	288	272	272	267	
Pentachlorophenol (PCP)	PM18C	C12	296	295	300	286	294	284	
Sodium m-arsenite	PM18C	D01	19	24	18	24	21	23	0.063
Sodium m-arsenite	PM18C	D02	18	20	23	15	16	15	
Sodium m-arsenite	PM18C	D03	19	24	20	18	16	13	
Sodium m-arsenite	PM18C	D04	15	18	20	18	16	11	
Sodium bromate	PM18C	D05	291	292	298	289	292	299	0.376
Sodium bromate	PM18C	D06	308	311	305	317	310	309	
Sodium bromate	PM18C	D07	316	301	305	304	301	310	
Sodium bromate	PM18C	D08	309	314	317	300	298	301	
Lidocaine	PM18C	D09	329	326	324	323	320	317	0.919
Lidocaine	PM18C	D10	327	321	324	321	320	317	
Lidocaine	PM18C	D11	31	34	34	42	32	29	
Lidocaine	PM18C	D12	29	43	70	32	35	29	
Sodium metasilicate	PM18C	E01	304	310	307	310	315	308	0.578
Sodium metasilicate	PM18C	E02	291	278	289	285	306	298	
Sodium metasilicate	PM18C	E03	270	262	269	287	281	267	
Sodium metasilicate	PM18C	E04	52	64	54	73		52	
Sodium periodate	PM18C	E05	294	297	300	301	300	296	0.956
Sodium periodate	PM18C	E06	301	287	294	304	306	300	
Sodium periodate	PM18C	E07	17	15	21	16	15	23	
Sodium periodate	PM18C	E08	21	23	24	26	22	25	
Antimony (III) chloride	PM18C	E09	296	297	307	299	294	288	0.937
Antimony (III) chloride	PM18C	E10	305	301	299	318	309	309	
Antimony (III) chloride	PM18C	E11	24	33	27	24	29	30	
Antimony (III) chloride	PM18C	E12	19	20	21	62	19	24	
Semicarbazide hydrochloride	PM18C	F01	272	263	272	280	272	277	0.327
Semicarbazide hydrochloride	PM18C	F02	260	258	267	278	272	270	
Semicarbazide hydrochloride	PM18C	F03	287	285	277	302	292	290	
Semicarbazide hydrochloride	PM18C	F04	256		261	56		71	
Tinidazole	PM18C	F05	291	280	288	302	290	294	0.074

Tinidazole	PM18C	F06	286	298	310	304	305	301	
Tinidazole	PM18C	F07	300	306	306	308	307	310	
Tinidazole	PM18C	F08	307	307	313	332	317	330	
Aztreonam	PM18C	F09	304	304	303	309	299	303	0.780
Aztreonam	PM18C	F10	292	294	294	295	291	292	
Aztreonam	PM18C	F11	278	279	275	298	287	280	
Aztreonam	PM18C	F12		25	24	25	48	26	
Triclosan	PM18C	G01	273	265	272	296	285	286	0.132
Triclosan	PM18C	G02	291	289	296	283	301	298	
Triclosan	PM18C	G03	291	301	299	310	301	283	
Triclosan	PM18C	G04	287	275	285	280	286	296	
3,5- Diamino-1,2,4-triazole (Guanazole)	PM18C	G05	294	308	300	315	307	293	0.032
3,5- Diamino-1,2,4-triazole (Guanazole)	PM18C	G06	307	298	299	311	312	313	
3,5- Diamino-1,2,4-triazole (Guanazole)	PM18C	G07	288	298	297	309	307	294	
3,5- Diamino-1,2,4-triazole (Guanazole)	PM18C	G08	286	275	275	290	293	295	
Myricetin	PM18C	G09	292	310	310	317	313	308	0.024
Myricetin	PM18C	G10	309	305	311	317	310	311	
Myricetin	PM18C	G11	309	306	307	324	326	324	
Myricetin	PM18C	G12	325	325	326	333	334	333	
5-Fluoro-5'-deoxyuridine	PM18C	H01	292	293	297	287	280	280	0.687
5-Fluoro-5'-deoxyuridine	PM18C	H02	295	287	291	285	287	290	
5-Fluoro-5'-deoxyuridine	PM18C	H03	284	284	282	293	287	290	
5-Fluoro-5'-deoxyuridine	PM18C	H04	286	278	284	297	285	281	
2- Phenylphenol	PM18C	H05	310	299	307	312	315	319	0.002
2- Phenylphenol	PM18C	H06	317	316	316	325	320	322	
2- Phenylphenol	PM18C	H07	314	315	319	320	322	319	
2- Phenylphenol	PM18C	H08	318	319	312	324	322	326	
Plumbagin	PM18C	H09	301	301	301	299	300	298	0.281
Plumbagin	PM18C	H10	316	314	311	301	297	306	
Plumbagin	PM18C	H11	313	312	317	315	311	308	
Plumbagin	PM18C	H12	321	316	319	323	320	319	
Josamycin	PM19	A01	295	283	300	306	292	295	0.434
Josamycin	PM19	A02	301	299	303	302	304	297	
Josamycin	PM19	A03	278	304	307	306	302	288	

Josamycin	PM19	A04	245	244	243	257	263	274	
Gallic Acid	PM19	A05	342	336	340	335	334	335	0.067
Gallic Acid	PM19	A06	362	360	361	352	352	349	
Gallic Acid	PM19	A07	366	363	365	356	356	358	
Gallic Acid	PM19	A08	364	363	364	354	354	356	
Coumarin	PM19	A09	293	296	294	298	300	297	0.815
Coumarin	PM19	A10	293	292	301	305	309	308	
Coumarin	PM19	A11	272	291	289	294	300	297	
Coumarin	PM19	A12	68	56	37	69	63	66	
Chloride	PM19	B01	291	291	295	289	280	278	0.979
Chloride	PM19	B02	298	302	302	295	298	282	
Chloride	PM19	B03	290	294	296	298	299	290	
Chloride	PM19	B04	17	16	15	32	29	53	
Harmane	PM19	B05	309	313	314	304	302	291	0.906
Harmane	PM19	B06	318	317	319	312	314	301	
Harmane	PM19	B07	295	292	291	293	295	288	
Harmane	PM19	B08		50	41	50		51	
2,4-Dintrophenol	PM19	B09	307	309	312	294	299	288	0.856
2,4-Dintrophenol	PM19	B10	302	310	303	300	299	296	
2,4-Dintrophenol	PM19	B11	298	305	306	292	288	289	
2,4-Dintrophenol	PM19	B12	134	132	141	155	151	144	
Chlorhexidine	PM19	C01	287	295	293	290	293	283	0.001
Chlorhexidine	PM19	C02	301	297	300	281	281	275	
Chlorhexidine	PM19	C03	282	300	301	293	298	290	
Chlorhexidine	PM19	C04	298	297	302	281	282	272	
Umbelliferone	PM19	C05	302	307	312	303	300	289	0.000
Umbelliferone	PM19	C06	301	314	314	295	300	273	
Umbelliferone	PM19	C07	306	312	308	287	295	287	
Umbelliferone	PM19	C08	311	299	302	298	296	285	
Cinnamic Acid	PM19	C09	303	304	304	288	292	282	0.015
Cinnamic Acid	PM19	C10	300	301	297	274	274	274	
Cinnamic Acid	PM19	C11	289	290	289	269	270	268	
Cinnamic Acid	PM19	C12		251	254	263	259	242	
Disulphiram	PM19	D01	295	294	297	299	296	289	0.031
Disulphiram	PM19	D02	294	298	301	292	289	284	
Disulphiram	PM19	D03	301	303	303	302	298	290	

Disulphiram	PM19	D04	298	302	304	301	299	297	
Iodonitro Tetrazolium Violet	PM19	D05	344	343	343	341	343	339	0.754
Iodonitro Tetrazolium Violet	PM19	D06	358	355	358	354	355	354	
Iodonitro Tetrazolium Violet	PM19	D07	346	331	327	333	354	325	
Iodonitro Tetrazolium Violet	PM19	D08	340	322	330	327	332	321	
Phenyl-Methyl-Sulfonyl-Fluoride (PMSF)	PM19	D09	305	307	310	301	302	298	0.006
Phenyl-Methyl-Sulfonyl-Fluoride (PMSF)	PM19	D10	311	307	308	302	303	295	
Phenyl-Methyl-Sulfonyl-Fluoride (PMSF)	PM19	D11	307	312	308	297	294	289	
Phenyl-Methyl-Sulfonyl-Fluoride (PMSF)	PM19	D12	299	295		299	314	294	
FCCP	PM19	E01	282	288	294	290	289	282	0.177
FCCP	PM19	E02	289	285	288	300	300	298	
FCCP	PM19	E03	295	305	304	311	316	307	
FCCP	PM19	E04	308	284	279	286	299	291	
D,L-Thioctic Acid	PM19	E05	302	306	308	307	305	301	0.764
D,L-Thioctic Acid	PM19	E06	309	305	310	316	313	308	
D,L-Thioctic Acid	PM19	E07	268	290	301	301	291	295	
D,L-Thioctic Acid	PM19	E08		25	31	31	34	24	
Lawsone	PM19	E09	320	318	319	318	318	314	0.924
Lawsone	PM19	E10	324	317	324	327	328	326	
Lawsone	PM19	E11	325	325	326	332	332	333	
Lawsone	PM19	E12	247	239	242	238	238	240	
Phenethicillin	PM19	F01	288	284	285	293	289	291	0.674
Phenethicillin	PM19	F02	266	265	274	288	267	261	
Phenethicillin	PM19	F03	278	273	261	261	286	268	
Phenethicillin	PM19	F04	27	19	26	24	20		
Blasticidin S	PM19	F05	298	302	292	289	295	288	0.966
Blasticidin S	PM19	F06	295	292	289	295	286	291	
Blasticidin S	PM19	F07		33	31	39		27	
Blasticidin S	PM19	F08	37	25	27	23	41	19	
Sodium Caprylate	PM19	F09	301	274	294	304	292	292	0.835
Sodium Caprylate	PM19	F10	290	278	273	282	290	277	
Sodium Caprylate	PM19	F11		176	136	53		77	
Sodium Caprylate	PM19	F12	40	20	40	64	23	50	
Lauryl sulfobetaine	PM19	G01	306	294	310	325	325	321	0.679

Lauryl sulfobetaine	PM19	G02	291	280	292	303	295	288	
Lauryl sulfobetaine	PM19	G03	187		164	175		152	
Lauryl sulfobetaine	PM19	G04	227	229	238	250	271	222	
Dihydrostreptomycin	PM19	G05	301	287	289	292	289	274	0.641
Dihydrostreptomycin	PM19	G06	293	288	279	298	296	305	
Dihydrostreptomycin	PM19	G07	289	294	288	288	287	269	
Dihydrostreptomycin	PM19	G08	295	284	278	292	300	295	
Hydroxylamine	PM19	G09	283	277	294	296	290	284	0.009
Hydroxylamine	PM19	G10	292	290	281	295	293	291	
Hydroxylamine	PM19	G11	280	274	279	302	297	297	
Hydroxylamine	PM19	G12	296	291	303	308	302	294	
Hexaminecobalt (III) Chloride	PM19	H01	281	296	316	293	296	281	0.543
Hexaminecobalt (III) Chloride	PM19	H02	300	304	311	293	303	284	
Hexaminecobalt (III) Chloride	PM19	H03	298	292	275	305	305	292	
Hexaminecobalt (III) Chloride	PM19	H04	317	298	290	326	317	325	
Thioglycerol	PM19	H05	292	296	283	288	290	274	0.607
Thioglycerol	PM19	H06	284	300	292	289	306	292	
Thioglycerol	PM19	H07	256	234	252	269	255	281	
Thioglycerol	PM19	H08	261	249	261	264	277	229	
Polymyxin B	PM19	H09	295	285	286	286	285	277	0.518
Polymyxin B	PM19	H10		27	33	290	281		
Polymyxin B	PM19	H11	33	32	34	20	19	16	
Polymyxin B	PM19	H12	37	38	47	21	23	25	
Amitriptyline	PM20B	A01		205	216	304	311	300	0.628
Amitriptyline	PM20B	A02	296	288	289	301	303	298	
Amitriptyline	PM20B	A03	320	320	320	310	310	300	
Amitriptyline	PM20B	A04	14	13	14	26	30	26	
Apramycin	PM20B	A05	295	289	290	294	299	295	0.109
Apramycin	PM20B	A06	297	289	294	302	298	292	
Apramycin	PM20B	A07	291	285	288	292	301	291	
Apramycin	PM20B	A08	297	291	290	291	288	288	
Benserazide	PM20B	A09	309	304	306	307	309	306	0.899
Benserazide	PM20B	A10	322	317	318	329	330	326	
Benserazide	PM20B	A11	176	173	183	171	183	175	
Benserazide	PM20B	A12	231	226	232	226	242	232	
Orphenadrine	PM20B	B01	289	282	288	286	285	283	0.954

Orphenadrine	PM20B	B02	291	289	289	290	289	282	
Orphenadrine	PM20B	B03	109		122	128	106	126	
Orphenadrine	PM20B	B04	14	14	11	22	29	18	
D,L-Propranolol	PM20B	B05	288	282	286	289	292	283	0.985
D,L-Propranolol	PM20B	B06	305	299	301	309	301	297	
D,L-Propranolol	PM20B	B07							
D,L-Propranolol	PM20B	B08	15	17	18	14	19	18	
Tetrazolium Violet	PM20B	B09	344	346	344	340	338	337	0.935
Tetrazolium Violet	PM20B	B10	352	350	351	336	339	337	
Tetrazolium Violet	PM20B	B11	193	229	206	212	201	195	
Tetrazolium Violet	PM20B	B12	53	51	53	60	67	60	
Thioridazine	PM20B	C01	308	296	299	303	301	297	0.031
Thioridazine	PM20B	C02	317	316	316	295	302	294	
Thioridazine	PM20B	C03	325	305	315	292	318	308	
Thioridazine	PM20B	C04	290	317	331	312	289		
Atropine	PM20B	C05	290	280	292	293	291	285	0.940
Atropine	PM20B	C06	286	276	290	297	284	279	
Atropine	PM20B	C07		152	117	96		124	
Atropine	PM20B	C08	15	20	16	13	16	11	
Ornidazole	PM20B	C09	278	278	277	269	276	263	0.815
Ornidazole	PM20B	C10	280	278	274	266	261	261	
Ornidazole	PM20B	C11	294	289	298	276	272	269	
Ornidazole	PM20B	C12		43	38		59	52	
Proflavine	PM20B	D01	295	288	293	301	302	294	0.607
Proflavine	PM20B	D02	294	287	292	283	296	285	
Proflavine	PM20B	D03	305	303	286	306	308	306	
Proflavine	PM20B	D04	308	298	310	293	302	304	
Ciprofloxacin	PM20B	D05	283	277	279	252	284	280	0.095
Ciprofloxacin	PM20B	D06	296	291	287	294	286	283	
Ciprofloxacin	PM20B	D07	286	289	283	284	281	271	
Ciprofloxacin	PM20B	D08	286	291	299	292	281	283	
18-Crown-6-Ether	PM20B	D09	282	279	279	278	278	273	0.715
18-Crown-6-Ether	PM20B	D10	273	274	281	275	272	271	
18-Crown-6-Ether	PM20B	D11	249	250	253	248	246	246	
18-Crown-6-Ether	PM20B	D12		117	111	129	129	126	
Crystal Violet	PM20B	E01	290	290	291	289	288	286	0.500

Crystal Violet	PM20B	E02	270	268	272	281	283	273	
Crystal Violet	PM20B	E03	293	289	291	298	300	294	
Crystal Violet	PM20B	E04	314	315	316	318	323	322	
Dodine	PM20B	E05	286	292	276	293	285	283	0.963
Dodine	PM20B	E06	283	287	294	280	285	287	
Dodine	PM20B	E07	279	276	277	297	286	270	
Dodine	PM20B	E08	16	16	18	23	19	20	
Hexachlorophene	PM20B	E09	274	285	270	274	280	272	0.314
Hexachlorophene	PM20B	E10	287	283	265	281	276	283	
Hexachlorophene	PM20B	E11	250	272	261	279	277	261	
Hexachlorophene	PM20B	E12	217	221	197	236	222	267	
4-Hydroxycoumarin	PM20B	F01	295	288	293	294	298	295	0.594
4-Hydroxycoumarin	PM20B	F02	269	267	270	286	291	288	
4-Hydroxycoumarin	PM20B	F03	271	258	267	280	277	275	
4-Hydroxycoumarin	PM20B	F04	66	50	43	49	34		
Oxytetracycline	PM20B	F05	278	289	265	286	288	280	0.518
Oxytetracycline	PM20B	F06	292	297	295	303	296	282	
Oxytetracycline	PM20B	F07	276	286	293	278	282	280	
Oxytetracycline	PM20B	F08	290	292	288	277	276	285	
Pridinol	PM20B	F09	279	286	275	284	293	287	0.869
Pridinol	PM20B	F10	280	278	283	286	276	267	
Pridinol	PM20B	F11		216	255	128		124	
Pridinol	PM20B	F12	60	70	54	125	111	81	
Captan	PM20B	G01	271	269	272	291	290	288	0.006
Captan	PM20B	G02	266	264	265	277	297	281	
Captan	PM20B	G03	283	289	275	300	297	298	
Captan	PM20B	G04	300	296	300	294	300	310	
3,5-Dinitrobenzene	PM20B	G05	290	289	285	290	292	286	0.995
3,5-Dinitrobenzene	PM20B	G06	306	297	303	314	312	305	
3,5-Dinitrobenzene	PM20B	G07	299	301	321	302	310	292	
3,5-Dinitrobenzene	PM20B	G08	24	21	20	18	15	16	
8-Hydroxyquinoline	PM20B	G09	282	291	274	300	289	290	0.956
8-Hydroxyquinoline	PM20B	G10	274	268	276	270	275	268	
8-Hydroxyquinoline	PM20B	G11	203						
8-Hydroxyquinoline	PM20B	G12	29	28	32	31	40	26	
Patulin	PM20B	H01	297	285	299	290	287	286	0.985

Patulin	PM20B	H02	28						
Patulin	PM20B	H03	27	24	27	12	14	16	
Patulin	PM20B	H04	41	33	40	33	28	35	
Tolylfluanid	PM20B	H05	290	280	282	287	287	279	0.812
Tolylfluanid	PM20B	H06	290	280	290	293	286	289	
Tolylfluanid	PM20B	H07	287	284	286	282	291	278	
Tolylfluanid	PM20B	H08	287	289	294	298	290	285	
Troleandomycin	PM20B	H09	290	279	283	277	293	281	0.120
Troleandomycin	PM20B	H10	293	292	286	272	277	262	
Troleandomycin	PM20B	H11	281	277	280	275	281	277	
Troleandomycin	PM20B	H12	275	248			137	138	

Supplementary material

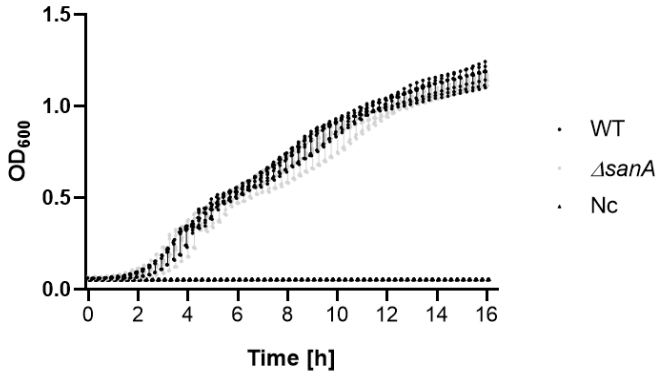

Fig. S1 Growth curves of *S.* Typhimurium 4/74

Growth curves of *S.* Typhimurium 4/74 and its deletion mutant *ΔsanA* in LB medium. Optical density (OD_{600}) was measured 16 h in 15 min intervals at 37°C. Data shown are means and SEM for at least three independent experiments.

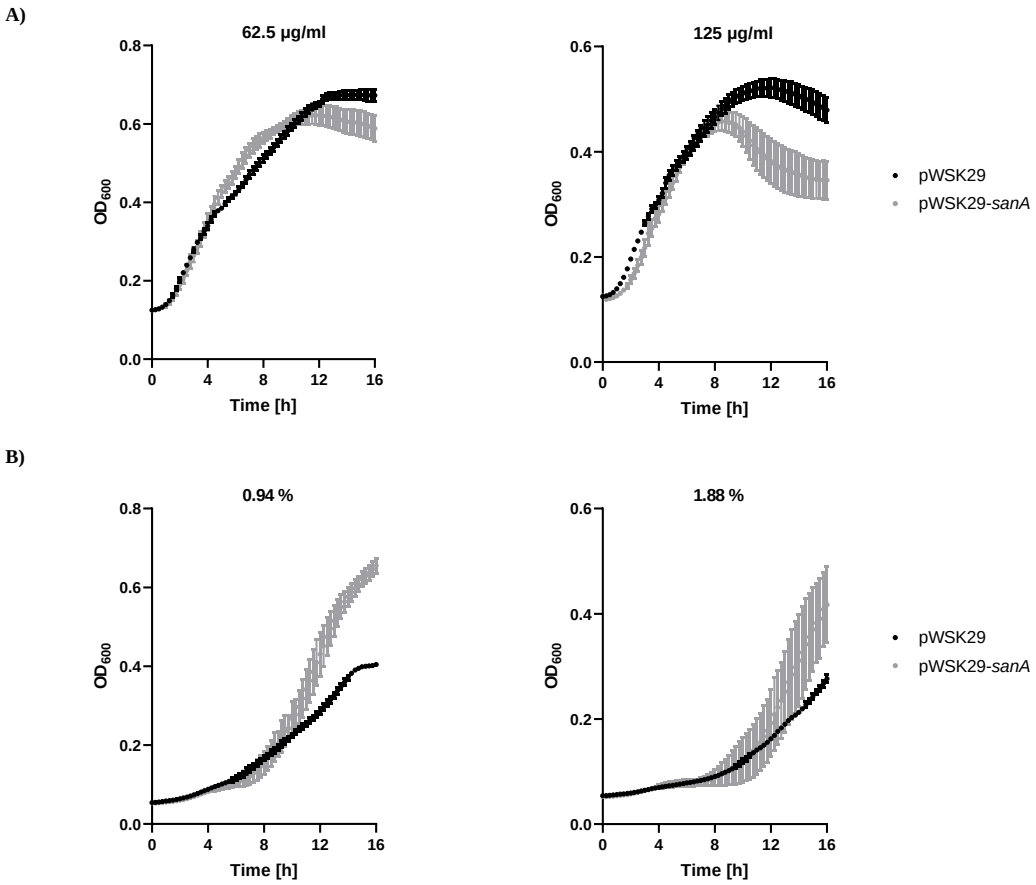

Fig. S2 Growth curve of *S*. Typhimurium 4/74 transformed with empty pWSK29 plasmid or vector with *sanA* in the presence of vancomycin or bile salts

Growth curve of *S*. Typhimurium 4/74 transformed with empty pWSK29 plasmid or vector with *sanA* in the presence of: **A)** vancomycin in the concentration 62.5 and 125 µg/ml, **B)** bile salts in the concentration 0.94 and 1.88 %. Optical density (OD_{600}) was measured 16 h in 15 min intervals at 37°C. Data shown are means and SEM for at least three independent experiments.

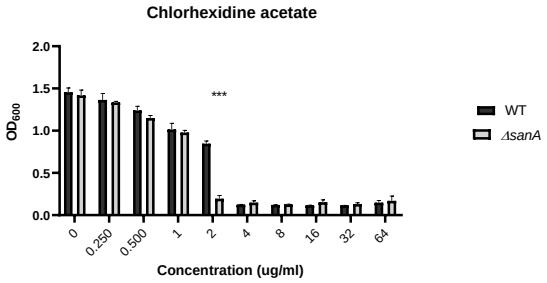
Chlorhexidine acetate
OD600
2.0
1.5
1.0
0.5
0.0
***
0
0.250
0.500
1
2
4
8
16
32
64
Concentration (ug/ml)
WT
ΔsanA

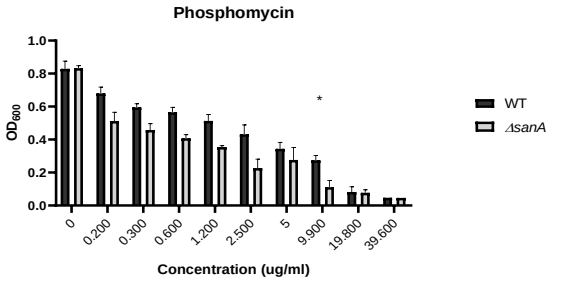
Phosphomycin
OD600
1.0
0.8
0.6
0.4
0.2
0.0
*
0
0.200
0.300
0.600
1.200
2.500
5
9.900
19.800
39.600
Concentration (ug/ml)
WT
ΔsanA

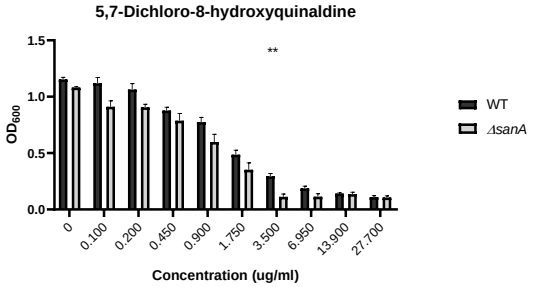
5,7-Dichloro-8-hydroxyquinaldine
OD600
1.5
1.0
0.5
0.0
**
0
0.100
0.200
0.450
0.900
1.750
3.500
6.950
13.900
27.700
Concentration (ug/ml)
WT
ΔsanA

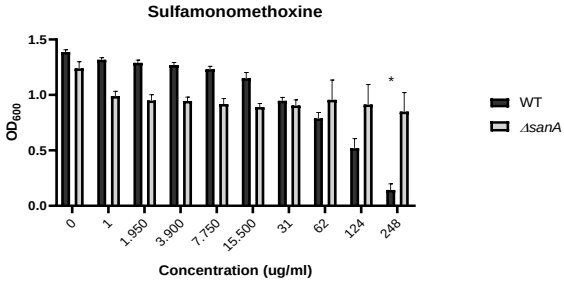
Sulfamonomethoxine
OD600
1.5
1.0
0.5
0.0
*
0
1
1.950
3.900
7.750
15.500
31
62
124
248
Concentration (ug/ml)
WT
ΔsanA

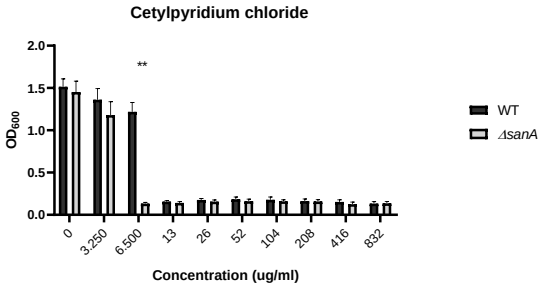
Cetylpyridium chloride
OD600
2.0
1.5
1.0
0.5
0.0
**
0
3.250
6.500
13
26
52
104
208
416
832
Concentration (ug/ml)
WT
ΔsanA

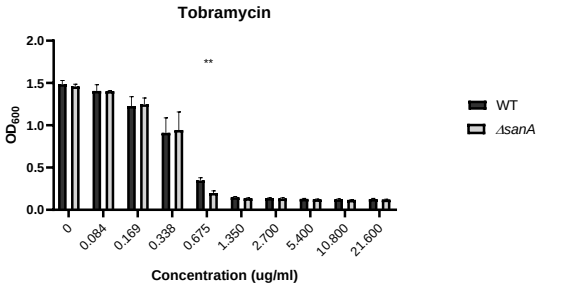
Tobramycin
OD600
2.0
1.5
1.0
0.5
0.0
**
0
0.084
0.169
0.338
0.675
1.350
2.700
5.400
10.800
21.600
Concentration (ug/ml)
WT
ΔsanA

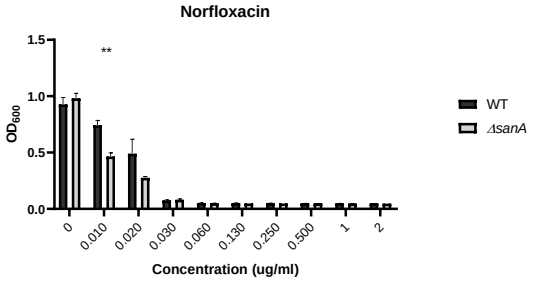
Norfloxacin
OD600
1.5
1.0
0.5
0.0
**
0
0.010
0.020
0.030
0.060
0.130
0.250
0.500
1
2
Concentration (ug/ml)
WT
ΔsanA

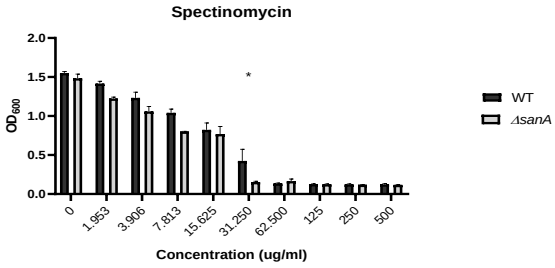
Spectinomycin
OD600
2.0
1.5
1.0
0.5
0.0
*
0
1.953
3.906
7.813
15.625
31.250
62.500
125
250
500
Concentration (ug/ml)
WT
ΔsanA

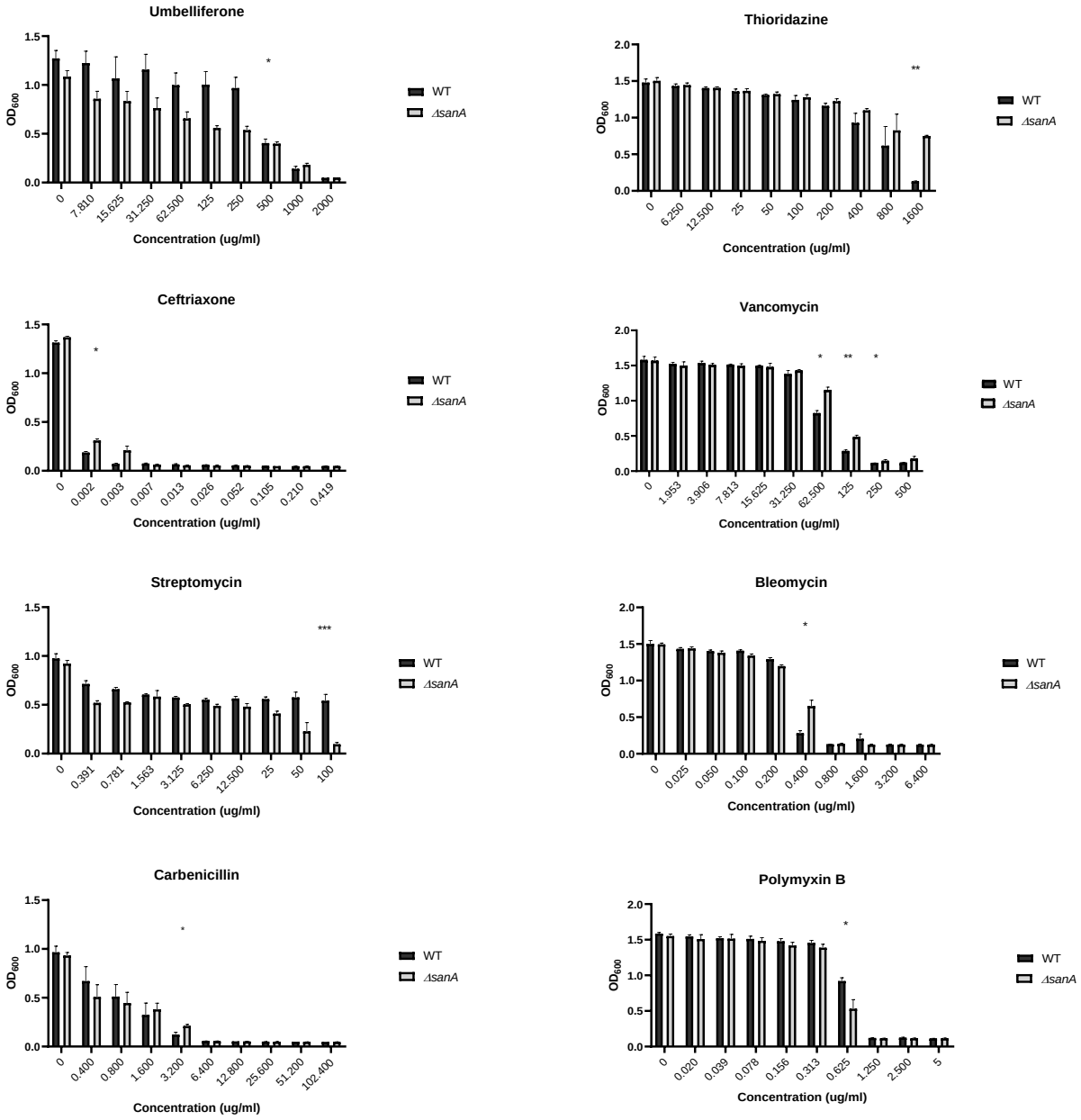

Fig. S3 Growth of *S.* Typhimurium 4/74 and its deletion mutant *ΔsanA* in MHB medium in the presence of different agents

Optical density (OD_{600}) was measured after 16 h incubation at 37°C. Data shown are means and SEM for at least three independent experiments. Statistical significance was determined by two-way ANOVA with Tukey's correction (*, $p<0.05$; **, $p<0.01$; ***, $p<0.001$). Concentrations with statistically significant differences indicated with asterix were chosen to the further analysis.

A) **B)**

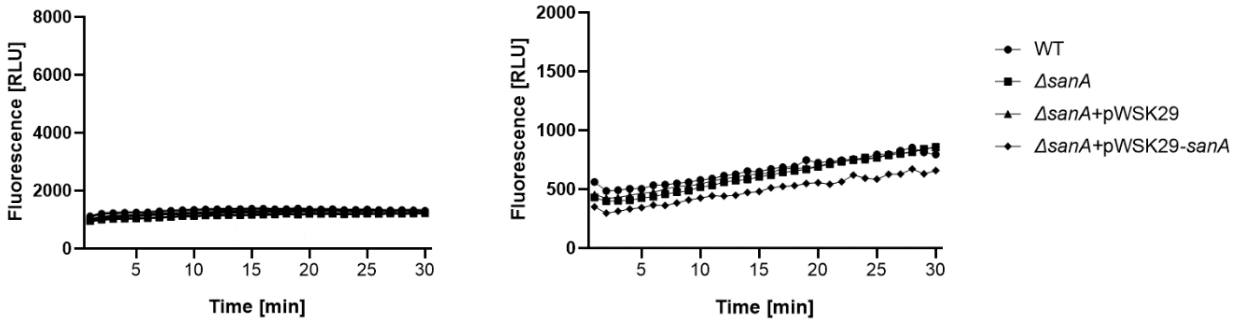

Fig. S4 Outer membrane permeability of *S*. Typhimurium 4/74

Outer membrane permeability of *S*. Typhimurium 4/74, its deletion mutant *ΔsanA* and *ΔsanA* transformed with empty pWSK29 plasmid or vector with *sanA* **A)** cationic dye ethidium bromide uptake **B)** neutral dye Nile red uptake. The assay was conducted in the absence of CCCP to measure a passive dyes uptake with the interference of efflux mechanisms. Data shown are representative of at least three independent experiments with similar results.

A)

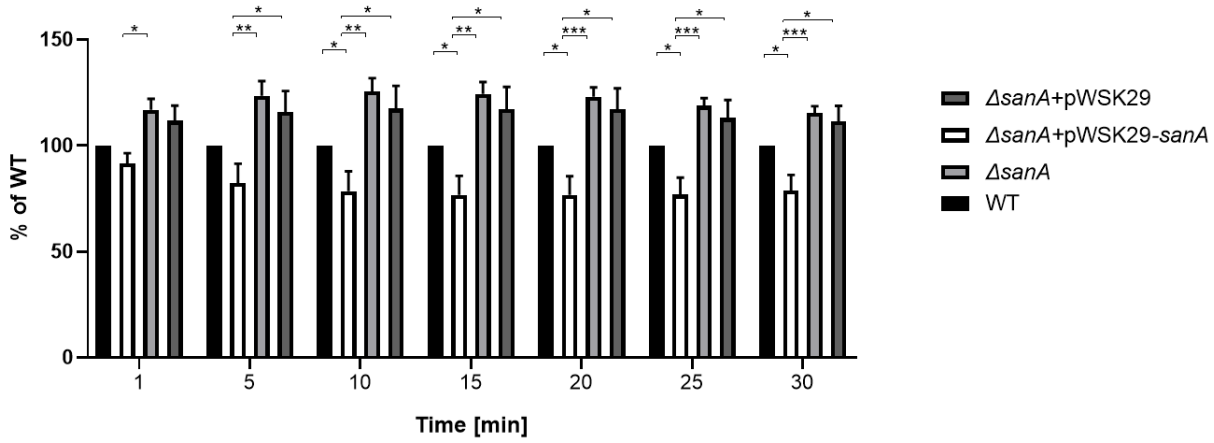

B)

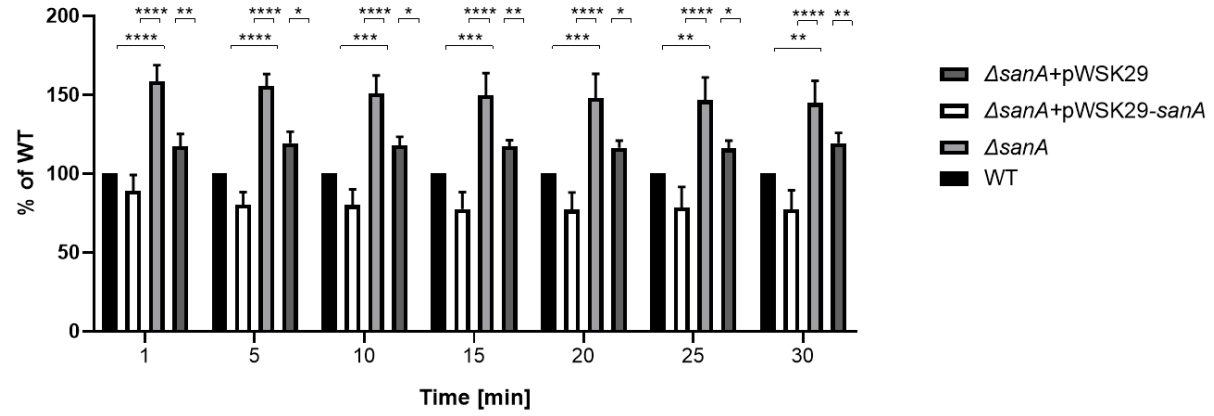

Fig. S5 Outer membrane permeability of *S.* Typhimurium 4/74 deletion mutant *ΔsanA* transformed with empty pWSK29 plasmid or vector with *sanA* wild type version; *ΔsanA*, and WT **A)** cationic dye ethidium bromide uptake **B)** neutral dye Nile red uptake. The assays were conducted in the presence of CCCP to prevent the efflux of compound by active pump to measure only passive permeability. Data are represented as the percent of isolate's permeability relative to WT. Data shown are means and SEM for at least three independent experiments. Statistical significance was determined by two-way ANOVA with Tukey's correction (*, $p<0.05$; **, $p<0.01$; ***, $p<0.001$; ****, $p<0.0001$).

9.2. Supplementary material for the 2nd manuscript

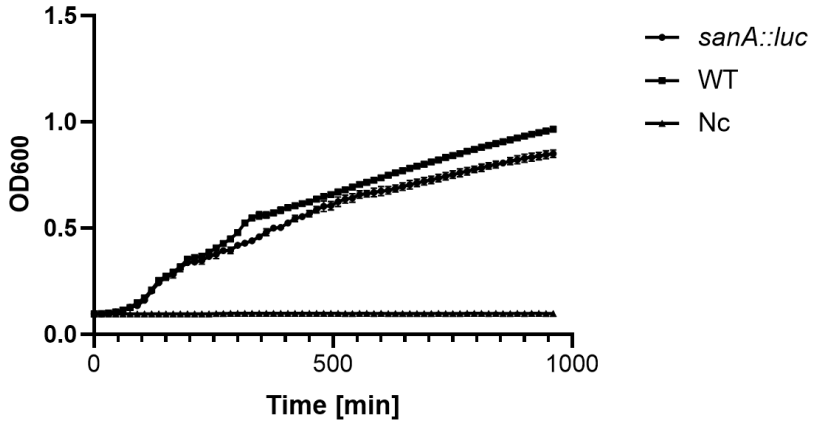

Figure S1 Growth curves of *S*. Typhimurium 4/74 WT and *sanA*$_{RBS}$*::luc* in LB medium. Nc indicates medium without bacteria. The data are shown as mean values and SEM of at least three separate experiments.

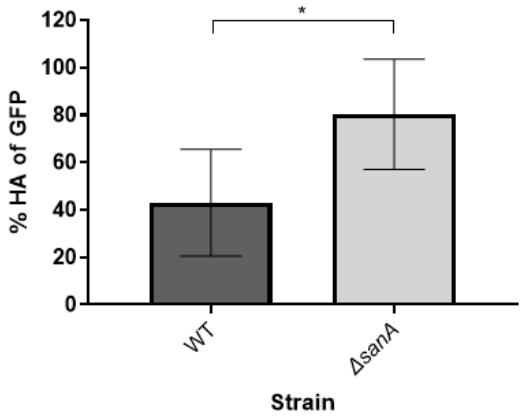

Figure S2 Densitometric analysis of protein bands imaged with the ChemiDoc MP. The average relative density of SicA was compared to the relative difference in GFP quantity of protein load for the *S*. Typhimurium lysates. The data are shown as mean values and SEM of at least three separate experiments. Statistical differences were analyzed by Student's t-test (*, $p<0.05$; **, $p < 0.01$).

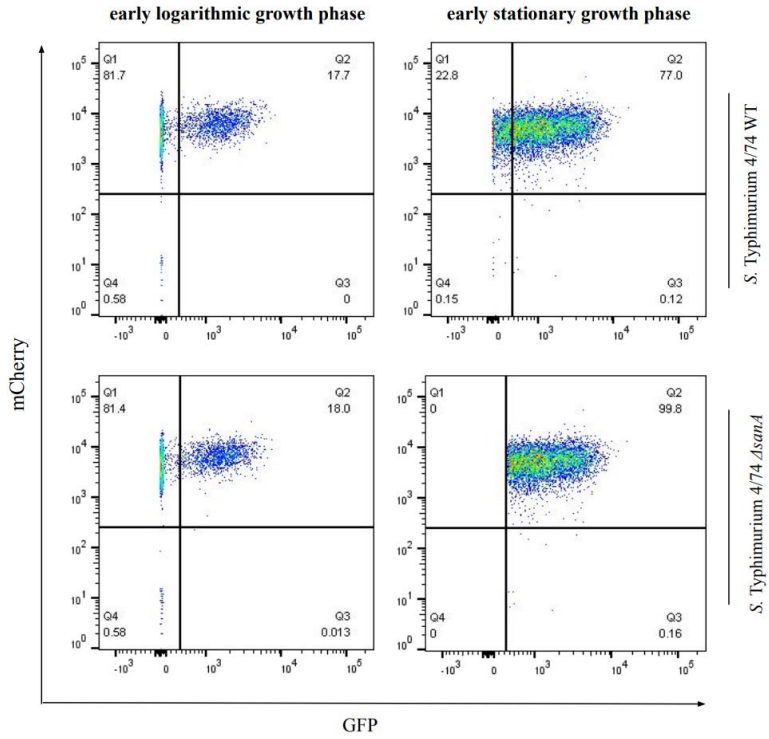

Figure S3 Fraction of cells expressing *sicA*. The fraction of cells in the on state was determined relative to the negative control (100% in the off state), which consisted of the measured fluorescence of cells not expressing the GFP. Early logarithmic growth phase corresponding to OD_{600}=0.5; early stationary growth phase corresponding to OD_{600}=2.0.

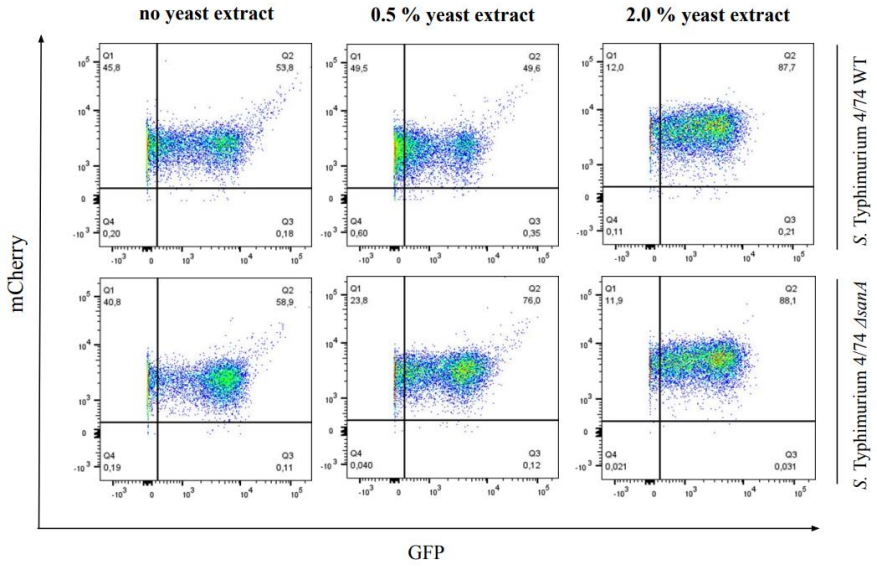

Figure S4 Fraction of cells expressing *sicA*. The fraction of cells in the on state was determined relative to the negative control (100% in the off state), which consisted of the measured fluorescence of cells not expressing the GFP.

10. Statements

Adrianna Aleksandrowicz Wrocław, 17.01.2024

Department of Biochemistry and Molecular Biology,
Faculty of Veterinary Medicine,
Wrocław University of Environmental and Life Sciences, Poland

STATEMENT

I declare that in the work: Adrianna Aleksandrowicz, Rafał Kolenda, Karolina Baraniewicz, Teresa Thurston, Jarosław Suchański, Krzysztof Grzymajło; 2024; *Membrane properties modulation by SanA: Implications for xenobiotic resistance in Salmonella Typhimurium*; Frontiers in Microbiology. 4:1340143. doi: 10.3389/fmicb.2023.1340143, my contribution consisted of:

1. Performing all described experiments: *in silico* analysis using bioinformatics tools; cloning using the classical ligation method; preparation of growth curves of the studied strains by measuring optical density; analysis of the studied strains' resistance to xenobiotics using the Biolog system; validation of results by measuring the minimum concentration of antibiotics inhibiting the growth of microorganisms; analysis of permeability and surface charge of the membrane using ethidium bromide, Nile red, and cytochrome c, respectively; isolation of primary mouse macrophages and analysis of the intracellular survival level of *Salmonell*a rods in this model.
2. Conducting statistical analysis of the results illustrated in Figures 2, 4, 5, S2, and S4, and in Table S1.
3. Preparing the initial and final version of the manuscript included in all chapters.

……..

Ph.D. student

I confirm the contents of the statement. ……..

Supervisor

Adrianna Aleksandrowicz Wrocław, 17.01.2024

Department of Biochemistry and Molecular Biology,
Faculty of Veterinary Medicine,
Wrocław University of Environmental and Life Sciences, Poland

STATEMENT

I declare that in the work: Adrianna Aleksandrowicz, Rafał Kolenda, Teresa Thurston, Krzysztof Grzymajło; 2024; *SanA is an inner membrane protein mediating early stages of Salmonella infection.* bioRxiv preprint doi: https://doi.org/10.1101/2024.01.05.574334, my contribution consisted of:

1. Performing all described experiments: cloning using the classical ligation method; preparation of growth curves of the studied strains through optical density measurement; preparation of transcriptional fusion and reporter systems; subcellular localization analysis of SanA using fractionation; determination of *sanA* expression level depending on environmental conditions; analysis of the invasiveness level of *Salmonella* in a model of mouse macrophages and human epithelial cells; analysis of the correlation of SanA with Type I Pathogenicity Island using flow cytometry.
2. Conducting statistical analysis of the experimental results illustrated in Figures 2, 3, 4, 5, and S2.
3. Preparing the initial and final versions of the manuscript included in all chapters.

……..

Ph.D. student

I confirm the contents of the statement. ……..

Supervisor